Regulation of glutathione transferase P1-1 by *S*-nitrosation

David Balchin 0600215W

November 2013

A Thesis submitted to the Faculty of Science, University of the Witwatersrand, Johannesburg in fulfilment of the requirements for the degree of Doctor of Philosophy

Supervisor: Professor Heini W. Dirr

Declaration

I, David Balchin (0600215W), am a student registered for the degree of Doctor of Philosophy (PhD) in the academic year 2013.

I hereby declare the following:

- I am aware that plagiarism (the use of someone else's work without their permission and/or without acknowledging the original source) is wrong.
- I confirm that the work submitted for assessment for the above degree is my own unaided work except where explicitly indicated otherwise.
- I have followed the required conventions in referencing the thoughts and ideas of others.
- I understand that the University of the Witwatersrand may take disciplinary action against me if there is a belief that this is not my own unaided work or that I have failed to acknowledge the source of the ideas or words in my writing.

Signature:  Date: 6 December 2013

Abstract

S-Nitrosation is a post-translational modification of protein cysteine residues, which occurs in response to cellular oxidative stress. Although it is increasingly being linked to physiologically important processes, the molecular basis for protein regulation by this modification remains poorly understood. Biophysical methods were used to elucidate the mechanism and molecular consequences of *S*-nitrosation of glutathione transferase (GST) P1-1, a ubiquitous homodimeric detoxification enzyme and important target for cancer therapeutics. Transient kinetic techniques, isothermal titration calorimetry and protein engineering were used to develop a minimal mechanism for *S*-nitrosation of GSTP1-1, the first for any protein. Cys^{47} of GSTP1-1 is *S*-nitrosated according to a conformational selection mechanism, with the chemical step limited by a pre-equilibrium between the open and closed conformations of a dynamic helix at the active site. Cys^{101}, in contrast, is *S*-nitrosated in a single step but is subject to negative cooperativity due to steric hindrance at the dimer interface. *S*-Nitrosation at Cys^{47} and Cys^{101} was found to reduce the detoxification activity of GSTP1-1 by 94%. Circular dichroism spectroscopy, acrylamide quenching and amide hydrogen-deuterium exchange mass spectrometry experiments revealed that the loss of activity is due to the introduction of local disorder at the active site. Furthermore, the modification destabilises domain 1 of GSTP1-1 against denaturation, smoothing the unfolding energy landscape of the protein and introducing a refolding defect. These data elucidate the physical basis for the regulation of GSTP1-1 by *S*-nitrosation, and provide general insight into the mechanism of *S*-nitrosation and its effect protein stability and dynamics.

Research outputs

Original publications

Publications forming part of PhD thesis

1. Balchin, D., Stoychev, S.H., and Dirr, H.W. (2013) *S*-Nitrosation destabilises glutathione transferase P1-1. *Biochemistry* **DOI:** 10.1021/bi401414c

2. Balchin, D., Wallace, L.A., Dirr, H.W. (2013) *S*-Nitrosation of glutathione transferase P1-1 is controlled by the conformation of a dynamic active site helix. *J. Biol. Chem*. **288**, 14973–14984.

Other publications

3. Balchin, D., Dirr, H.W. and Sayed, Y. (2011) Energetics of ligand binding to human glutathione transferase A1-1: Tyr-9 associated localisation of the C-terminal helix is ligand-dependent. *Biophys. Chem.* 156, 153-158.

4. Balchin, D., Fanucchi, S., Achilonu, I., Adamson, R.J., Burke, J., Fernandes, M., Gildenhuys, S. and Dirr, H.W. (2010) Stability of the domain interface contributes towards catalytic function at the H-site of class alpha glutathione transferase A1-1. *Biochim. Biophys. Acta* 1804, 2228-2233.

5. Gildenhuys, S., Wallace, L.A., Burke, J.P., Balchin, D., Sayed, Y. and Dirr, H.W. (2010) Class Pi glutathione transferase unfolds via a dimeric and not monomeric intermediate: functional implications for an unstable monomer. *Biochemistry* 49, 5074-5081.

Conference outputs

Conference presentations during PhD thesis

1. University of the Witwatersrand postgraduate symposium 2013. *Poster presentation*. "Mechanism and biophysical consequences of *S*-nitrosation of GSTP1-1". David Balchin and Heini W. Dirr.

2. Molecular Biosciences Research Thrust Research day, Johannesburg 2012. *Poster presentation*. "Redox signalling at a molecular level: mechanism and consequences of protein *S*-nitrosation." David Balchin, Stoyan S. Stoychev and Heini W. Dirr.

3. 26th Symposium of the Protein Society, San Diego 2012. *Poster presentation*. "Redox signalling at a molecular level: mechanism and consequences of protein *S*-nitrosation." David Balchin, Stoyan S. Stoychev and Heini W. Dirr.

4. South African Society for Biochemistry and Molecular Biology conference, Drakensberg 2012. *Oral presentation*. "*S*-nitrosylation modulates the stability of glutathione transferase P1-1." David Balchin, Stoyan S. Stoychev and Heini W. Dirr.

5. Molecular Biosciences Research Thrust Research day, Johannesburg 2011. *Oral presentation*. "*S*-nitrosylation modulates the stability of glutathione transferase P1-1." David Balchin, Stoyan S. Stoychev and Heini W. Dirr.

Other conference presentation

6. South African Society for Biochemistry and Molecular Biology conference, Bloemfontein 2010. *Oral presentation*. "The role of a topologically conserved interdomain interaction in the function of human glutathione transferase A1-1". David Balchin, Samantha Gildenhuys and Heini W. Dirr.

Acknowledgements

I would like to acknowledge Tata Africa, the National Research Foundation (SARChI) grant to H.W. Dirr) and the University of the Witwatersrand for their generous financial support.

I would like to thank the following people:

Dr. S. Y. Blond for her kind gift of the expression vector encoding wild-type His^6-hGSTP1-1.

Dr. Stoyan Stoychev for his invaluable technical and intellectual contribution to the hydrogen-deuterium exchange mass-spectrometry experiments.

Professor Yasien Sayed, Dr. Ikechukwu Achilonu and Nishal Parbhoo for their generous help with numerous theoretical and technical aspects of this research.

Professor Heini Dirr for his excellent supervision throughout my postgraduate career.

Contents

List of figures

List of abbreviations

α2	Helix 2 of glutathione transferase P1-1
CDNB	2-chloro-dinitrobenzene
DXMS	Hydrogen-deuterium exchange mass spectrometry
GSH	Reduced glutathione
GSNO	*S*-Nitrosoglutathione
GST	Glutathione transferase
JNK	c-Jun N-terminal kinase
NMR	Nuclear magnetic resonance
NO	Nitric oxide
NOS	Nitric oxide synthase
SASA	Solvent accessible surface area
SNO	*S*-Nitrosothiol

Chapter 1

Introduction

1.1 Post-translational modifications expand the genetic code

Following synthesis at the ribosome and subsequent folding (or not [1]) to achieve their functional form, proteins are often covalently modified. These post-translational modifications are diverse, highly prevalent in eukaryotes, and serve numerous critical functions (reviewed in [2,3]). Covalent modifications can diversify the function of a single protein, regulate protein activity, amplify cellular signals (in signal transduction cascades), modulate protein-protein interactions, or target proteins to specific parts of the cell.

Several post-translational modifications modulate cellular events by promoting or inhibiting key protein-protein interactions. Nucleotidylations such as adenylylation inhibit the interaction between Rab proteins and their effectors [4], and ubiquitination targets proteins for degradation by facilitating their interaction with the proteasome system [5]. Another well-characterised example is histone acetylation, which alters protein interactions critical to the activation of transcription [6].

Covalent protein modifications can also act to selectively target proteins to cellular membranes. This typically involves the conjugation of lipid groups to the protein, which serve as membrane anchors. Examples include prenylation [7], palmitoylation [8] and myristoylation [9]. Such lipidation events typically occur at cysteine residues via thioester linkages, and are usually irreversible. These modifications are therefore not involved in dynamic signalling processes.

Reversible post-translational modifications play a critical role in cellular signal transduction. This is exemplified by protein phosphorylation, which is tightly regulated by kinase [10] and phosphatase enzymes. Phosphorylation at serine, threonine or tyrosine residues induces local changes in protein structure, which often alter enzyme activity [11]. Furthermore, kinases are themselves typically activated by phosphorylation. An important consequence of this is that successive steps of enzyme activation can amplify the signal associated with the initial

phosphorylation event. Phosphorylation and other reversible post-translational modifications add layers of complexity to the behaviour of eukaryotic cells, and allow protein function to be fine-tuned in reponse to physiological or pathophysiological stimuli.

1.2 Redox regulation of proteins: cysteines are redox switches

The cysteine thiol (Figure 1) is the most reactive amino acid functional group. In addition, the pK_a of a solvent exposed thiol group is close to physiological pH [12,13]. It is therefore unsurprising that cysteine residues in proteins participate in a variety of functionally important reactions. These reactions can be partitioned into three classes: catalytic, structural and regulatory. Catalytic cysteines are those that participate directly in chemical catalysis at an enzyme active site, for example in oxidoreductases, proteases and acyltransferases [12]. Structural cysteines stabilise protein structure by forming disulfide bonds. Finally, regulatory cysteines are responsible for the fine control of protein function by accepting a variety of post-translational modifications [13]. It is this latter function that enables cysteine to be classed as a redox-sensitive switch [14].

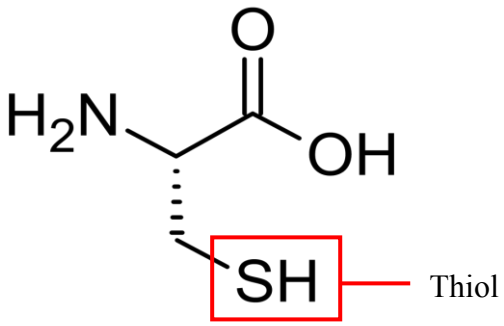

Figure 1. L-Cysteine. The thiol group is indicated. Adapted from the PubChem database (http://pubchem.ncbi.nlm.nih.gov/).

Cysteine pK_a (and therefore reactivity) can be finely modulated by the microenvironment of the cysteine thiol [15]. Cysteines are therefore extremely sensitive to physiological stimuli, such as changes to the redox status of the cell. Furthermore, this sensitivity allows for a graded response to cellular stimuli, such that a single cysteine can display a range of redox

modifications, depending on the level of oxidative or nitrosative stress (Figure 2) [14]. At one end of the scale are poorly reversible sulfonic acid and sulfinic acid modifications, associated with diseased states. At the other end are sulfenic acid, disulfides, *S*-nitrosation and *S*-glutathionylation: readily reversible signalling modifications associated with healthy cells [16,17].

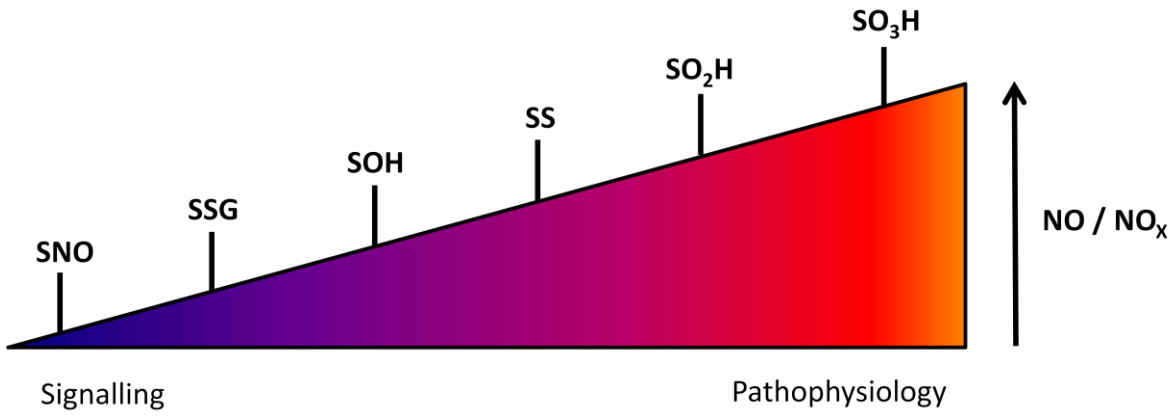

Figure 2. Redox modifications of cysteine in response to increasing oxidative/nitrosative stress. Sulfonic acid (SO_3H), sulfinic acid (SO_2H), sulfenic acid (SOH), disulfides (SS), *S*-nitrosation (SNO) and *S*-glutathionylation (SSG). Adapted from Hess *et al*. [16].

1.3 Protein *S*-nitrosation

Cellular nitric oxide (NO) is predominantly generated by nitric oxide synthases (NOS), which catalyse the reaction between arginine and molecular oxygen, forming citrulline as a byproduct [18]. Alternatively, NO may be produced by the oxidation or reduction of exogenous nitrates or nitrites [19]. NO may then react with metals [20], ferrous heme [21] or cysteine thiols [22]. The effects of NO were initially thought to be confined to the regulation of heme-containing proteins such as haemoglobin [23] and guanylate cyclase [24]. More recently, protein thiols have emerged as a major target of NO, with more than five hundred protein *S*-nitrosation sites identified to date [25].

Protein *S*-nitrosation is recognised to control a number of important physiological processes such as vascular homeostasis [26], autophagy [27], the innate immune response [28] and a spectrum of other post-translational modifications [29]. In this context, it is unsurprising that dysregulation of protein *S*-nitrosation is associated with several diseases, including neurodegenerative disorders, various cancers, and diabetes (reviewed in [30]). The study of *S*-nitrosation at a molecular level is therefore highly relevant from a therapeutic perspective.

1.4 *S*-Nitrosothiol structure, chemistry and stability

Crystallographic studies of various small *S*-nitrosated molecules [31] as well as several *S*-nitrosated proteins [32–35] have provided valuable insight into the structure of *S*-nitrosothiols structure (Figure 3).

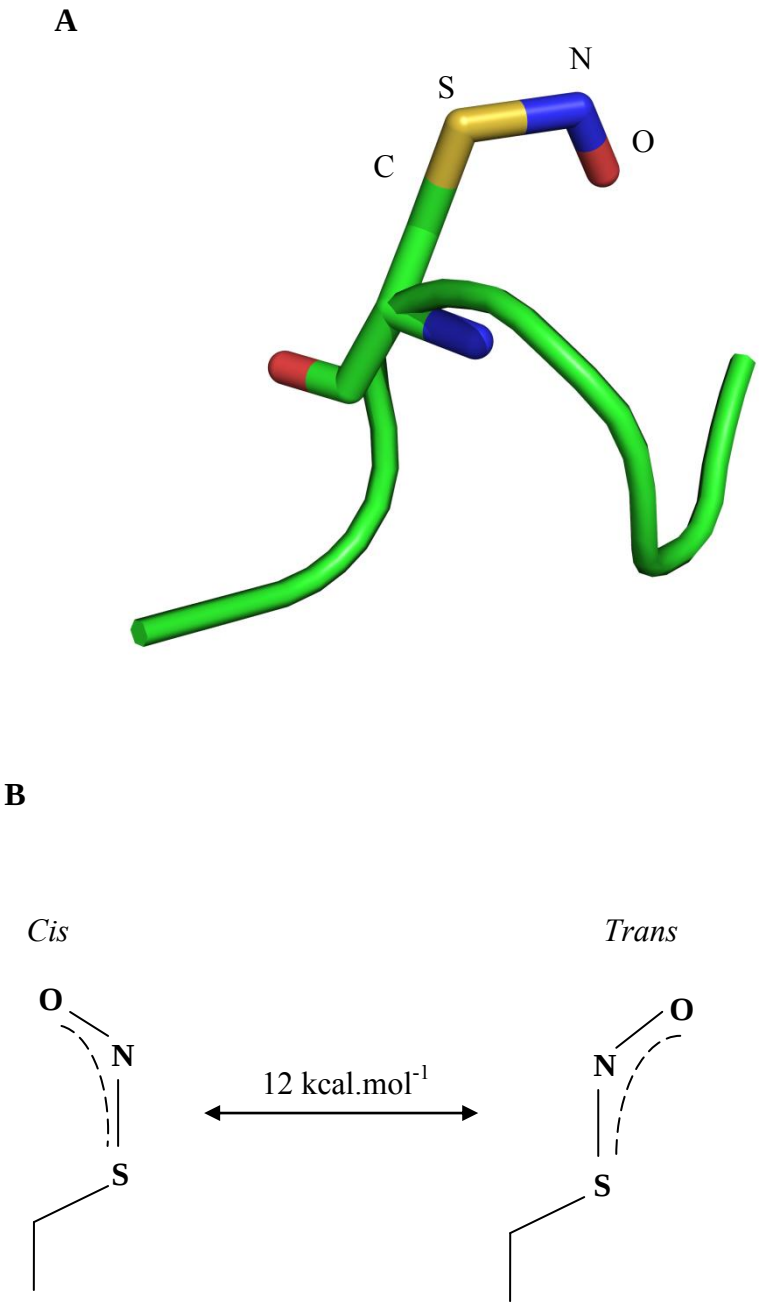

Figure 3. *S*-Nitrosocysteine structure. *A*, *S*-nitrosocysteine at position 10 in *S*-nitrosated blackfin tuna myoglobin. The C-S-N-O dihedral, with *cis* planar configuration, is indicated. The peptide backbone is coloured green. The image was generated from 2NRM [33] using PyMol (www.pymol.sourceforge.net). *B*, schematic of *cis* or *trans S*-nitrosothiol. The dashed lines illustrate delocalisation of the N=O π electrons, conveying partial double-bond character to the S-N bond. The energy barrier for rotation between the two conformers is 12 kcal.mol^{-1} [36].

S-Nitrosothiols show significant S-N double-bond character [31] due to delocalization of the N=O π electrons. Consistent with this, quantum mechanical calculations place energy minima for the C-S-N-O dihedral at 0 ° and 180 ° (*cis* and *trans* respectively) and estimate a 12 kcal.mol^{-1} energy barrier for the rotation between these conformers [36] (Figure 3B). Although both the *cis* and *trans* conformers have been observed for small molecule *S*-nitrosothiols [31], the *cis* conformer appears to dominate in the structures of *S*-nitrosated proteins solved thus far. This is possibly because of steric clashes with the peptide backbone in the *trans* configuration, although too few structures have been solved to allow a definitive explanation. The exception to this trend is Cys*β*93-NO of S-nitrosohemoglobin, for which a dihedral of approximately 90 ° was reported [32]. It was later concluded, however, that this was more likely a thionitroxide radical (C-S-NH-O•) than a conventional *S*-nitrosated cysteine residue [36].

Bond dissociation enthalpies for homolysis of the S-N bond of model *S*-nitrosothiols (SNOs) have been computed to range from approximately 94 to 132 kJ.mol^{-1}, which covers a predicted SNO half-life of seconds to years [16,37]. This variation results from differences in the RSNO R-substituent and the length (double-bond character) of the S-N linkage [37]. In proteins, these factors can be tuned by the local environment of the SNO: hydrophobicity, steric hindrance and the presence of groups which might stabilise or destabilise the SNO dissociation products [16]. For SNOs in solution at physiological pH, however, the major route of decomposition is not spontaneous, but catalysed by trace monovalent copper ions [38]. Photolysis, particularly at the absorption maximum of SNOs (335 or 550 nm) is another significant mechanism of S-N cleavage [39]. Finally, any reducing agent will destroy the S-N linkage, by either protonating the thiolate anion, or reducing Cu^{2+} to form Cu^{+} [40]. Therefore, contingent on the thermal stability of the S-N bond, SNOs should be significantly stable in the dark and in the presence of copper chelators. This appears to be true for at least some protein-SNOs *in vitro*; *S*-nitrosated blackfin tuna myoglobin is reported to be stable for at least 1 month in the absence of light and metal ions [33]. *In vivo*, *S*-nitrosated proteins are sufficiently stable to transduce cellular signals over at least the lifetime of the stimulus (typically oxidative or nitrosative stress) [16]. In fact, a small subset of *S*-nitrosated proteins *in vivo* have been shown to be persist beyond the timescale of the nitrosative stimulus, even in the presence of cellular reductants such as glutathione [41]. This suggests a complexity to SNO

decomposition in proteins that is beyond the simple chemistry of small model *S*-nitrosothiols, possibly involving protein conformational changes which protect Cys-NOs from reduction [41].

1.5 Mechanism and kinetics of *S*-nitrosation and denitrosation

The nitric oxide radical (NO) is generated *in vivo* by the endothelial, neuronal and inducible isoforms of nitric oxide synthase (NOS) [42]. Several pathways for the formation of *S*-nitrosothiols from NO have been proposed (Figure 4): radical-radical recombination, transition metal catalysed, and NO_2 mediated.

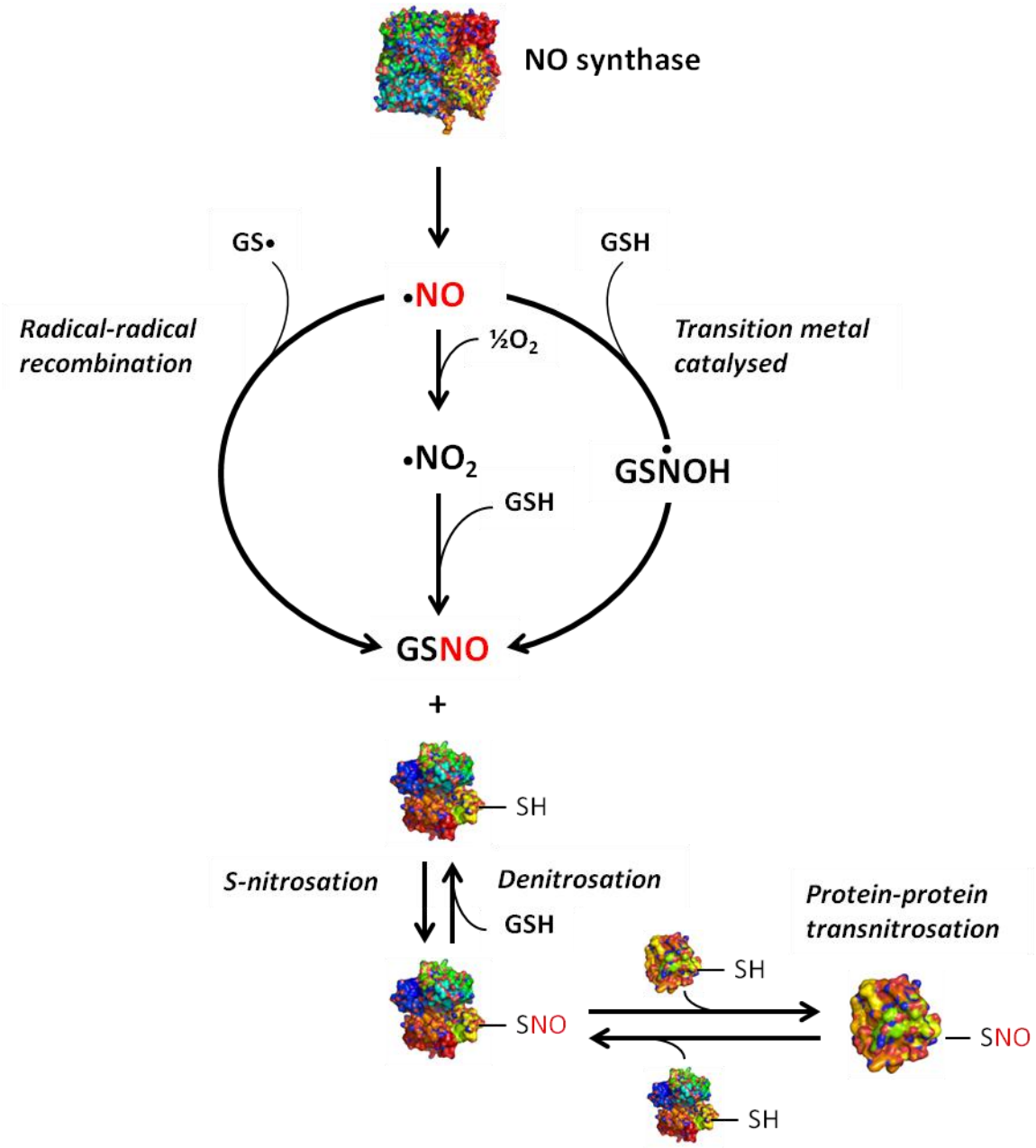

Figure 4. Mechanisms of protein *S*-nitrosation. NO radical produced in a reaction catalysed by NO synthase (1NOD) can react with GSH to form GSNO in three ways: 1) radical recombination with the GS radical, 2) via NO_2, 3) via GSNOH, catalysed by transition metals. GSNO is able to transnitrosate protein thiols, which can themselves transnitrosate other proteins. Denitrosation reactions are mediated by free thiols on GSH or proteins. Adapted from Smith and Marletta [43].

The physiological relevance of *S*-nitrosothiol formation via radical-radical recombination is controversial. Initial calculations based on model systems assumed a rate constant for the reaction of the thiyl radical with NO of approximately 1 x 10^9 $M^{-1}.s^{-1}$ (near the diffusion controlled limit) [44]. However, subsequent experimental work derived rate constants of 3 x 10^7 $M^{-1}.s^{-1}$ (laser flash photolysis) [45] or 2 x 10^9 $M^{-1}.s^{-1}$ (pulse radiolysis and kinetic competition assays) [46] for the same reaction. If the former (smaller) rate constant is correct, then at physiological NO concentrations and pH, the reaction between GS• and •NO would be outcompeted by rapid rearrangement of the thiyl radical to form the carbon-centred radical of glutathione [45,47,48]. If the higher rate constant (2 x 10^9 $M^{-1}.s^{-1}$) is correct, however, then radical-radical recombination is a plausible route for *S*-nitrosation of glutathione *in vivo*, a conclusion which is supported by kinetic modeling [49].

The reaction between NO and glutathione can also be catalysed by electron acceptors with sufficiently large electrode potentials, such as transition metal ions [50]. This has been demonstrated for ferric cytochrome c [51], ferric soluble guanylate cyclase [52] and methaemoglobin [53,54]. In the case of ferric cytochrome c, the protein binds GSH before reacting with NO to yield ferrous cytochrome c and GSNO [51]. The protein acts as an electron sink, stabilising the intermediate radical GSNOH and facilitating its oxidation to GSNO. Ferric soluble guanylate cyclase and methaemoglobin appear to catalyse *S*-nitrosation by first undergoing reductive nitrosylation, whereby the ferric (Fe^{3+}) oxidation state of the haem group binds NO to form Fe^{2+} - NO [52,53]. This complex is then readily able to *S*-nitrosate nearby thiolates, forming *S*-nitrosothiols.

Thiol nitrosation has also been proposed to occur via NO_2 [55], a process that is energetically favourable by – 37 ± 5 $kJ.mol^{-1}$ at pH 7 [50]. However, cellular nitrosothiol formation has been shown to occur independently of oxygen under certain conditions [56,57]. NO_2 – mediated nitrosation, which requires oxidation of the NO radical (Figure 5), may therefore be of limited physiological relevance, or may occur only in permissive cellular compartments. NO_2 can also undergo further oxidation to form N_2O_3, and it was initially proposed that N_2O_3 was the predominant thiol nitrosating species [58]. Although this notion is still prevalent in the literature, the formation of nitrosothiols from N_2O_3 is unlikely for several reasons. First, *S*-nitrosation is (under certain conditions) favoured in the absence of oxygen [56]. Second, the formation of N_2O_3 from NO_2 is easily outcompeted by the reaction of NO_2 with free thiols and urate *in vivo* [59]. Third, the formation of N_2O_3 from NO_2 is energetically unfavourable by

59 kJ.mol^{-1} [50]. Fourth, the hydrolysis of N_2O_3 is too slow to compete with its dissociation into NO and NO_2 [50].

GSH is the most abundant thiol in human cells, reaching concentrations of up to 10 mM, depending on the cellular redox status [60]. It follows that GSNO is the most abundant cellular *S*-nitrosothiol [61], and therefore transnitrosation reactions between GSNO and free protein thiols are significant *in vivo*. This conclusion is supported by the fact that GSNO treatment is efficiently stimulates protein *S*-nitrosation *in vitro*, in cultured yeast [62] and in human cells [41]. Furthermore, knockout of GSNO reductase in mice was shown to result in increased protein *S*-nitrosation, implying that cellular GSNO is in equilibrium with protein-SNO [63]. Transnitrosation reactions are second-order [64], and are limited by the rate of the nucleophilic attack of the target thiolate on the nitrogen of the SNO moiety [65] (Scheme 1). The reaction proceeds via a nitroxyl disulfide intermediate (R-SN[O]S-R) [66] and has an activation energy of approximately 95 kJ.mol^{-1} (obtained for the model compound *S*-nitrosocysteine ethyl ester) [67]. Second order rate constants for the transnitrosation reaction of small molecule thiols by GSNO range from approximately 30 to 170 $M^{-1}.s^{-1}$ [64]. Protein transnitrosation by GSNO occurs with similarly slow kinetics, depending on the target cysteine, with values of 6 and 112 $M^{-1}s^{-1}$ reported for bovine serum albumin and Cys112 on the β chain of haemoglobin, respectively [68]. Although it clearly occurs *in vivo*, transnitrosation of proteins by GSNO is likely to achieve physiologically significant rates only at high concentrations of GSNO (under conditions of intense nitrosative stress, for example [57,69]), or in the presence of an appropriate catalyst. Alternatively, the gradual accumulation of stably *S*-nitrosated protein [41,57] may cause long term cellular effects and comprise an important part of the cellular stress response.

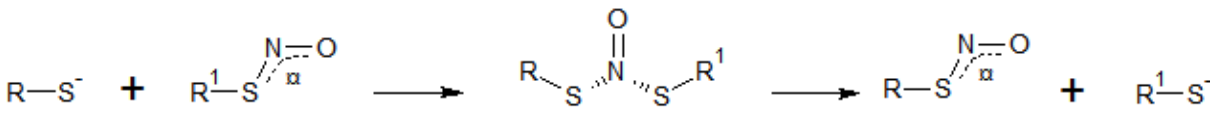

Scheme 1. Generic transnitrosation reaction. A nitrosothiol group (RSNO) transfers NO to free thiolate (RS^-). The reaction proceeds via a nitroxyl disulfide intermediate (R-SN[O]S-R) [66].

Although *S*-nitrosothiol formation appears to be predominantly non-enzymatic, several enzymes also contribute to protein *S*-nitrosation, allowing more complex regulation of NO signalling [70]. Thioredoxin catalyses both nitrosation [71] and denitrosation [72], depending on its redox state [73], while superoxide dismutase specifically catalyses the conformation-dependent *S*-nitrosation of haemoglobin [74]. Ferric cytochrome-c has also been shown to accelerate the formation of protein *S*-nitrosothiols by acting as an electron sink, as described above [75]. In addition, protein transnitrosation by GSNO is indirectly modulated by GSNO reductase [63] and carbonyl reductase 1 [76], which control the levels of GSNO *in vitro.*

For protein *S*-nitrosation to transduce cellular signals, the cysteine modification must be reversible. Because cellular GSH concentrations are high, most *S*-nitrosated proteins are likely to be rapidly reduced by GSH *in vivo*. A subset of *S*-nitrosated proteins are, however, resistant to GSH-mediated denitrosation [57]. This has been proposed to be due to conformational changes which shield the SNO moiety from GSH [41], but kinetic and structural analyses defining this important process are lacking. In addition to spontaneous denitrosation by GSH, several enzymes have been proposed to function as denitrosases *in vivo* (reviewed in [77]), although only thioredoxin is unambiguously established to function in this regard [72].

The mechanisms of *S*-nitrosothiol formation *in vivo* remain controversial. Furthermore, transnitrosation and denitrosation reactions have been properly characterised only for small molecule model systems: the physiologically important reaction between GSNO and protein thiols is poorly understood. Although several studies have attempted to describe the kinetics of protein transnitrosation by GSNO [68,73], a kinetic mechanism has yet to be derived. A detailed understanding of the sequence of events associated with protein transnitrosation and denitrosation is also likely to give insight into how the specificity of *S*-nitrosation is achieved.

1.6 *S*-Nitrosation motifs

Not all cysteine-containing proteins are *S*-nitrosated, and not all cysteines on *S*-nitrosated proteins are modified. The microenvironment of a cysteine residue must therefore in some way define the susceptibility of that cysteine to *S*-nitrosation. A number of methodologies have been developed for detecting *S*-nitrosated proteins and identifying *S*-nitrosated cysteines [78], which has resulted in a large and expanding database of protein *S*-nitrosation sites [25]. Despite this, there is still a lack of consensus on the molecular determinants for protein *S*-nitrosation – the features of an *S*-nitrosation motif.

From proteomics data, the first proposal for a *S*-nitrosation motif was an acid-base motif in primary sequence, with acidic and basic residues flanking the target cysteine [79]. Potentially important secondary structural elements were later hypothesised, in particular the N-termini of alpha-helices and active site loops [62]. Recently, it has been increasingly recognized that protein tertiary structure around the target thiol is likely to ultimately define its susceptibility to *S*-nitrosation. Promisingly, two recent structure-based analyses identified new acid-base *S*-nitrosation motifs with exposed charged groups [80,81]. Furthermore, several earlier hypotheses were rejected, such as a low thiol pK_a and a hydrophobic cysteine microenvironment [82].

Transnitrosation by reaction with GSNO is likely a major mechanism of protein S-nitrosation [16]. In this case, the ability of GSNO to dock to a site near to the target cysteine residue has been suggested as an important criterion for *S*-nitrosation specificity [81] and has been demonstrated for several proteins [14,28]. A further intriguing possibility is that *S*-nitrosation specificity is conferred by specific protein-protein interactions between the target protein and an *S*-nitrosated partner [80,81]. GAPDH [83], thioredoxin [84] and inducible NOS [85] have all been shown to participate in specific protein-protein transnitrosation reactions. In the case of NOS, an alternative explanation is that *S*-nitrosation is spatially regulated by the production of locally concentrated NO [86].

1.7 Molecular consequences of protein *S*-nitrosation

S-Nitrosation has been shown to regulate enzyme function in a large number of cases. These include the inhibition of caspase-3 [87] and thioredoxin [88], and activation of the bacterial transcription factor OxyR [89]. The activity of several ion channels is also modulated by *S*-nitrosation, including ryanodine receptor [90] and the potassium channel KCNQ1 [91]. Furthermore, the allosteric behavior of hemoglobin appears to be under post-translational control by targeted *S*-nitrosation [92].

Despite the plethora of examples of *S*-nitrosation altering protein function, there is little information concerning the molecular origins of these effects. This is especially true in cases where the modified cysteine is not catalytic. Biophysical data linking the *S*-nitrosation event to its functional consequence have only been collected for a limited set of proteins. Far-UV circular dichroism spectroscopy revealed a small loss in alpha-helical content upon *S*-nitrosation of OxyR [14] and the chloride channel CLIC4 [93]. A subtle change in the tertiary structure of *S*-nitrosated CLIC4 was also suggested by trypsin digestion and thermal

denaturation experiments [93]. At the level of quaternary structure, *S*-nitrosation has been found to regulate the immune response in plants by triggering the oligomerisation of NPR1 [94].

Only five crystal structures and two solution structures (by nuclear magnetic resonance, NMR) have been solved for *S*-nitrosated proteins to date: myoglobin [33], thioredoxin [34], protein-tyrosine phosphatase 1B [35], nitrophorin [95], soluble guanylyl cyclase [96], $p21^{Ras}$ [97] (NMR) and S100A1 [98] (NMR). *S*-Nitrosation has very little effect on the structures of protein-tyrosine phosphatase 1B and $p21^{Ras}$. However, distinct structural consequences were apparent for the other *S*-nitrosated proteins. In all cases, a "wedging apart" [33] of secondary structural elements to accommodate the bulk of the NO moiety was observed. In the case of nitrophorin, this opening of the protein structure was accompanied by enhanced local dynamics and a loss of hydrogen bonds [95]. Although the structural data obtained thus far are valuable, the small size of the data set limits our ability to identify trends or make predictions about the consequences of *S*-nitrosation to protein structure. In addition, structural data need to be linked to changes in protein function, stability and dynamics to completely elucidate *S*-nitrosation on a molecular level.

1.8 Glutathione transferase P1-1: structure, stability and cysteine reactivity

The glutathione transferases (GSTs) are a major class of drug detoxification enzymes ubiquitous in aerobes [99]. These proteins are of keen therapeutic interest due to their apparent involvement in cancer drug resistance (reviewed in [100]), with class pi GST in particular observed to be up-regulated in tumor cell lines ([101] and references therein). This latter observation is likely due to the involvement of GSTP1-1 in the regulation of signal transduction pathways relevant to oncogenesis [102]. Specifically, GSTP1-1 binds and inhibits the phosphorylated form of the pro-apoptotic protein, c-jun N-terminal kinase [103]. GSTP1-1 has also been shown to modulate cellular redox activity and energy homeostasis by binding 1-cys peroxiredoxin [104] and AMP-activated protein kinase [105], respectively.

GSTP1-1 is a native homodimer [106], with each subunit comprising two non-identical domains [107] (Figure 5). Domain 1 forms a thioredoxin-like fold while domain 2 is exclusively alpha-helical. The active site is situated primarily in domain 1 but is fully formed by inter-domain and inter-subunit contacts. The detoxification reaction catalysed by GSTs involves the conjugation of reduced GSH to a variety of hydrophobic, electrophilic substrates (reviewed

by Armstrong [108]). Glutathione binds at the G-site of the protein, while the hydrophobic substrate occupies the H-site [109] (see the glutathionyl and *S*-hexyl moieties of *S*-hexylglutathione at the active site in Figure 5). Substrate specificity varies between the GST classes, and is influenced by the flexibility of structural elements at the active site [110].

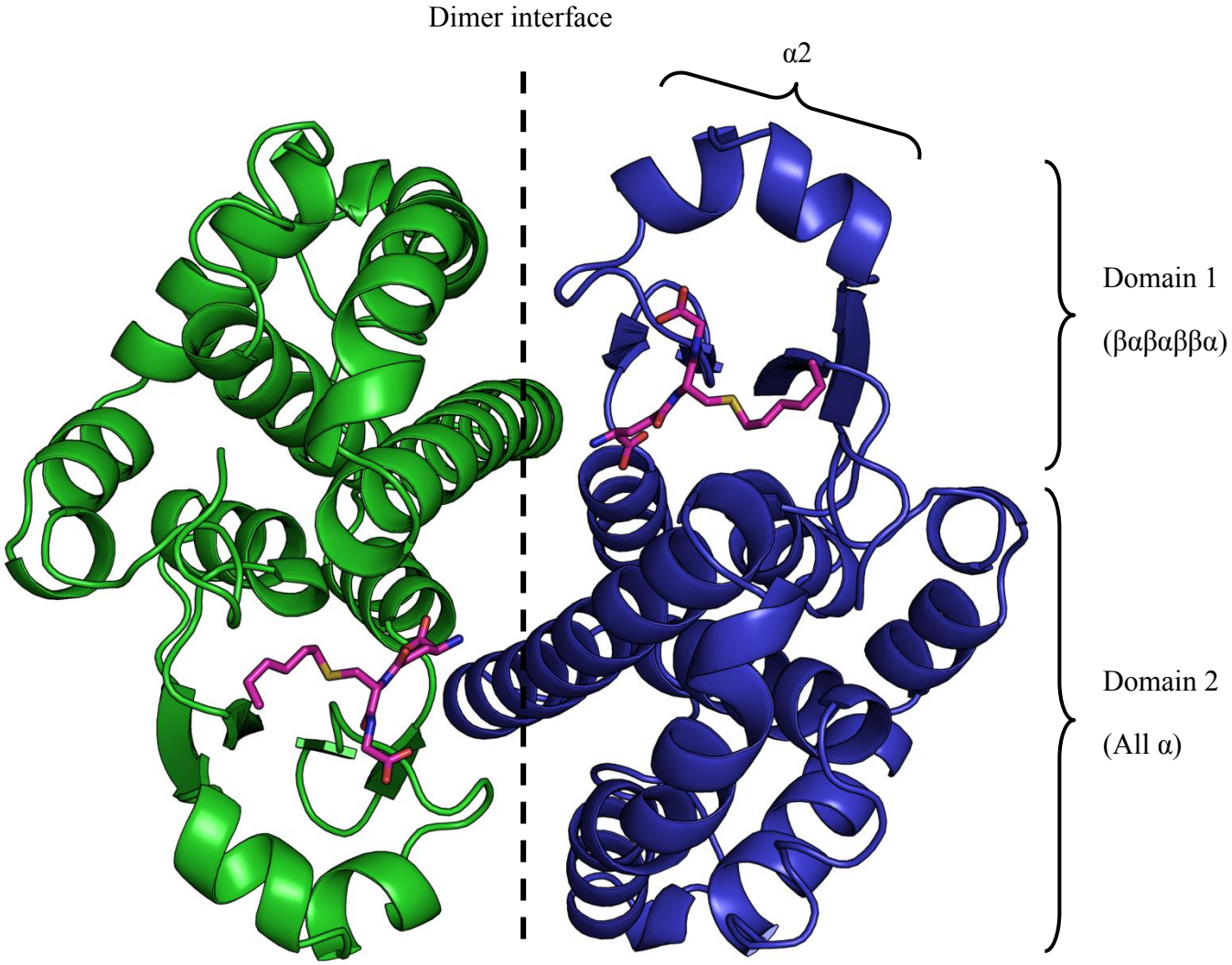

Figure 5. Quaternary structure of hGSTP1-1. The dimer interface, domains 1 and 2 and the active site helix, α2, are indicated. The active site is located by the position of *S*-hexylglutathione (magenta). The image was generated using PyMol (www.pymol.sourceforge.net) from 9GSS [111].

An intriguing structural feature in class pi GST is a highly flexible helix, α2, at the active site. α2 is characterised by high crystallographic B-factors [111] (Figure 6) and is partially disordered in the apo-enzyme at temperatures above 17 °C [112]. The docking of α2 onto the bulk protein appears to be important for catalysis and is the rate-limiting step for the reaction between CDNB and GSH [113].

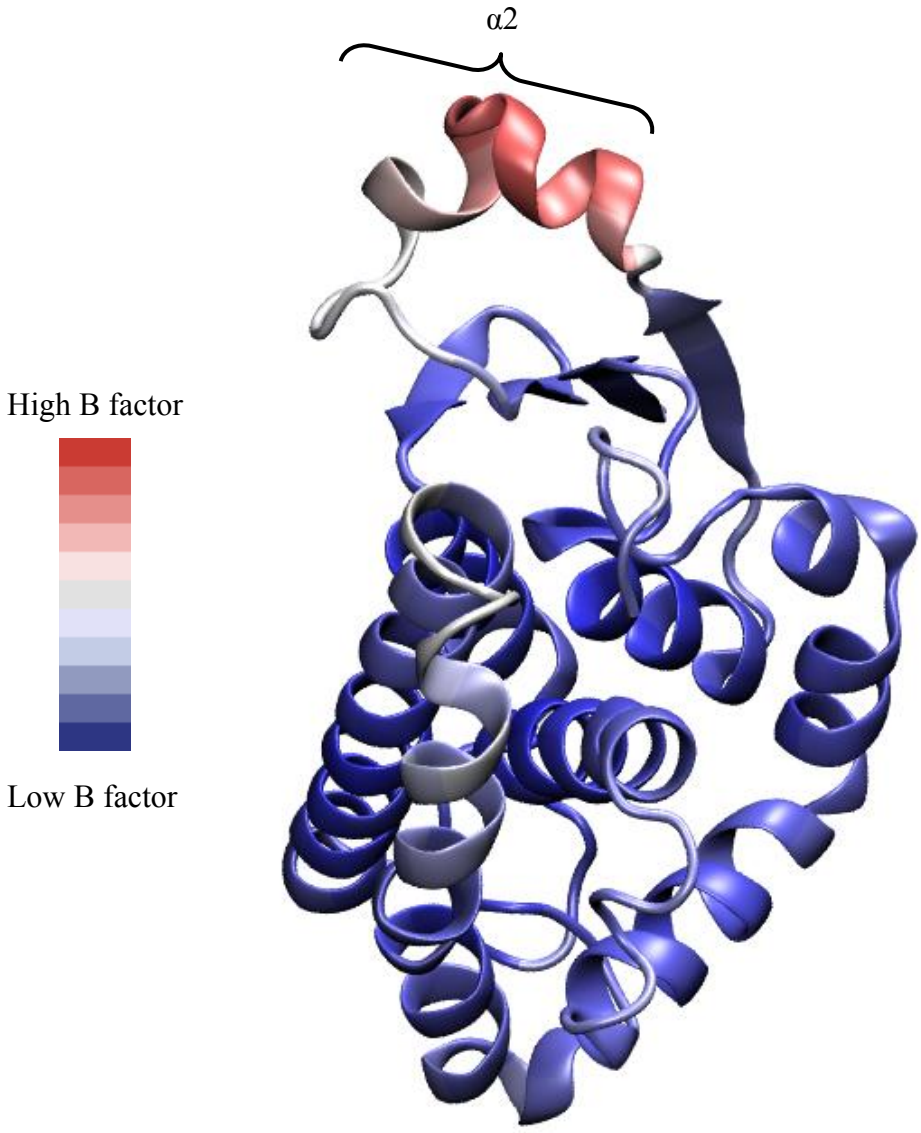

Figure 6. Helix α2 is highly dynamic in crystals of the GSTP1-1 apoenzyme (PDB code: 16GS [111]). Subunit of GSTP1-1 coloured according to B factor, where blue and red denote low and high B factors, respectively. The figure was generated using VMD [114].

Recently, the unfolding of human GSTP1-1 has been mapped in some detail using a combination of equilibrium and kinetic unfolding studies, and multiple spectroscopic probes [115]. GSTP1-1 appears to unfold via a thermodynamically stable intermediate which has native like quaternary structure but an unfolded α2. This intermediate is destabilised and disappears from the unfolding equilibrium when the protein is in complex with glutathione sulfonate (GSO_3^-). GSO_3^- forces the closed conformation of α2 [112], preventing or delaying its unfolding. The unfolding kinetics are more complex, with three resolvable phases: fast, medium and slow [115]. The fast phase appears to correspond to the unfolding of α2. In addition, native state heterogeneity was observed, and attributed to different conformations of folded α2.

Human GSTP1-1 contains four cysteine residues per monomer, at positions 14, 47, 101 and 169 (Figure 7). Cys47 has an unusually low pK_a due to stabilisation of the thiolate anion [116] and is the most reactive of the four cysteine residues [117]. Although Cys47 does not participate directly in catalysis [118], chemical modifications of this residue inactivate the enzyme [119–121]. This is likely due to a perturbation of active site conformation or dynamics [122]. Interestingly, Cys47 is unreactive when the glutathione-binding site of the enzyme is occupied [123]. This is probably a consequence of the ligand-dependent dynamics of α2 [112]: the Cys47 thiol becomes buried in a hydrophobic pocket when α2 is in its closed conformation (Figure 8). Cys47 and Cys101 have also been observed to spontaneously form an unusual long-range intra-subunit disulfide bond *in vitro* [124]. The formation of the disulfide requires extensive rearrangement of α2 [125] and inactivates the enzyme. Of more physiological relevance, GSTP1-1 has been shown to be subject to *S*-glutathionylation *in vivo* [126]. *S*-Glutathionylation at Cys47 and Cys101 causes a small loss of alpha-helical structure and impairs catalytic activity [126], suggesting that cellular GSTP1-1 is regulated by this modification.

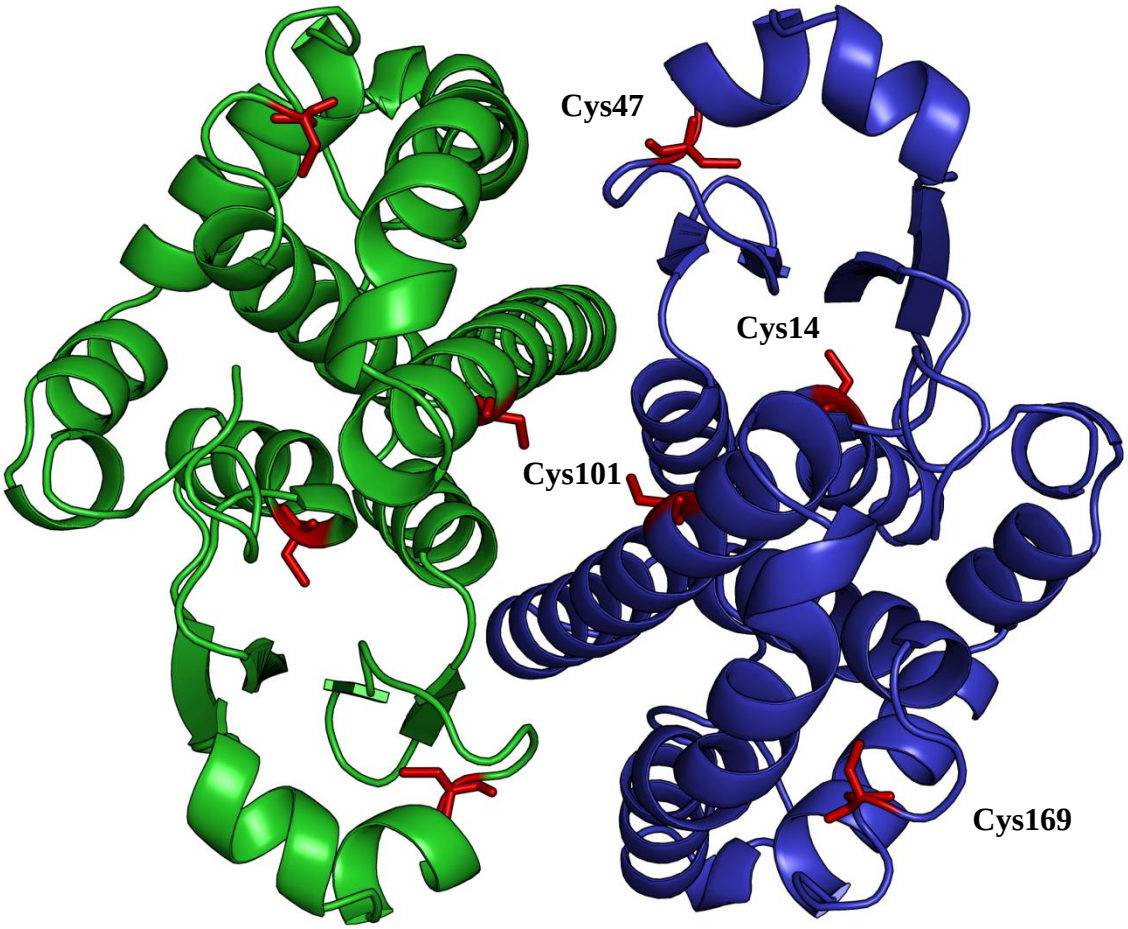

Figure 7. Location of cysteine residues in human GSTP1-1 (PDB code: 9GSS [111]). Cysteines 14, 47, 101 and 169 are coloured red and labelled on one monomer of the homodimer. The image was generated using PyMol (www.pymol.sourceforge.net).

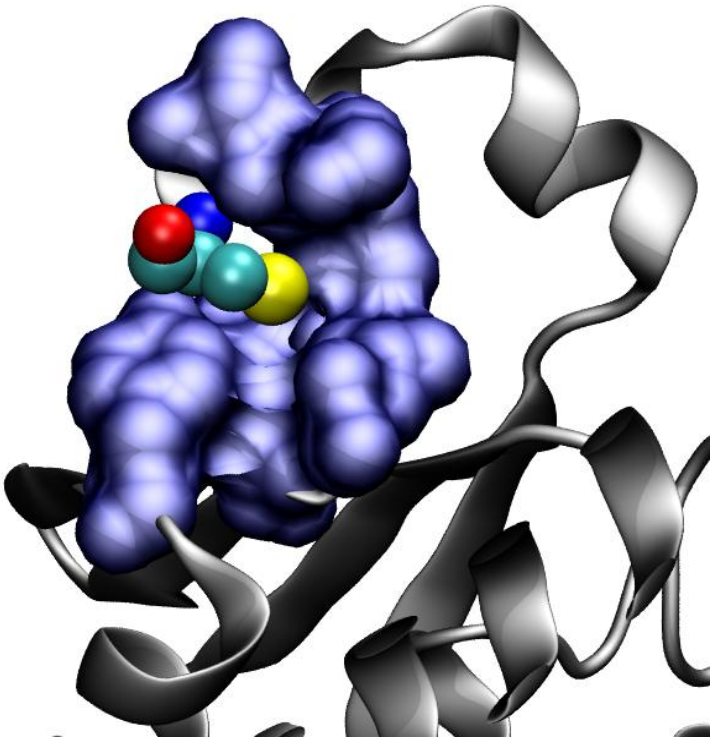

Figure 8. The Cys47 thiol (yellow) is buried in a hydrophobic pocket at the active site of liganded human GSTP1-1 (PDB code: 6GSS [127]). The figure was generated using VMD [114].

1.9 *S*-Nitrosation of glutathione transferase P1-1

S-Nitrosated GSTP1-1 has previously been generated *in vitro* by reaction with GSNO [128,129]. A stoichiometry of three SNOs per protein dimer was observed and a 30 % decrease in enzyme activity was attributed to a higher K_M^{GSH} for *S*-nitrosated GSTP1-1 [128]. The *S*-nitrosation sites were identified by site-directed mutagenesis as Cys47 and Cys101, although only modification at Cys47 affected enzyme activity [128]. Importantly, *S*-nitrosated GSTP1-1 has also been identified *in vivo* in oxidatively stressed cells [130] by mass spectrometry. In two separate studies, either Cys47 [131] or Cys101 [41] of GSTP1-1 were identified as the sites of *S*-nitrosation. Intriguingly, Cys101 was identified as an unusually long-lived protein-SNO, persisting beyond the timescale of the nitrosative stimulus even in the presence of the cellular reducing agent, GSH [41]. The fact that GSTP1-1 is readily *S*-nitrosated *in vitro,* and that the same sites are nitrosated in a physiological context, makes this protein a good model for more detailed *in vitro* studies on protein *S*-nitrosation.

1.10 Objective and aims

Despite its importance in cellular physiology and pathophysiology [30], protein *S*-nitrosation is a poorly understood phenomenon, particularly at a molecular level. The objective of this research was to contribute to a molecular understanding of *S*-nitrosation of GSTP1-1 by 1) deriving a kinetic mechanism for the *S*-nitrosation process and 2) evaluating the consequences to protein activity, stability, structure and dynamics upon *S*-nitrosation.

Specifically, the aims of this research were:

1. Express and purify recombinant GSTP1-1.
2. Generate *S*-nitrosated GSTP1-1 *in vitro.*
3. Determine a minimal mechanism for transnitrosation of GSTP1-1 using site-directed mutagenesis, isothermal titration calorimetry and transient kinetic methods.
4. Probe the structure of *S*-nitrosated GSTP1-1 using spectroscopic techniques.
5. Investigate the unfolding energy landscape of *S*-nitrosated GSTP1-1 using equilibrium and transient kinetic methods.
6. Evaluate the dynamics of *S*-nitrosated GSTP1-1 using hydrogen-deuterium exchange mass spectrometry.

Chapter 2

S-Nitrosation of glutathione transferase P1-1 is controlled by the conformation of a dynamic active site helix

Balchin, D., Wallace, L.A., Dirr, H.W.

J. Biol. Chem. **288**, 14973–14984, 2013

In this publication, a minimal mechanism was derived for the transnitrosation and denitrosation of GSTP1-1.

Author contributions: David Balchin performed all experimental work except the temperature dependence of α2 unfolding (Figure 4C), analysed the data and wrote the manuscript. Louise A. Wallace performed the experiment in Figure 4C. Heini W. Dirr supervised the project and assisted in data analysis and interpretation.

THE JOURNAL OF BIOLOGICAL CHEMISTRY VOL. 288, NO. 21, pp. 14973–14984, May 24, 2013

S-Nitrosation of Glutathione Transferase P1-1 Is Controlled by the Conformation of a Dynamic Active Site Helix*

Received for publication, February 19, 2013, and in revised form, April 2, 2013 Published, JBC Papers in Press, April 9, 2013, DOI 10.1074/jbc.M113.462671

David Balchin, Louise Wallace, and Heini W. Dirr[1]

From the Protein Structure-Function Research Unit, School of Molecular and Cell Biology, University of the Witwatersrand, Johannesburg, South Africa

Background: *S*-Nitrosation is an emerging post-translational modification that is not yet well understood on a molecular level.
Results: We propose a mechanism for *S*-nitrosation of glutathione transferase P1-1 by *S*-nitrosoglutathione.
Conclusion: Cys^{101} is nitrosated in a single step, but Cys^{47} nitrosation is limited by the rate of helix 2 opening.
Significance: Detailing the mechanism of spontaneous transnitrosation is crucial to understanding how protein *S*-nitrosation is controlled.

S*-Nitrosation is a post-translational modification of protein cysteine residues, which occurs in response to cellular oxidative stress. Although it is increasingly being linked to physiologically important processes, the molecular basis for protein regulation by this modification remains poorly understood. We used transient kinetic methods to determine a minimal mechanism for spontaneous *S*-nitrosoglutathione (GSNO)-mediated transnitrosation of human glutathione transferase (GST) P1-1, a major detoxification enzyme and key regulator of cell proliferation. Cys^{47} of GSTP1-1 is *S*-nitrosated in two steps, with the chemical step limited by a pre-equilibrium between the open and closed conformations of helix α2 at the active site. Cys^{101}, in contrast, is *S*-nitrosated in a single step but is subject to negative cooperativity due to steric hindrance at the dimer interface. Despite the presence of a GSNO binding site at the active site of GSTP1-1, isothermal titration calorimetry as well as nitrosation experiments using *S*-nitrosocysteine demonstrate that GSNO binding does not precede *S*-nitrosation of GSTP1-1. Kinetics experiments using the cellular reductant glutathione show that Cys^{101}-NO is substantially more resistant to denitrosation than Cys^{47}-NO, suggesting a potential role for Cys^{101} in long term nitric oxide storage or transfer. These results constitute the first report of the molecular mechanism of spontaneous protein transnitrosation, providing insight into the post-translational control of GSTP1-1 as well as the process of protein transnitrosation in general.

S-Nitrosation is a post-translational modification resulting from the covalent linkage of nitric oxide (NO) to cysteine thiols. The experimentally verified *S*-nitrosoproteome is rapidly increasing (1) and *S*-nitrosation is recognized to control a number of important physiological processes such as vascular homeostasis (2), autophagy (3), the innate immune response (4), and a spectrum of other post-translational modifications (5). Unsurprisingly, dysregulation of protein *S*-nitrosation has been associated with several diseases, including neurodegenerative disorders, various cancers, and diabetes (reviewed in Ref. 6).

S-Nitrosothiols are formed either by the direct, diffusion controlled reaction between the thiyl radical and NO (7) or via the intermediate N_2O_3 (8). Several enzymes have been identified as catalysts of protein *S*-nitrosation reactions (reviewed in Ref. 9). However, the cellular abundance of GSH (10) means that *S*-nitrosoglutathione (GSNO)[2] is the major *S*-nitrosothiol *in vivo* (11) and therefore spontaneous transnitrosation of protein thiols by GSNO is a significant route for protein *S*-nitrosation. In support of this, cellular GSNO appears to be in equilibrium with protein-SNOs, with an increase in GSNO levels leading to increased protein *S*-nitrosation (12). In addition, GSNO treatment causes widespread *S*-nitrosation of yeast proteins (13) and GSNO is commonly used to stimulate *S*-nitrosation of purified protein *in vitro*.

Rates of transnitrosation by GSNO or other NO donors have been measured for small molecule thiols (14), bovine serum albumin (15), hemoglobin (16), and thioredoxin (17). However, the kinetic mechanism of transnitrosation has yet to be reported for any protein. Because protein *S*-nitrosation is largely not under enzymatic control, elucidating possible mechanisms of spontaneous GSNO-mediated transnitrosation is crucial to understanding how *S*-nitrosation is controlled, as well as targeted to specific cysteines.

Human glutathione transferase P1-1 is a well characterized detoxification enzyme that also functions to regulate cell proliferation by inhibiting c-Jun N-terminal kinase (18). GSTP1-1 *S*-nitrosated at cysteines 47 and 101 has previously been discovered *in vivo* (19–21) and produced *in vitro* (22, 23). The modification is highly disruptive, significantly impairing the catalytic activity of the enzyme (22). Here, we establish a minimal mechanism for GSTP1-1 transnitrosation and denitrosation at both

* This work was supported by the University of the Witwatersrand, South African National Research Foundation Grants 60810, 65510, and 68898 and South African Research Chairs Initiative of the Department of Science and Technology and National Research Foundation Grant 64788.
[1] To whom correspondence should be addressed. Tel.: 27-11-717-6352; E-mail: heinrich.dirr@wits.ac.za.

[2] The abbreviations used are: GSNO, *S*-nitrosoglutathione; CysNO, *S*-nitrosocysteine; α2, helix 2 of glutathione transferase P1-1; ITC, isothermal titration calorimetry.

Cys^{47} and Cys^{101}. This model gives new insight into the post-translational control of GSTP1-1 activity, as well as protein transnitrosation reactions in general.

EXPERIMENTAL PROCEDURES

Protein Expression, Purification, and S-Nitrosation—The pET-15b vector encoding N-terminal His_6-tagged GSTP1-1 was a kind gift from S. Y. Blond (Centre for Pharmaceutical Biotechnology, University of Illinois, Chicago, IL). His_6-GSTP1-1 was expressed in *Escherichia coli* T7 cells and purified by Co^{2+} affinity chromatography as described previously (24). C47S, C101S, and C47S/C101S mutant GSTP1-1 were prepared by site-directed mutagenesis and purified identically to the wild-type protein. *S*-Nitrosated GSTP1-1 was prepared by mixing fully reduced protein with a 50-fold molar excess of GSNO or CysNO at 37 °C for 1 h. Excess nitrosating agent was removed by dialysis or buffer exchange. *S*-Nitrosation stoichiometry was determined by UV-difference spectroscopy as described in Ref. 22 based on an S-NO extinction coefficient of 750 M^{-1} cm^{-1} at 330 nm.

Synthesis of GSNO and CysNO—GSNO and CysNO were synthesized as described previously (25) and frozen in aliquots at −80 °C. SNO concentrations were determined by UV absorbance and confirmed after thawing. Solutions were protected from light throughout subsequent experiments to limit photolysis of the S-NO bond (26).

Steady-state Fluorescence—Steady-state fluorescence measurements were performed on a Jasco FP-6300 fluorimeter. Excitation was at 280 nm and emission light was collected at 342 nm. Equilibrium titrations were performed by measuring the fluorescence intensity of 2 μM *S*-nitrosated protein prepared as described above but with varying concentrations of GSNO or CysNO. The fluorescence intensities showed a hyperbolic dependence on reagent concentration, with the exception of the reaction between GSNO and C47S GSTP1-1, which fit better to a Hill equation with $n = -0.5$.

Kinetics Experiments—Kinetics of GSTP1-1 nitrosation or denitrosation were measured by following the change in intrinsic protein fluorescence using an SX-18MV stopped-flow instrument (Applied Photophysics). Excitation was at 280 nm and emission light was collected using a 320-nm long-pass filter. Final protein concentrations were 1 μM and all experiments were performed in 20 mM phosphate buffer with 150 mM NaCl, 2 mM EDTA, and 0.02% NaN_3. At least three traces were recorded and averaged at each ligand concentration. α2 unfolding rates were measured under the same conditions by following the initial increase in protein fluorescence following mixing with 7.5 M urea (27).

Kinetic Data Analysis—Fluorescence transients for C101S or C47S GSTP1-1 nitrosation were fit to a double-exponential function using SigmaPlot version 11.0 or the stopped-flow instrument software. The second exponent was fixed to the k_{obs} value from a single-exponential fit of the fluorescence transient for the reaction of C47S/C101S GSTP1-1 with GSNO. In this way, the kinetics data of the single mutants were corrected for the slow, substoichiometric *S*-nitrosation at the third site. The first exponent from the fits is subsequently reported here as the k_{obs} for Cys^{47} nitrosation (C101S mutant) or Cys^{101} nitrosation (C47S mutant). The quality of the fits was judged by inspection of the residuals.

The data for Cys^{101} nitrosation were fit to Equation 1, for a single-step reaction.

$$k_{obs} = k_{-NO}^{cys\text{-}101} + k_{+NO}^{cys\text{-}101}[GSNO] \quad \text{(Eq. 1)}$$

For *S*-nitrosation at Cys^{47} at all temperatures, the data were fit to Equation 2, for a two-step reaction following a conformational selection mechanism.

$$k_{obs} = \frac{k_{open}}{1 + \frac{k_{closed}}{k_{+NO}^{Cys\text{-}47}[GSNO]}} + \frac{k_{-NO}^{Cys\text{-}47}}{1 + \frac{k_{+NO}^{Cys\text{-}47}[GSNO]}{k_{closed}}} \quad \text{(Eq. 2)}$$

k_{open} and k_{closed} are the forward and reverse rate constants for the pre-nitrosation conformational equilibrium, and $k_{+NO}^{Cys\text{-}47}$ and $k_{-NO}^{Cys\text{-}47}$ are the rate constants for Cys^{47} nitrosation and denitrosation, respectively.

The data for GSH-mediated denitrosation at either Cys^{47}-NO or Cys^{101}-NO were fit to Equation 3, describing a single-step denitrosation dependent on GSH concentration.

$$k_{obs} = k_{+NO} + k_{-NO}^{GSH}[GSH] \quad \text{(Eq. 3)}$$

The temperature dependence of Cys^{47} nitrosation or α2 unfolding was analyzed using an Eyring plot generated from Equation 4 (28).

$$\ln\left(\frac{kh}{k_BT}\right) = \left(-\frac{\Delta H^{\ddagger}}{R}\right)\left(\frac{1}{T}\right) + \frac{\Delta S^{\ddagger}}{R} \quad \text{(Eq. 4)}$$

Where k is the nitrosation rate constant, h is Planck's constant, k_B is the Boltzmann constant, T is absolute temperature, and R is the universal gas constant. $\Delta H^{\ddagger}$ was calculated from the slope of a plot of the left-hand side of Equation 4 against $1/T$. $\Delta S^{\ddagger}$ was determined from Equations 5 and 6.

$$\Delta G^{\ddagger} = -RT\ln\left(\frac{kh}{k_BT}\right) \quad \text{(Eq. 5)}$$

$$\Delta S^{\ddagger} = \frac{\Delta H^{\ddagger} - \Delta G^{\ddagger}}{T} \quad \text{(Eq. 6)}$$

Isothermal Titration Calorimetry—ITC experiments were performed using a MicroCal VP-ITC instrument. 9.4 mM GSNO or 2 mM GSO_3^- in the syringe was injected into the sample cell containing 61.4 μM (C47S/C101S) or 114 μM (C101S) protein in 20 mM phosphate buffer with 150 mM NaCl, 2 mM EDTA, and 0.02% NaN_3. The temperature was kept constant at 37 °C to match the kinetics experiments. Data were analyzed using Origin 7.0 (MicroCal).

RESULTS

GSTP1-1 S-Nitrosation Probed by Tryptophan Fluorescence—GSTP1-1 *S*-nitrosated at cysteines 47 and 101 has previously been discovered *in vivo* (19–21) and produced *in vitro* (22, 23) by reaction with GSNO. Here, we generated a series of cysteine mutants with the aim of examining the kinetics of nitrosation of GSTP1-1 in detail. Reaction of wild-type GSTP1-1 with GSNO or CysNO resulted in *S*-nitrosated protein with a stoichiometry

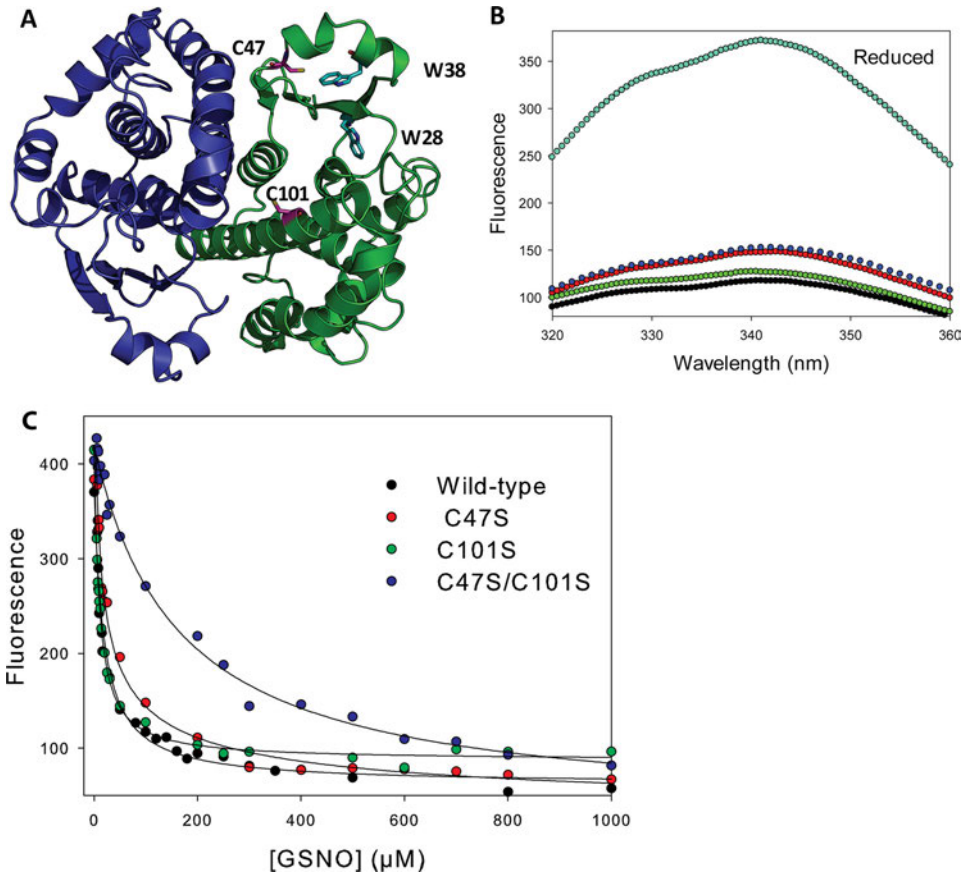

FIGURE 1. **Fluorescence equilibrium titration of cysteine mutants of GSTP1-1 with GSNO.** *A*, representation of dimeric human GSTP1-1 (Protein Data Bank code 6GSS). The sites of nitrosation, Cys^{47} and Cys^{101}, are indicated (*pink*). Trp^{28} and Trp^{38} (*cyan*) are probes of the nitrosation events. *B,* quenching of fluorescence upon reacting 2 μM wild-type and mutant GSTP1-1 with 100 μM GSNO at 37 °C for 1 h. Reduced (*cyan*), wild-type (*black*), C101S (*green*), C47S (*red*), C47S/C101S (*blue*) are indicated (λ_{ex} = 280 nm). *C,* 2 μM protein was titrated with increasing amounts of GSNO and equilibrated for 1 h at 37 °C with λ_{ex} = 280 nm and λ_{em} = 342 nm. The *solid lines* are hyperbolic fits to the data, except for the C47S mutant, where a Hill equation with $n = -0.52$ gave a better fit. K_D values from the fits are reported in Table 1.

of 2 ± 0.1 *S*-nitrosothiols per subunit, consistent with previous reports. Furthermore, mutation of either Cys^{47} or Cys^{101} to serine reduced the number of *S*-nitrosocysteines to 1.2 ± 0.1 per subunit. Surprisingly, we also detected a substoichiometric (0.3 ± 0.1/subunit) *S*-nitrosation of C47S/C101S double mutant GSTP1-1. The identity of the third *S*-nitrosation site (or sites) is unclear, but may represent *S*-nitrosation at another cysteine, or even nitration of tryptophan or tyrosine residues (29). Electrospray ionization-mass spectrometry did not suggest the presence of any additional modifications such as *S*-glutathionylation (data not shown), consistent with the mass spectrometric analysis of Lo Bello *et al.* (22). This alternate nitrosation event is unlikely to be physiologically interesting because it has not been detected *in vivo*, affects only a minor subpopulation of protein and occurs with very slow kinetics (Figs. 1*C* and 2*B*). We therefore corrected all kinetics data for *S*-nitrosation at the alternate site, as described under "Experimental Procedures." In this way, only *S*-nitrosation at Cys^{47} (C101S mutant) or Cys^{101} (C47S mutant) were studied.

Cys^{101}, and Cys^{47} especially, are located close to the two tryptophan residues (Trp^{28} and Trp^{38}) in domain 1 of GSTP1-1 (Fig. 1*A*). These residues provide a convenient probe of *S*-nitrosation, as the modification results in significant quenching of intrinsic protein fluorescence, probably due to FRET between the indole ring and *S*-NO moiety (30) (Fig. 1*B*). Equilibrium fluorescence titrations of wild-type and mutant GSTP1-1 reveal that both Cys^{47} and Cys^{101} are *S*-nitrosated with relatively low affinity (low micromolar K_D values) by either GSNO or CysNO (Fig. 1*C* and Table 1). The equilibrium titration of Cys^{101} with GSNO shows some evidence of negative cooperativity, with the data better described by a Hill equation with $n = -0.5$. This is discussed below with reference to Fig. 6. Consistent with the kinetics data in Fig. 2*B*, the alternate nitrosation site (C47S/C101S mutant) has a K_D 10-fold higher than either of the canonical sites.

The quenching of tryptophan fluorescence upon *S*-nitrosation of GSTP1-1 was used to probe the kinetics of the modification at Cys^{47} and Cys^{101}. Representative transients from mixing 500 μM nitrosating agent with 1 μM protein reveal distinct differences between the rates and amplitudes of nitrosation at Cys^{47} and Cys^{101} (Fig. 2*B*). *S*-Nitrosation at Cys^{47} occurs more rapidly and produces a larger fluorescence change than at Cys^{101}, whereas changing the nitrosation agent to CysNO results in even faster reaction kinetics. To demonstrate that the kinetics of nitrosation of the Cys-mutant GSTP1-1 reliably reports on the reactions of the wild-type protein, the fluorescence transient for wild-type GSTP1-1 mixed with GSNO was fit to a triple-exponential function (Fig. 2*C*). By fixing the three

observed rate constants to the k_{obs} calculated from fits to the C101S, C47S, and C47S/C101S nitrosation transients, respectively, an excellent fit was obtained for the wild-type data. This demonstrates that GSTP1-1 *S*-nitrosation kinetics at different sites can be reliably partitioned by cysteine mutagenesis.

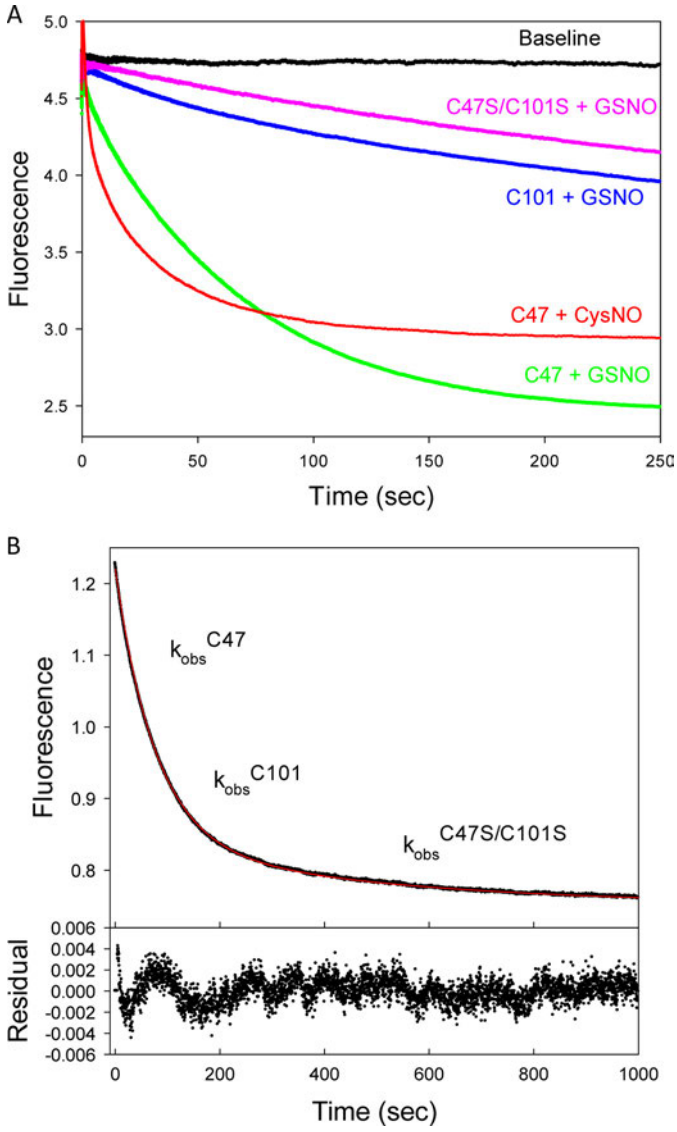

FIGURE 2. **Kinetics of GSTP1-1 nitrosation monitored by intrinsic fluorescence.** *A,* representative transients showing the decrease in fluorescence when 1 μM of different cysteine mutants of GSTP1-1 was mixed with 500 μM nitrosating agent (GSNO or CysNO) at 37 °C. *Curves* were normalized to have the same starting fluorescence. *B, S*-nitrosation of 1 μM wild-type GSTP1-1 with 500 μM GSNO. The data were fit to a triple-exponential function. The residuals show an excellent fit to the data when the three exponential terms are fixed to the observed rate constants for nitrosation at Cys^{47}, Cys^{101}, and the alternate site, respectively, determined from fitting the data in *B*.

S-Nitrosation at Cys^{47} Is Preceded by the Isomerization of Helix α2—To characterize the kinetics of Cys^{47} nitrosation, the concentration dependence of the observed rates at 37 °C were evaluated for both GSNO and CysNO under pseudo-first order conditions (Fig. 3). For both nitrosating agents, the plots appeared hyperbolic, indicating that more than one event contributes to Cys^{47} *S*-nitrosation kinetics. Assuming the simplest case (a two-step mechanism), two common scenarios are consistent with these data: 1) low affinity *S*-nitrosation of Cys^{47} followed by a slow conformational change (induced-fit, rapid equilibrium assumption); or 2) a slow equilibrium between protein conformers, followed by the chemical *S*-nitrosation event (conformational selection) (31). If the induced fit model is correct, then the data should correspond to an increasing hyperbolic function, whatever the relative magnitudes of the rate constants for the first and second steps. A conformational selection mechanism, however, will produce an inverted hyperbolic dependence on ligand concentration if the forward rate constant for the first step becomes smaller than the reverse rate constant for the second step. We therefore sought to discriminate between these two scenarios by following the reaction between GSNO and Cys^{47} of GSTP1-1 at different temperatures, potentially altering the relative magnitudes of the conformational and chemical steps. Fig. 4*A* clearly demonstrates that at 15 °C the concentration dependence of Cys^{47} nitrosation inverts to give a decreasing hyperbolic function. This is strong evidence that the formation of *S*-nitrosated GSTP1-1 is limited by a pre-equilibrium between protein conformers. With reference to Scheme 1, lowering the temperature to 15 °C causes k_{open} to become smaller than $k_{-NO}^{Cys\text{-}47}$, giving the plot in Fig. 4*A*. Above 20 °C, k_{open} is larger than $k_{-NO}^{Cys\text{-}47}$, resulting in an increasing hyperbolic function. The data at all temperatures were therefore fit to Equation 2, derived from Scheme 1. Because the two steps are not independently resolved in the fluorescence transients, only k_{open} (the saturation value) and $k_{-NO}^{Cys\text{-}47}$ (the *y* intercept) can be resolved from these data. Deriving $k_{-NO}^{Cys\text{-}47}$ from the plot in Fig. 3 is error-prone because the *y* intercept is close to 0, so this value was instead determined in an independent experiment (Fig. 7). Kinetic constants for *S*-nitrosation of Cys^{47} at 37 °C are reported in Table 1.

Helix α2, covering the active site of GSTP1-1, is known to be highly dynamic in the apoenzyme (32) and has been linked to the reactivity of Cys^{47} (33). We therefore hypothesize that the conformational equilibrium that precedes chemical modification of Cys^{47} is between the open and closed states of α2 (Fig. 4*D*). When α2 is in its closed conformation, the Cys^{47} thiol is buried in a hydrophobic pocket in domain 1, inaccessible to transnitrosation by GSNO or CysNO. The rate of Cys^{47} nitrosa-

TABLE 1
Kinetic and equilibrium constants for *S*-nitrosation of GSTP1-1 according to Scheme 1

Ligand	Nitrosation site	$k_{open}^{\alpha 2}$	k_{+NO}	k_{-NO}	k_{-NO}^{GSH}	K_D
		s^{-1}	$M^{-1}s^{-1}$	s^{-1}	$M^{-1}s^{-1}$	μM
GSNO	Cys^{47}	0.022 ± 0.001	ND[a]	0.0008 ± 0.0001	46 ± 3	10 ± 0.5
	Cys^{101}	NA	40 ± 3[b]	0.001 ± 0.0002	1.4 ± 0.06	4 ± 4
CysNO	Cys^{47}	0.07 ± 0.02	ND	0.0008 ± 0.0001	NA[c]	8 ± 0.6
	Cys^{101}	NA	100 ± 5	0.001 ± 0.0002	NA	15 ± 2

[a] ND, not determined.
[b] Estimated from fit to linear portion of curve.
[c] NA, not applicable.

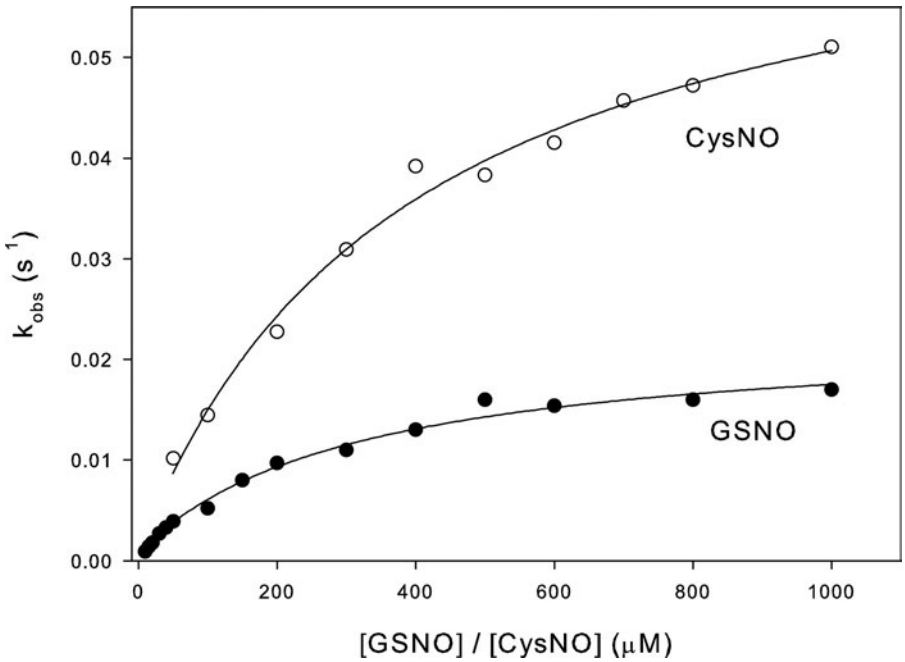

FIGURE 3. **Concentration dependence of the rate of *S*-nitrosation of Cys^{47} reveals a multistep mechanism.** 1 μM C101S GSTP1-1 was mixed with varying concentrations of GSNO (*closed circles*) or CysNO (*open circles*) under pseudo-first order conditions at 37 °C. The primary data were fit to a double exponential function. One exponential term was fixed to the observed nitrosation rate of C47S/C101S GSTP1-1, and the second rate is reported here as k_{obs}, representing the nitrosation of Cys^{47} alone. The data in the figure were fit to Equation 2.

tion would therefore be limited by k_{open}, the rate constant for accessing the open state of α2. Eyring analysis of k_{open} gives $\Delta H^{\ddagger} = 114 \pm 23$ kJ mol^{-1} and $T\Delta S^{\ddagger} = 26 \pm 23$ kJ mol^{-1} (Fig. 4*B*), suggesting a large, entropically favorable conformational change, such as the unfolding of α2. To test this with an independent approach, we examined the temperature dependence of the unfolding of α2 in 7.5 M urea (Fig. 4*C*). At high urea concentrations, α2 unfolding occurs rapidly, before the rest of the protein, and can be measured independently by stopped-flow fluorescence (27). Eyring analysis of the unfolding rate of α2 gives $\Delta H^{\ddagger} = 118 \pm 3$ kJ mol^{-1} and $T\Delta S^{\ddagger} = 50 \pm 3$ kJ mol^{-1}, in excellent agreement with the energetics of k_{open}. These values are also very close to estimates of α2 unfolding enthalpy from NMR (32) and ligand binding (34) experiments. Finally, high glycerol is known to impair GSTP1-1 activity by dampening α2 dynamics (33), and we found that 40% glycerol caused a 10-fold decrease in k_{open} (data not shown). Together, these data constitute strong evidence that *S*-nitrosation of GSTP1-1 at Cys^{47} is limited by an equilibrium between the open and closed conformations of α2.

GSNO binding has been proposed to precede *S*-nitrosation of GSTP1-1 (23). In support of this, GSNO was co-crystallized with GSTP1-1 and was found to bind the active site in essentially the same orientation as GSH (23, 35) (Fig. 5*D*). However, our finding that CysNO can readily nitrosate Cys^{47} of GSTP1-1 (Fig. 3) does not support the idea that GSNO binding necessarily precedes Cys^{47} *S*-nitrosation. To test this further, we examined the interaction of GSNO with GSTP1-1 at 37 °C using isothermal titration calorimetry. Titration of C101S GSTP1-1 with GSNO revealed at least one exothermic event (Fig. 5*C*), consistent with previous reports (23). However, we find no evidence from ITC for GSNO binding to C47S/C101S GSTP1-1 (Fig. 5*A*), with the heats essentially identical to those for GSNO titrated into buffer (Fig. 5*B*). This result does not appear to be due to an alteration of the protein structure by the C47S mutation, as the double mutant retains substantial activity (36) and binds glutathione sulfonate with similar affinity to the wild-type (data not shown), suggesting that the G-site of the protein is intact. The exothermic heats in Fig. 5*A* are too small to be attributed to any significant binding event, but may represent *S*-nitrosation at the third site. After correction for heats of dilution, the data for the interaction of GSNO with C101S GTP1-1 were fit to a model for a single set of binding sites. Accurate values for enthalpy and stoichiometry could not be derived from these data because the interaction was too weak to establish a thermogram pre-transition baseline. However, the K_D, calculated from the slope of the transition, was 14.1 ± 0.8 μM, in good agreement with the K_D determined from fluorescence titration for Cys^{47} nitrosation (Table 1).

S-Nitrosation at Cys^{101} Occurs in a Single Step, Limited by Steric Hindrance at the Dimer Interface—The rate of *S*-nitrosation of Cys^{101}, at the dimer interface of GSTP1-1, was also investigated at 37 °C with increasing concentrations of GSNO or CysNO. Unlike *S*-nitrosation of Cys^{47}, the concentration dependence of the observed rate constants for Cys^{101} nitrosation is qualitatively different for GSNO or CysNO (Fig. 6*A*). The rate of the reaction between Cys^{101} and CysNO shows a linear dependence on CysNO concentration, indicating that *S*-nitrosation occurs in a single step. In contrast, the same plot for Cys^{101} nitrosation by GSNO shows some curvature at high GSNO concentrations. Given that GSNO and CysNO function essentially identically as NO donors in transnitrosation reactions, it is unlikely that they would nitrosate Cys^{101} by substantially different mechanisms. In addition, there is no known GSNO (or GSH) binding site near Cys^{101}, so it is also unlikely that a direct interaction between GSNO and the protein occurs

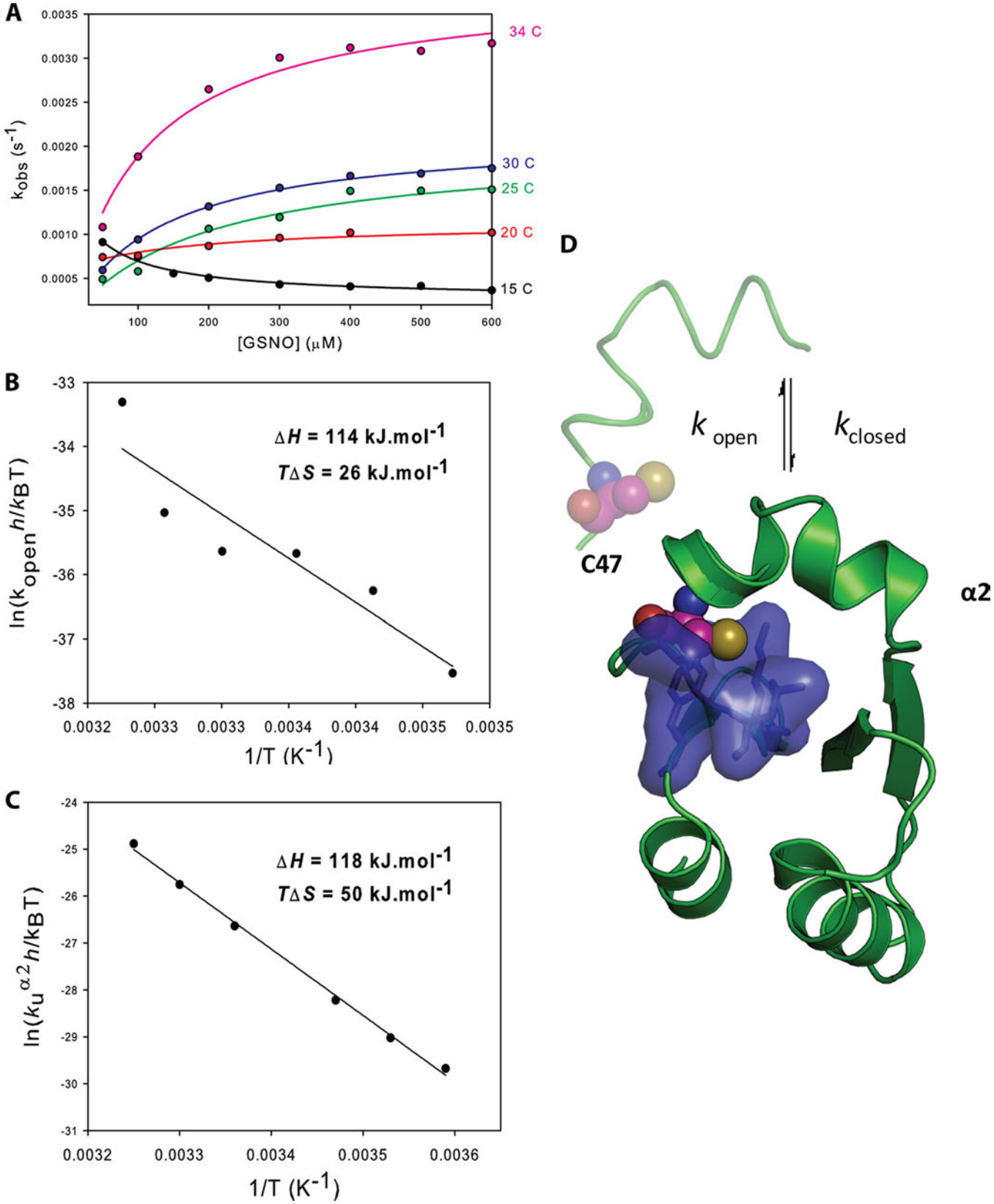

FIGURE 4. **Temperature dependence of Cys^{47} *S*-nitrosation suggests that a conformational equilibrium limits the chemical step.** *A*, the experiment described in the legend to Fig. 3 was repeated at different temperatures, with varying [GSNO] and 1 μM C101S GSTP1-1. The *solid lines* are fits to Equation 4. Values of k_{open} from the fits were analyzed with an Eyring plot (*B*), yielding $\Delta H = 114 \pm 23$ kJ mol^{-1} and $T\Delta S = 26 \pm 23$ kJ mol^{-1}. *C*, the energetics of α2 unfolding were determined independently in an Eyring plot of the temperature dependence of the rate of unfolding of α2 (k_U) in 7.5 M urea, yielding $\Delta H = 118 \pm 3$ kJ mol^{-1} and $T\Delta S = 50 \pm 3$ kJ mol^{-1}. *D*, domain 1 of GSTP1-1. When α2 is closed, the thiol of Cys^{47} is buried in a hydrophobic pocket (*blue surface*) at the active site. *S*-Nitrosation at Cys^{47} requires α2 to be in its open conformation, and is therefore limited by the equilibrium between the open and closed states (k_{closed}/k_{open}).

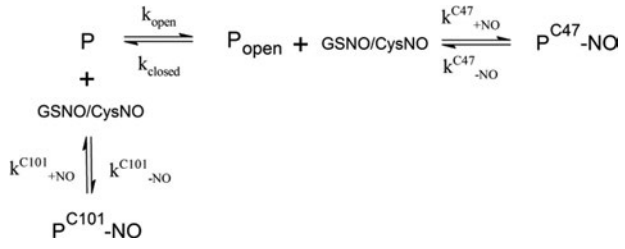

SCHEME 1

before *S*-nitrosation of the cysteine thiol. Instead, we propose that the saturation effect in the plot in Fig. 6*A* is a result of negative cooperativity between Cys^{101} nitrosation sites on each subunit. This interpretation is consistent with the equilibrium titrations in Fig. 1*C*, where Cys^{101} nitrosation fits a Hill equation with $n = -0.5$. The solvent accessible cleft at the dimer interface of GSTP1-1 is relatively narrow, with only 6.5 Å separating the Cys^{101} thiols on each chain. Unless considerable structural rearrangement occurs, this space is insufficient to accommodate two GSNO molecules simultaneously without significant steric clashes. The situation can be visualized in Fig. 6*B*: GSH attached to Cys^{101} on one subunit (analogous to a hypothetical intermediate in the transnitrosation reaction with GSNO) occupies most of the solvent accessible region surrounding Cys^{101} on the adjacent subunit. At high concentrations of GSNO, steric hindrance could plausibly limit the rate of *S*-nitrosation of GSNO, giving the behavior in Fig. 6*A*. CysNO, in contrast, is much smaller than GSNO (Fig. 6*C*) and is therefore unlikely to experience competition for nitrosation sites at the dimer interface, resulting in linear dependence of the nitrosation rate on CysNO concentration. The rate of *S*-nitrosation of Cys^{101} by GSNO or CysNO was calculated from a fit of the data in Fig. 6*A* to Equation 1, for a single step reaction. For the GSNO reaction, $k_{+NO}^{Cys\text{-}101}$ was estimated from the initial linear portion of the curve. All kinetic constants are reported in Table 1.

S-Nitrosated Cys^{101} Is More Resistant Than Cys^{47}-NO to Reduction by GSH—To fully understand signaling by *S*-nitrosation, the mechanism and rates of denitrosation as well as nitrosation must be determined. We measured spontaneous denitrosation rates for GSTP1-1 as well as denitrosation mediated by GSH, the most abundant cellular thiol and therefore the most relevant cellular reducing agent. As with the nitrosation rates, denitrosation rates were corrected for denitrosation at the alternate site (C47S/C101S GSTP1-1). After *S*-nitrosating GSTP1-1 at either Cys^{47} or Cys^{101} by mixing with GSNO at 37 °C, excess GSNO was removed by buffer exchange and spontaneous denitrosation was measured by following the restoration of intrinsic protein fluorescence (Fig. 7*A*). The rate constant for spontaneous denitrosation was essentially the same for Cys^{101}-NO and Cys^{47}-NO, and is reported in Table 1. These rates were likely accelerated by the 280 nm excitation light (26) and are therefore not generally applicable beyond our experimental set-up. Of more interest are the rates of denitrosation in the presence of GSH. In this case, Cys^{101}-NO and Cys^{47}-NO were denitrosated at quite different rates. The linear dependence of the observed denitrosation rate on GSH concentration suggests that both Cys^{47}-NO and Cys^{101}-NO are denitrosated in a single step (Fig. 7*B*). Fitting the data to Equation 3 gives k_{-NO}^{GSH} 30-fold larger for Cys^{47}-NO than Cys^{101}-NO (Table 1), indicating that Cys^{101}-NO is substantially more resistant than Cys^{47}-NO to denitrosation by GSH. To test whether the mechanism of GSH-mediated denitrosation is related to GSH binding to the protein, we also performed denitrosation by DTT (Fig. 7*A*). Although DTT restored protein fluorescence at a much higher rate than GSH, the fluorescence transients were qualitatively similar to those for GSH, and also fit well to a triple exponential function (with two of the rates fixed to the spontaneous denitrosation rate and the rate of denitrosation of C47S/C101S GSTP1-1-NO, respectively).

DISCUSSION

Recently, protein *S*-nitrosation has emerged as an important cellular signaling mechanism, with a broad range of targets (37, 1) and significant implications for human health (6, 4). Unlike other physiologically important post-translational modifications (*e.g.* phosphorylation, glycosylation, and ubiquitination), *S*-nitrosation is largely not under enzymatic control. Instead, the dominant route of protein *S*-nitrosation appears to be transnitrosation by cellular GSNO, which exists in equilibrium with the pool of *S*-nitroso-proteins (12). It is therefore not obvious how *S*-nitrosation is controlled and how specific proteins and cysteines are targeted *in vivo*. Here, we examined in detail the mechanism of transnitrosation of the detoxification enzyme GSTP1-1, with the aim of providing insight into the molecular basis for the specificity and sensitivity of protein *S*-nitrosation. From transient kinetic analyses, we propose a minimal model for *S*-nitrosation of GSTP1-1 at both Cys^{47} and Cys^{101} (Scheme 1).

Cys^{101} is transnitrosated in a single step, whereas *S*-nitrosation at Cys^{47} is limited by a pre-equilibrium between the open and closed states of α2. The mechanism reported here suggests an intricate regulation of GSTP1-1 *S*-nitrosation. Because the rate of opening of helix α2 controls Cys^{47} nitrosation, ligands that bind the G-site and lock α2 into a closed conformation will prevent this residue from being modified. These include GSH, GSSG (oxidized glutathione disulfide), and the dinitrosyl-diglutathionyl-iron complex (38). The latter compound is an NO carrier *in vivo*, suggesting that Cys^{47} *S*-nitrosation can be either stimulated or inhibited depending on whether cellular NO is sequestered as GSNO or the dinitrosyl-diglutathionyl-iron complex. Cys^{101} nitrosation is less complex, occurring in a single step. However, modification of this cysteine is limited by negative cooperativity due to steric hindrance (Fig. 6), mitigating nitrosation at high GSNO. Cys^{101} is therefore nitrosated slowly, but is unusually stable; the rate constant for GSH-mediated denitrosation at Cys^{101}-NO is 30 times smaller than at Cys^{47}-NO (Table 1). This is consistent with a previous study that identified Cys^{101}-NO of GSTP1-1 as an unusually long-lived nitrosation site *in vivo* (19). A possible explanation for this is the limited accessibility of Cys^{101}-NO to GSH due to steric hindrance at the dimer interface (Fig. 6*B*). Consistent with this interpretation, the rate of spontaneous denitrosation was essentially identical for Cys^{47}-NO and Cys^{101}-NO. DTT-mediated denitrosation was qualitatively similar to denitrosation by GSH (Fig. 7*A*), suggesting that GSH binding does not influence

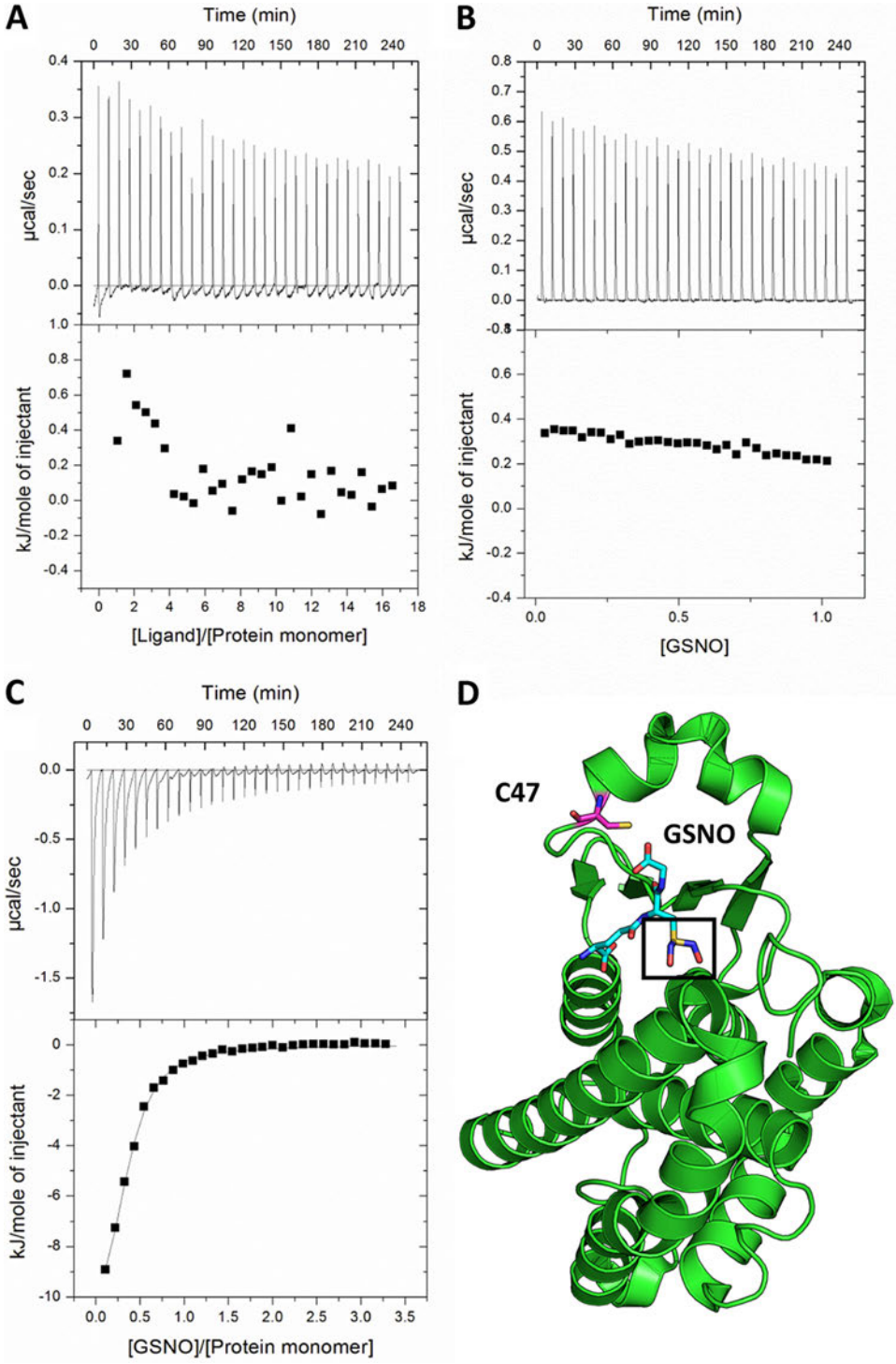

FIGURE 5. **GSNO binding does not precede Cys^{47} *S*-nitrosation.** 9.4 mM GSNO in the ITC syringe was titrated into: *A*, 61.4 μM C47S/C101S GSTP1-1; *B*, buffer; or *C*, 114 μM C101S GSTP1-1. Injection volumes were 5 μl and the temperature was 37 °C for all experiments. The data in *C* was fit to a single-site binding model, giving a K_D of 14 μM. *D*, single subunit of GSTP1-1, showing the binding mode of GSNO and the proximity of the NO moiety (*black box*) to the Cys^{47} thiol (Protein Data Bank code 2A2S).

the process of denitrosation at either site. Instead, GSH seems to be acting simply as a reducing agent.

Several enzymes capable of catalyzing denitrosation reactions have been identified (39). However, given the high cellular concentration of GSH and the lability of the *S*-nitrosothiols, spontaneous GSH-mediated denitrosation is likely highly significant physiologically. Physiological GSH concentrations can reach 1 to 10 mM (10). Based on the rate constants we report here (Table 1), Cys^{47}-NO of GSTP1-1 would be denitrosated at a rate of 0.05–0.5 s^{-1}, whereas Cys^{101}-NO would be denitrosated at 0.001–0.01 s^{-1}. This compares to nitrosation rates at physiological GSNO concentrations (1–5 μM (11)) of 0.0002 s^{-1} at Cys^{101} and 0.02 s^{-1} at Cys^{47} (k_{open}), indicating that nitrosation of GSTP1-1 is disfavored at high GSH concentrations.

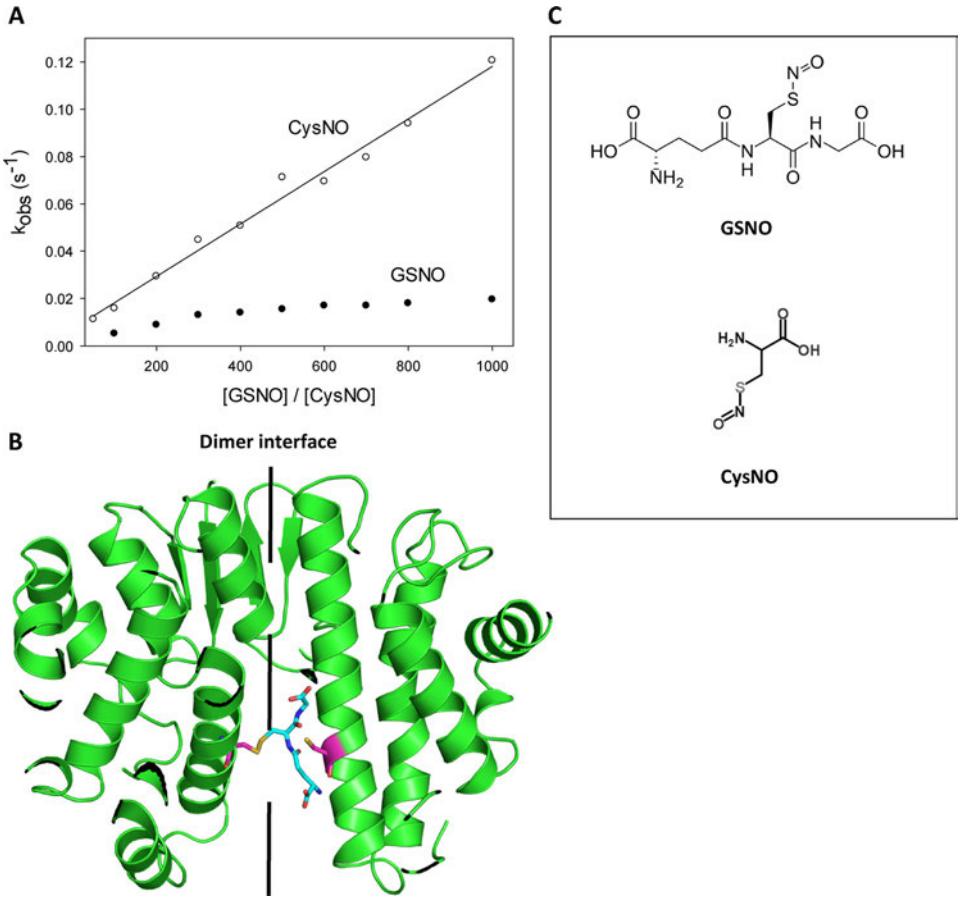

FIGURE 6. **Cys[101] nitrosation kinetics.** *A*, 1 μM C47S GSTP1-1 was mixed with varying concentrations of GSNO (*closed circles*) or CysNO (*open circles*) under pseudo-first order conditions at 37 °C. The primary data were fit to a double exponential function. One exponential term was fixed to the observed nitrosation rate of C47S/C101S GSTP1-1, and the second rate is reported here as k_{obs}, representing the nitrosation of Cys[101] alone. The data for the CysNO reaction correspond to a one-step mechanism and were fit to Equation 1. Rate constants are reported in Table 1. The rate of the GSNO reaction appears to saturate at high [GSNO], which is likely due to steric hindrance at the dimer interface, visualized in *B*. *B*, model of GSTP1-1 (Protein Data Bank code 6GSS) showing GSH (*cyan*) attached to Cys[101] (*pink*) on one subunit in a hypothetical transnitrosation reaction. It is apparent that a second GSNO molecule is not readily accommodated at the dimer interface, resulting in negative cooperativity for *S*-nitrosation of Cys[101] on the adjacent subunit. *C*, structures of GSNO and CysNO.

The rates reported here are consistent with those determined previously for L-cysteine (14), bovine serum albumin, and hemoglobin (15) and show that spontaneous protein transnitrosation by GSNO is generally not a rapid signaling mechanism. It is, however, clearly relevant to the function of many proteins, and can be regulated by a combination of ligand binding and the relative concentrations of GSNO and GSH.

S-Nitrosation of Cys[47] significantly perturbs the detoxification activity of GSTP1-1 (22). Because Cys[47] does not directly participate in catalysis (40), this is likely due to a disruption of the structure or dynamics of the active site. Nitrosation of Cys[101] does not substantially affect the enzymatic function of the protein (22). Cys[101] nitrosation may, however, affect the ability of GSTP1-1 to bind JNK (18) or peroxiredoxin (41). The unusual persistence of Cys[101]-NO *in vivo* also raises the possibility that this residue acts as a NO storage site or a shuttle for NO in protein-protein transnitrosation reactions.

The mechanism of *S*-nitrosation of GSTP1-1 provides some insight into *S*-nitrosation specificity. Although there is no clear consensus as to what constitutes an "*S*-nitrosation motif," two recent structure-based analyses suggest a distant (within 8 Å) acid-base motif with exposed charged groups (42, 43). Cys[101] of GSTP1-1 is not proximal to any obvious acid-base motif, but instead is distinguished from the three other cysteines on each chain of the protein by its high solvent accessibility. This factor is also important for Cys[47] nitrosation: Cys[47] is modified only when α2 is open and the thiol is solvent accessible. Lys[44] has been proposed to enhance the reactivity of Cys[47] by stabilizing the cysteine thiolate (44), and has also been identified as a relevant nitrosation motif for GSTP1-1 in dbSNO, a database of nitrosation sites (1). However, because the α2 equilibrium limits its nitrosation at Cys[47], its low pK_a does not ultimately determine its reactivity. Eyring analysis in Fig. 4 reveals that activation enthalpy of k_{open} is essentially identical to the activation enthalpy for α2 unfolding in high urea. This suggests that α2 is unfolded or disordered in the open state, consistent with NMR data (32) and the lack of clear electron density for α2 in crystal structures of apo-GSTP1-1 (45). This further implies that, whereas the tertiary protein structure may be important for regulating the solvent accessibility of *S*-nitrosated cysteines, significant tertiary or even secondary structures are not necessary for *S*-nitrosation to occur. A similar association between intrinsic disorder and susceptibility to post-translational modifications has been observed for several proteins, including p53 (46) and histone tails (47). The ability of GSNO to dock to a site near the target cysteine residue has also been suggested as an

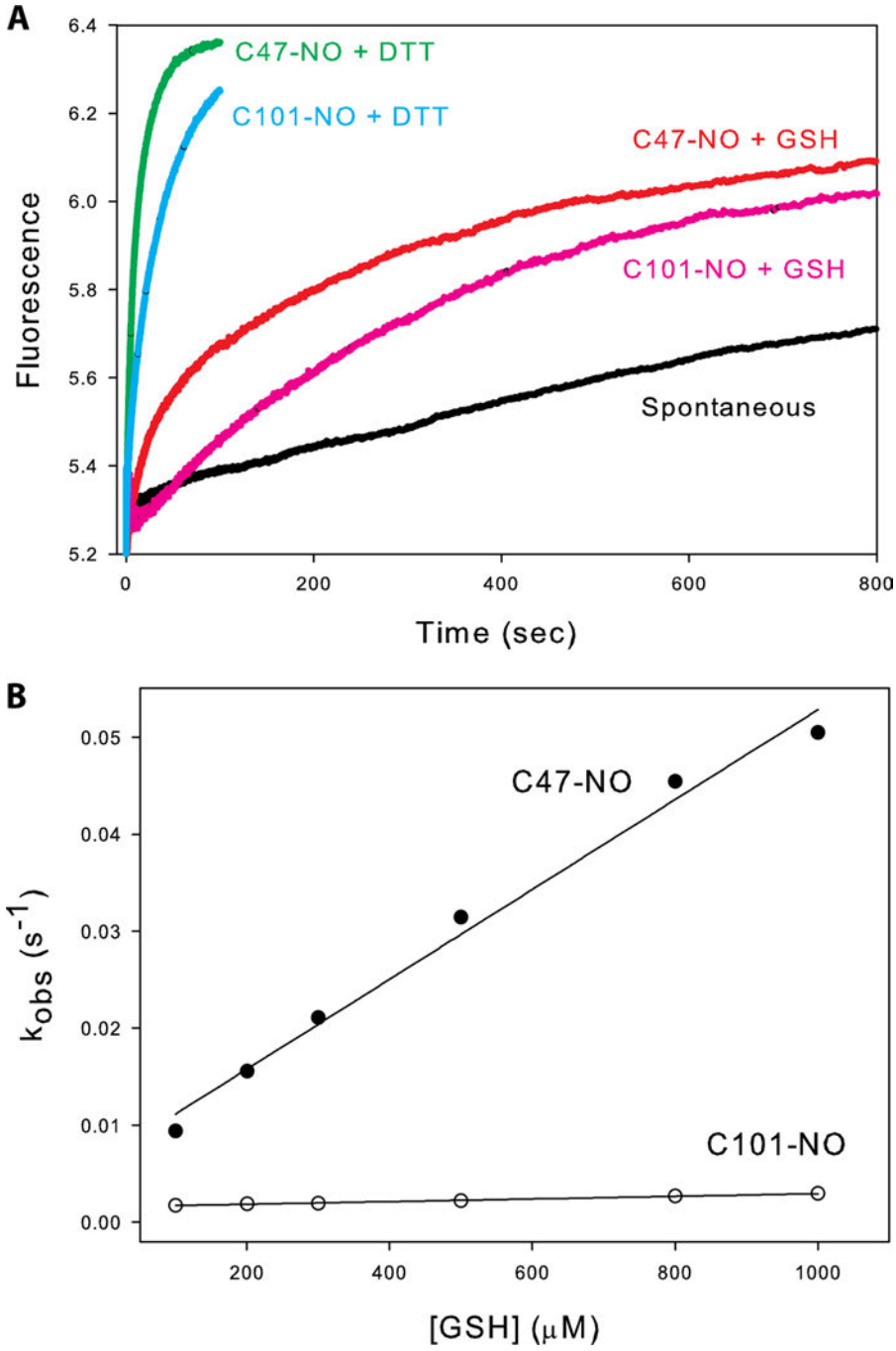

FIGURE 7. **Denitrosation of GSTP1-1-NO.** *A*, *S*-nitrosated cysteine mutants of GSTP1-1 (μM) were prepared as described under "Experimental Procedures" and denitrosated using 1 mM GSH or DTT at 37 °C, causing an increase in intrinsic protein fluorescence. Observed rate constants for Cys^{47} (*closed circles*) or Cys^{101} (*open circles*) denitrosation with GSH were determined by fitting the primary data to a triple exponential function. Two of the exponents were fixed to the spontaneous denitrosation rate and the rate of denitrosation of C47S/C101S GSTP1-1, respectively, and the third rate is reported here as k_{obs}, representing the rate of GSH-mediated denitrosation of Cys^{47} or Cys^{101} alone. The GSH concentration dependence of these rates is shown in *B* and the *solid line* is a fit to Equation 3.

important criterion for *S*-nitrosation specificity (43), and this has been demonstrated for several proteins (4, 48). GSNO has been co-crystallized with GSTP1-1, prompting the proposal that GSNO binding precedes Cys^{47} nitrosation (23). However, close analysis of the binding mode of GSNO does not support this proposal. Unsurprisingly, GSNO binds GSTP1-1 identically to GSH, which positions the NO group of GSNO distant from the Cys^{47} thiol (Fig. 5*D*). To transfer the NO group to Cys^{47}, GSNO would have to undergo an energetically costly reorientation that would locate the GS^- moiety at an unprecedented binding site. We therefore propose that, even if GSNO does bind GSTP1-1, this is not a precursor for *S*-nitrosation at Cys^{47}. Consistent with this, CysNO (which has no known binding site on GSTP1-1) is able to *S*-nitrosate Cys^{47} with similar kinetics to GSNO (Fig. 3). Furthermore, our ITC experiments indicate that GSNO does not bind to GSTP1-1 with significant affinity (Fig. 5). Titrating C101S GSTP1-1 with GSNO resulted in larger exothermic events (Fig. 5*C*), which were attributed to

GSNO binding by Téllez-Sanz *et al.* (23). In light of our results, these heats are more plausibly attributed to the *S*-nitrosation of Cys^{47} as well as any associated protein conformational changes. Consistent with this interpretation, the K_D determined from ITC was very similar to the K_D from the fluorescence titration (Table 1), which is not contributed to by GSNO binding (GSNO was removed by dialysis after *S*-nitrosation in the fluorescence experiments). Notably, the rate constant for the opening of $\alpha 2$, k_{open}, is three times lower when GSNO rather than CysNO is used as the nitrosating agent (Table 1). A possible explanation for this is that GSH, produced when GSNO donates NO to the protein, binds to the active site and reduces the apparent k_{open} by biasing the closed state of $\alpha 2$.

In this study, we present the mechanism of transnitrosation of GSTP1-1, a detoxification enzyme and key regulator of cell proliferation through the JNK pathway. The mechanism we report here is significant to understanding how this protein is regulated by spontaneous *S*-nitrosation, and also provides more general insights into the *S*-nitrosation of other proteins. Detailed mechanistic studies of *S*-nitrosation such as this one are vital to understanding how protein transnitrosation by small molecules is controlled and targeted.

REFERENCES

1. Lee, T.-Y., Chen, Y.-J., Lu, C.-T., Ching, W.-C., Teng, Y.-C., Huang, H.-D., and Chen, Y.-J. (2012) dbSNO. A database of cysteine *S*-nitrosylation. *Bioinformatics* **28,** 2293–2295
2. Liu, L., Yan, Y., Zeng, M., Zhang, J., Hanes, M. A., Ahearn, G., McMahon, T. J., Dickfeld, T., Marshall, H. E., Que, L. G., and Stamler, J. S. (2004) Essential roles of *S*-nitrosothiols in vascular homeostasis and endotoxic shock. *Cell* **116,** 617–628
3. Sarkar, S., Korolchuk, V. I., Renna, M., Imarisio, S., Fleming, A., Williams, A., Garcia-Arencibia, M., Rose, C., Luo, S., Underwood, B. R., Kroemer, G., O'Kane, C. J., and Rubinsztein, D. C. (2011) Complex inhibitory effects of nitric oxide on autophagy. *Mol. Cell* **43,** 19–32
4. Savidge, T. C., Urvil, P., Oezguen, N., Ali, K., Choudhury, A., Acharya, V., Pinchuk, I., Torres, A. G., English, R. D., Wiktorowicz, J. E., Loeffelholz, M., Kumar, R., Shi, L., Nie, W., Braun, W., Herman, B., Hausladen, A., Feng, H., Stamler, J. S., and Pothoulakis, C. (2011) Host *S*-nitrosylation inhibits clostridial small molecule-activated glucosylating toxins. *Nat. Med.* **17,** 1136–1141
5. Hess, D. T., and Stamler, J. S. (2012) Regulation by *S*-nitrosylation of protein posttranslational modification. *J. Biol. Chem.* **287,** 4411–4418
6. Foster, M. W., Hess, D. T., and Stamler, J. S. (2009) Protein *S*-nitrosylation in health and disease. A current perspective. *Trends Mol. Med.* **15,** 391–404
7. Madej, E., Folkes, L. K., Wardman, P., Czapski, G., and Goldstein, S. (2008) Thiyl radicals react with nitric oxide to form *S*-nitrosothiols with rate constants near the diffusion-controlled limit. *Free Radic. Biol. Med.* **44,** 2013–2018
8. Goldstein, S., and Czapski, G. (1996) Mechanism of the nitrosation of thiols and amines by oxygenated NO solutions. The nature of the nitrosating intermediates. *J. Am. Chem. Soc.* **118,** 3419–3425
9. Anand, P., and Stamler, J. S. (2012) Enzymatic mechanisms regulating protein *S*-nitrosylation. Implications in health and disease. *J. Mol. Med.* **90,** 233–244
10. Yap, L.-P., Sancheti, H., Ybanez, M. D., Garcia, J., Cadenas, E., and Han, D. (2010) Determination of GSH, GSSG, and GSNO using HPLC with electrochemical detection. *Methods Enzymol.* **473,** 137–147
11. Gaston, B. (1993) Endogenous nitrogen oxides and bronchodilator *S*-nitrosothiols in human airways. *Proc. Natl. Acad. Sci. U.S.A.* **90,** 10957–10961
12. Liu, L., Hausladen, A., Zeng, M., Que, L., Heitman, J., and Stamler, J. S. (2001) A metabolic enzyme for *S*-nitrosothiol conserved from bacteria to humans. *Nature* **410,** 490–494
13. Foster, M. W., Forrester, M. T., and Stamler, J. S. (2009) A protein microarray-based analysis of *S*-nitrosylation. *Proc. Natl. Acad. Sci. U.S.A.* **106,** 18948–18953
14. Hogg, N. (1999) The kinetics of *S*-transnitrosation. A reversible second-order reaction. *Anal. Biochem.* **272,** 257–262
15. Rossi, R., Lusini, L., Giannerini, F., Giustarini, D., Lungarella, G., and Di Simplicio, P. (1997) A method to study kinetics of transnitrosation with nitrosoglutathione. Reactions with hemoglobin and other thiols. *Anal. Biochem.* **254,** 215–220
16. Patel, R. P., Hogg, N., Spencer, N. Y., Kalyanaraman, B., Matalon, S., and Darley-Usmar, V. M. (1999) Biochemical characterization of human *S*-nitrosohemoglobin. *J. Biol. Chem.* **274,** 15487–15492
17. Barglow, K. T., Knutson, C. G., Wishnok, J. S., Tannenbaum, S. R., and Marletta, M. A. (2011) Site-specific and redox-controlled *S*-nitrosation of thioredoxin. *Proc. Natl. Acad. Sci. U.S.A.* **108,** E600–E606
18. Adler, V., Yin, Z., Fuchs, S. Y., Benezra, M., Rosario, L., Tew, K. D., Pincus, M. R., Sardana, M., Henderson, C. J., Wolf, C. R., Davis, R. J., and Ronai, Z. (1999) Regulation of JNK signaling by GSTp. *EMBO J.* **18,** 1321–1334
19. Paige, J. S., Xu, G., Stancevic, B., and Jaffrey, S. R. (2008) Nitrosothiol reactivity profiling identifies *S*-nitrosylated proteins with unexpected stability. *Chem. Biol.* **15,** 1307–1316
20. Beltrán, B., Orsi, A., Clementi, E., and Moncada, S. (2000) Oxidative stress and *S*-nitrosylation of proteins in cells. *Br. J. Pharmacol.* **129,** 953–960
21. Sinha, V., Wijewickrama, G. T., Chandrasena, R. E., Xu, H., Edirisinghe, P. D., Schiefer, I. T., and Thatcher, G. R. (2010) Proteomic and mass spectroscopic quantitation of protein *S*-nitrosation differentiates NO-donors. *ACS Chem. Biol.* **5,** 667–680
22. Lo Bello, M., Nuccetelli, M., Caccuri, A. M., Stella, L., Parker, M. W., Rossjohn, J., McKinstry, W. J., Mozzi, A. F., Federici, G., Polizio, F., Pedersen, J. Z., and Ricci, G. (2001) Human glutathione transferase P1-1 and nitric oxide carriers. A new role for an old enzyme. *J. Biol. Chem.* **276,** 42138–42145
23. Téllez-Sanz, R., Cesareo, E., Nuccetelli, M., Aguilera, A. M., Barón, C., Parker, L. J., Adams, J. J., Morton, C. J., Lo Bello, M., Parker, M. W., and García-Fuentes, L. (2006) Calorimetric and structural studies of the nitric oxide carrier *S*-nitrosoglutathione bound to human glutathione transferase P1-1. *Protein Sci.* **15,** 1093–1105
24. Chang, M., Bolton, J. L., and Blond, S. Y. (1999) Expression and purification of hexahistidine-tagged human glutathione *S*-transferase P1-1 in *Escherichia coli*. *Protein Expr. Purif.* **17,** 443–448
25. Hart, T. W. (1985) Some observations concerning the *S*-nitroso and *S*-phenylsulphonyl derivatives of L-cysteine and glutathione. *Tetrahedron Lett.* **26,** 2013–2016
26. Sexton, D. J., Muruganandam, A., McKenney, D. J., and Mutus, B. (1994) Visible light photochemical release of nitric oxide from *S*-nitrosoglutathione. *Photochem. Photobiol.* **59,** 463–467
27. Gildenhuys, S., Wallace, L. A., Burke, J. P., Balchin, D., Sayed, Y., and Dirr, H. W. (2010) Class Pi glutathione transferase unfolds via a dimeric and not monomeric intermediate. Functional implications for an unstable monomer. *Biochemistry* **49,** 5074–5081
28. Werbeck, N. D., Kellner, J. N., Barends, T. R., and Reinstein, J. (2009) Nucleotide binding and allosteric modulation of the second AAA^+ domain of ClpB probed by transient kinetic studies. *Biochemistry* **48,** 7240–7250
29. Nuriel, T., Hansler, A., and Gross, S. S. (2011) Protein nitrotryptophan. Formation, significance and identification. *J. Proteomics* **74,** 2300–2312
30. Chen, X., Wen, Z., Xian, M., Wang, K., Ramachandran, N., Tang, X., Schlegel, H. B., Mutus, B., and Wang, P. G. (2001) Fluorophore-labeled *S*-nitrosothiols. *J. Org. Chem.* **66,** 6064–6073
31. Vogt, A. D., and Di Cera, E. (2012) Conformational selection or induced-fit? A critical appraisal of the kinetic mechanism. *Biochemistry* **51,** 5894–5902
32. Hitchens, T. K., Mannervik, B., and Rule, G. S. (2001) Disorder-to-order transition of the active site of human class Pi glutathione transferase, GST P1-1. *Biochemistry* **40,** 11660–11669
33. Ricci, G., Caccuri, A. M., Lo Bello, M., Rosato, N., Mei, G., Nicotra, M., Chiessi, E., Mazzetti, A. P., and Federici, G. (1996) Structural flexibility

modulates the activity of human glutathione transferase P1-1. *J. Biol. Chem.* **271,** 16187–16192
34. Caccuri, A. M., Antonini, G., Ascenzi, P., Nicotra, M., Nuccetelli, M., Mazzetti, A. P., Federici, G., Lo Bello, M., and Ricci, G. (1999) Temperature adaptation of glutathione *S*-transferase P1-1. *J. Biol. Chem.* **274,** 19276–19280
35. Oakley, A. J., Lo Bello, M., Battistoni, A., Ricci, G., Rossjohn, J., Villar, H. O., and Parker, M. W. (1997) The structures of human glutathione transferase P1-1 in complex with glutathione and various inhibitors at high resolution. *J. Mol. Biol.* **274,** 84–100
36. Ricci, G., Lo Bello, M., Caccurri, A. M., Pastore, A., Nuccetelli, M., Parker, M. W., and Federici, G. (1995) Site-directed mutagenesis of human glutathione transferase P1-1. *J. Biol. Chem.* **270,** 1243–1248
37. Seth, D., and Stamler, J. S. (2011) The SNO-proteome. Causation and classifications. *Curr. Opin. Chem. Biol.* **15,** 129–136
38. De Maria, F., Pedersen, J. Z., Caccuri, A. M., Antonini, G., Turella, P., Stella, L., Lo Bello, M., Federici, G., and Ricci, G. (2003) The specific interaction of dinitrosyl-diglutathionyl-iron complex, a natural NO carrier, with the glutathione transferase superfamily. Suggestion for an evolutionary pressure in the direction of the storage of nitric oxide. *J. Biol. Chem.* **278,** 42283–42293
39. Benhar, M., Forrester, M. T., and Stamler, J. S. (2009) Protein denitrosylation. Enzymatic mechanisms and cellular functions. *Nat. Rev. Mol. Cell. Biol.* **10,** 721–732
40. Kong, K.-H., Inoue, H., and Takahashi, K. (1991) Non-essentiality of cysteine and histidine residues for the activity of human class Pi glutathione *S*-transferase. *Biochem. Biophys. Res. Commun.* **181,** 748–755
41. Ralat, L. A., Misquitta, S. A., Manevich, Y., Fisher, A. B., and Colman, R. F. (2008) Characterization of the complex of glutathione *S*-transferase π and 1-cysteine peroxiredoxin. *Arch. Biochem. Biophys.* **474,** 109–118
42. Doulias, P. T., Greene, J. L., Greco, T. M., Tenopoulou, M., Seeholzer, S. H., Dunbrack, R. L., and Ischiropoulos, H. (2010) Structural profiling of endogenous S-nitrosocysteine residues reveals unique features that accommodate diverse mechanisms for protein *S*-nitrosylation. *Proc. Natl. Acad. Sci. U.S.A.* **107,** 16958–16963
43. Marino, S. M., and Gladyshev, V. N. (2010) Structural analysis of cysteine *S*-nitrosylation. A modified acid-based motif and the emerging role of trans-nitrosylation. *J. Mol. Biol.* **395,** 844–859
44. Lo Bello, M., Parker, M. W., Desideri, A., Polticelli, F., Falconi, M., Del Boccio, G., Pennelli, A., Federici, G., and Ricci, G. (1993) Peculiar spectroscopic and kinetic properties of Cys-47 in human placental glutathione transferase. Evidence for an atypical thiolate ion pair near the active site. *J. Biol. Chem.* **268,** 19033–19038
45. Oakley, A. J., Lo Bello, M., Ricci, G., Federici, G., and Parker, M. W. (1998) Evidence for an induced-fit mechanism operating in π class glutathione transferases. *Biochemistry* **37,** 9912–9917
46. Bell, S., Klein, C., Müller, L., Hansen, S., and Buchner, J. (2002) p53 contains large unstructured regions in its native state. *J. Mol. Biol.* **322,** 917–927
47. Jenuwein, T., and Allis, C. D. (2001) Translating the histone code. *Science* **293,** 1074–1080
48. Kim, S. O., Merchant, K., Nudelman, R., Beyer, W. F., Jr., Keng, T., DeAngelo, J., Hausladen, A., and Stamler, J. S. (2002) OxyR. A molecular code for redox-related signaling. *Cell* **109,** 383–396

Chapter 3

S-Nitrosation destabilises glutathione transferase P1-1

Balchin, D., Stoyan H. Stoychev and Dirr, H.W.

Biochemistry, 2013 **DOI:** 10.1021/bi401414c

In this publication, the consequences of *S*-nitrosation to the activity, structure, stability and dynamics of GSTP1-1 were determined.

Author contributions: David Balchin performed all experiments, analysed the data and wrote the manuscript. Stoyan S. Stoychev assisted with the DXMS experiments. Heini W. Dirr supervised the project and assisted in data analysis and interpretation.

BIOCHEMISTRY
including biophysical chemistry & molecular biology

Article

pubs.acs.org/biochemistry

S-Nitrosation Destabilizes Glutathione Transferase P1-1

David Balchin,[†] Stoyan H. Stoychev,[‡] and Heini W. Dirr*[,†]

[†]Protein Structure-Function Research Unit, School of Molecular and Cell Biology, University of the Witwatersrand, Johannesburg, South Africa

[‡]CSIR Biosciences, Pretoria, South Africa

Supporting Information

ABSTRACT: Protein *S*-nitrosation is a post-translational modification that regulates the function of more than 500 human proteins. Despite its apparent physiological significance, *S*-nitrosation is poorly understood at a molecular level. Here, we investigated the effect of *S*-nitrosation on the activity, structure, stability, and dynamics of human glutathione transferase P1-1 (GSTP1-1), an important detoxification enzyme ubiquitous in aerobes. *S*-Nitrosation at Cys47 and Cys101 reduces the activity of the enzyme by 94%. Circular dichroism spectroscopy, acrylamide quenching, and amide hydrogen−deuterium exchange mass spectrometry experiments indicate that the loss of activity is caused by the introduction of local disorder at the active site of GSTP1-1. Furthermore, the modification destabilizes domain 1 of GSTP1-1 against denaturation, smoothing the unfolding energy landscape of the protein and introducing a refolding defect. In contrast, *S*-nitrosation at Cys101 alone introduces a refolding defect in domain 1 but compensates by stabilizing the domain kinetically. These data elucidate the physical basis for the regulation of GSTP1-1 by *S*-nitrosation and provide general insight into the consequences of *S*-nitrosation on protein stability and dynamics.

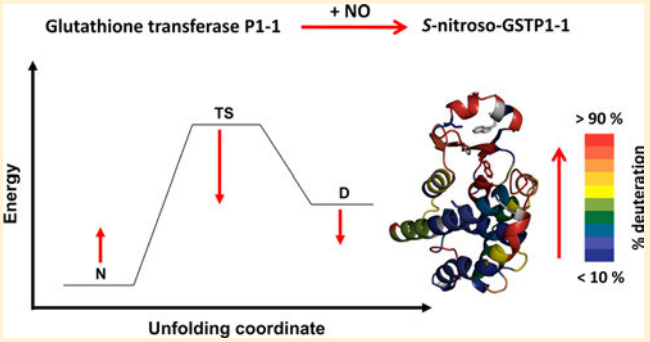

S-Nitrosation is a post-translational modification of cysteine residues in proteins that results from the formation of a covalent complex between NO and the cysteine thiol. Increasingly intensive study is confirming the importance of this modification alongside other, more extensively studied post-translational modifications such as phosphorylation, glycosylation, and ubiquitination. *S*-Nitrosation affects a wide range of proteins,[1] regulates a number of physiological phenomena,[2,3] and has been linked to several diseases.[4]

S-Nitrosation has been shown to induce enzyme activation[5] or inhibition[6] and to regulate the activity of several ion channels[7,8] and control the allosteric behavior of hemoglobin.[9] Despite the clear importance of *S*-nitrosation to the physiological regulation of protein function, relatively little is known about the molecular origins of these effects. Specifically, biophysical data linking the *S*-nitrosation event to its functional consequence are lacking. Far-UV circular dichroism spectroscopy revealed a small loss of α-helical content upon *S*-nitrosation of OxyR[10] and the chloride channel CLIC4,[11] and a subtle change in the tertiary structure of *S*-nitrosated CLIC4 was suggested by trypsin digestion and thermal denaturation experiments.[11] *S*-Nitrosation has also been shown to regulate the immune response in plants by triggering the oligomerization of NPR1.[12] Only four crystal structures and two solution structures [nuclear magnetic resonance (NMR)] have been determined for *S*-nitrosated proteins to date: myoglobin,[13] thioredoxin,[14] protein-tyrosine phosphatase 1B,[15] nitrophorin,[16] p21^{Ras}[17] (NMR), and S100A1[18] (NMR). The limited size of this structural data set makes it difficult to identify trends or make predictions about the consequences of *S*-nitrosation on protein structure. In addition, structural data need to be linked to changes in protein function, stability, and dynamics to completely elucidate *S*-nitrosation at a molecular level.

In this study, we explore the effect of *S*-nitrosation on the activity, structure, stability, and dynamics of human glutathione transferase P1-1 (GSTP1-1). GSTP1-1 is a homodimeric detoxification enzyme that solubilizes toxins by conjugation to glutathione and regulates cell proliferation by inhibition of c-jun N-terminal kinase. *S*-Nitrosated GSTP1-1 is known to exist *in vivo*,[19−21] and *in vitro* work has demonstrated that the modification affects the detoxification activity of the enzyme.[22] Given that the target cysteines are not directly involved in catalysis by GSTP1-1, it is not clear how the *S*-nitrosation event causes the apparent loss of activity. Here, we provide experimental evidence of a severe disruption of GSTP1-1 stability and domain 1 dynamics upon *S*-nitrosation at Cys47 and Cys101. These data detail the regulation of GSTP1-1 by *S*-nitrosation and provide insight into the biophysical basis for protein regulation by *S*-nitrosation in general.

Received: October 16, 2013
Revised: November 22, 2013

   dx.doi.org/10.1021/bi401414c | *Biochemistry* XXXX, XXX, XXX−XXX

EXPERIMENTAL PROCEDURES

Protein Expression, Purification, and *S*-Nitrosation. The pET-15b vector encoding N-terminally His_6-tagged GSTP1-1 was a kind gift from S. Y. Blond (Centre for Pharmaceutical Biotechnology, University of Illinois, Chicago, IL). His_6-GSTP1-1 was expressed in *Escherichia coli* T7 cells and purified by Co^{2+} affinity chromatography as described previously.[23] *S*-Nitrosated GSTP1-1 was prepared by mixing fully reduced protein (with or without a 50-fold molar excess of glutathione sulfonate) with a 50-fold molar excess of *S*-nitrosoglutathione (GSNO) at 37 °C for 1 h. Excess GSNO was removed by dialysis or buffer exchange. The *S*-nitrosation stoichiometry was determined by UV difference spectroscopy as described previously[22] based on an S-NO extinction coefficient of 750 M^{-1} cm^{-1} at 330 nm.

Steady-State Enzyme Kinetics. Enzyme activity was measured at 20 °C for the conjugation of GSH to CDNB.[24] GSH (1 mM) and CDNB (1 mM) were mixed with 1−10 nM enzyme in 100 mM sodium phosphate buffer (pH 6.5) with 1 mM EDTA, 0.02% sodium azide, and 3% (v/v) ethanol. Product formation was monitored by the absorbance at 340 nm. All measurements were performed in triplicate and corrected for the nonenzymatic reaction rate.

Steady-State Spectroscopic Measurements. Fluorescence emission spectra were recorded using a Jasco FP-6300 fluorescence spectrophotometer. Excitation was at 280 nm, and protein concentrations were 2 μM in 20 mM phosphate buffer (pH 7.4) with 150 mM NaCl, 2 mM EDTA, and 0.02% sodium azide. For the acrylamide quenching experiments, excitation was at 295 nm and emission was collected at 342 nm. The protein concentration was 1 μM, and the acrylamide concentration was varied between 0 and 0.3 M. For denatured-state quenching, the protein was equilibrated in 8 M urea before the fluorescence measurements, and *N*-acetyltryptophanamide was included as a control. The quenching data were fit to a modified form of the Stern−Volmer equation (Lehrer plot), for systems with multiple fluorophores:[25,26]#tab;

$$\frac{F_0}{F_0 - F} = \frac{1}{f_a K_Q [Q]} + \frac{1}{f_a}$$

where F_0 is the total fluorescence in the absence of a quencher (contributed by both the accessible and nonaccessible fractions of fluorophores), F is the fluorescence at a particular quencher concentration, K_Q is the Stern−Volmer quenching constant of the accessible fraction, [Q] is the concentration of quencher (acrylamide), and f_a is the fraction of the initial fluorescence accessible to the quencher.

Far-UV circular dichroism measurements were performed in triplicate on a Jasco J810 circular dichroism spectropolarimeter with 2 μM protein in the same buffer as the fluorescence measurements. The raw data were averaged and converted to mean residue ellipticity, $[\theta]$ (degrees square centimeters per decimole) using the following equation:#tab;

$$[\theta] = \frac{100\theta}{Cnl}$$

where θ is the measured ellipticity (millidegrees), C is the protein concentration (millimolar), n is the number of residues, and l is the path length (centimeters).

Equilibrium Unfolding and Refolding. Equilibrium unfolding experiments were conducted by mixing 1 μM protein [20 mM phosphate buffer (pH 7.4) with 150 mM NaCl, 2 mM EDTA, and 0.02% sodium azide] with 0−8 M urea. Refolding was initiated by diluting 10 μM protein in 8 M urea into 1−7.8 M urea with a final protein concentration of 1 μM. All solutions were prepared in triplicate and allowed to equilibrate for 30 min before the structure of the proteins was probed using fluorescence spectroscopy (λ_{ex} = 280 nm; λ_{em} = 342 nm) and circular dichroism at 222 nm.

Unfolding Kinetics. Unfolding kinetics were measured by intrinsic fluorescence using a stopped-flow instrument (Applied Photophysics SX-18MV). Excitation was at 280 nm, and emission was collected using a 320 nm long-pass filter. Final protein concentrations were 1 μM, and the urea concentration was varied from 5.5 to 8 M in 20 mM phosphate buffer (pH 7.4) with 150 mM NaCl, 2 mM EDTA, and 0.02% sodium azide. At least three traces were recorded and averaged at each urea concentration, and the data were fit to single- or double-exponential equations in SigmaPlot version 11.0. The dependence of the observed rate constants on urea concentration was fit to the following equation:

$$\log k_u = \log k_u^{H_2O} + \frac{m_u^{\ddagger}[\text{urea}]}{2.303RT}$$

where k_u is the observed unfolding rate constant, $k_u^{H_2O}$ is the unfolding rate constant in the absence of urea, and $m_u^{\ddagger}$ is the m value for the unfolding of the native state to form the transition state.

Hydrogen−Deuterium Exchange Mass Spectrometry. For the on-exchange reactions, 10 μL of reduced or *S*-nitrosated GSTP1-1 at a concentration of 8 mg/mL [20 mM phosphate buffer (pH 7.4) with 150 mM NaCl, 2 mM EDTA, and 0.02% sodium azide] was diluted with 40 μL of 100% D_2O at 20 °C for 10, 15, 30, 100, 300, or 3600 s before the simultaneous quench, reduction, and proteolysis as previously described.[27] Ice-cold quench buffer was added in an equal volume to the reaction buffer and contained 1 mg/mL pepsin (Sigma), 100 mM TCEP, and 2 M guanidinium chloride. For the fully deuterated control, deuteration was conducted overnight and the buffer was supplemented with 0.02% formic acid. The nondeuterated control experiment was performed as described above except MilliQ H_2O was used in place of D_2O. Following addition of the quench buffer, proteolysis was allowed to proceed for 5 min before the samples were injected onto an Aeris PEPTIDE 3.6 μm XB-C18 RP column (Phenomenex), submerged in ice, coupled to an AB SCIEX QSTAR Elite mass spectrometer via a six-port switching valve. Peptides were eluted at a rate of 300 μL/min with a linear acetonitrile gradient (5 to 95%) over 15 min. Initial peptide identification was performed using collision-induced dissociation (CID) in information-dependent acquisition (IDA) mode, and all subsequent samples were analyzed in MS mode. All reactions were performed in duplicate. The initial peptide pool was sequenced using PEAKS 6 (Bioinformatics Solutions Inc.), and deuterium exchange data were processed using HDExaminer 1.3 (Sierra Analytics).

RESULTS

***S*-Nitrosation of GSTP1-1 *in Vitro*.** GSTP1-1 *S*-nitrosated at Cys47 and Cys101 exists *in vivo*[19−21] and has previously been generated *in vitro*.[22,28] Here, we produced *S*-nitrosated GSTP1-1 by reaction with GSNO, the most prominent physiological transnitrosation agent.[29] *S*-Nitrosation was confirmed by ESI-

dx.doi.org/10.1021/bi401414c | *Biochemistry* XXXX, XXX, XXX−XXX

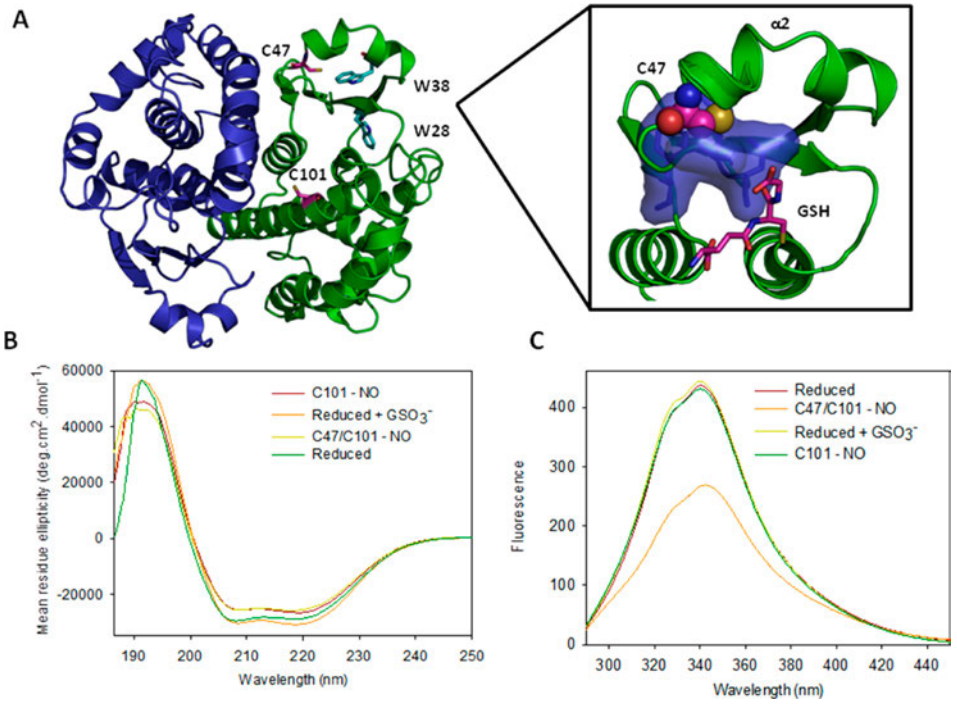

Figure 1. *S*-Nitrosation does not substantially alter the structure of GSTP1-1. (A) Dimeric human GSTP1-1 (PDB entry 6GSS). The sites of nitrosation, Cys47 and Cys101, are indicated (magenta), as are the locations of Trp28 and Trp38, the two tryptophan residues in each subunit (cyan). The inset shows the active site of GSTP1-1 showing the glutathione binding site and packing of Cys47. Glutathione (GSH, magenta sticks) does not interact directly with Cys47 of the protein, nor does the cysteine thiol participate in catalysis. Packing of Cys47 into a hydrophobic pocket (blue surface) maintains the conformation of helix α2 and the GSH binding site. (B) Circular dichroism spectra for reduced and *S*-nitrosated GSTP1-1. The raw data were converted to mean residue ellipticity (MRE) as described in Experimental Procedures. (C) Fluorescence spectra of reduced and *S*-nitrosated GSTP1-1 with a λ_{ex} of 280 nm.

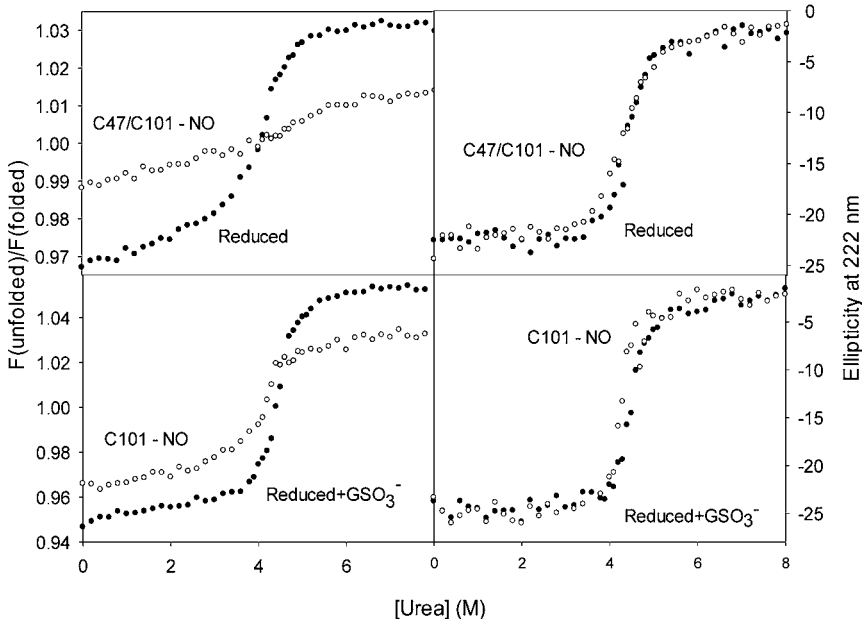

Figure 2. *S*-Nitrosation reduces the unfolding cooperativity in domain 1 of GSTP1-1. Urea-induced unfolding of reduced GSTP1-1 (●) and *S*-nitrosated variants (○) monitored by tryptophan fluorescence with a λ_{ex} of 280 nm (A and C) and circular dichroism at 222 nm (B and D). Data points are the average of three replicates.

MS,[30] and the stoichiometry of nitrosation was determined by UV absorption to be 2 ± 0.1 *S*-nitrosothiols per subunit, consistent with previous reports. Cys101 of GSTP1-1 has been identified as an unusually long-lived *S*-nitrosocysteine *in vivo*.[19] We produced GSTP1-1 Cys101-NO by saturating the protein with glutathione sulfonate (GSO_3^-) before reaction with GSNO. GSO_3^- binds the active site and prevents Cys47 nitrosation by inducing the closed state of α2,[30] resulting in an *S*-nitrosation stoichiometry of 1.2 ± 0.1 per subunit. In all subsequent experiments, GSTP1-1 Cys101-NO was compared

dx.doi.org/10.1021/bi401414c | *Biochemistry* XXXX, XXX, XXX−XXX

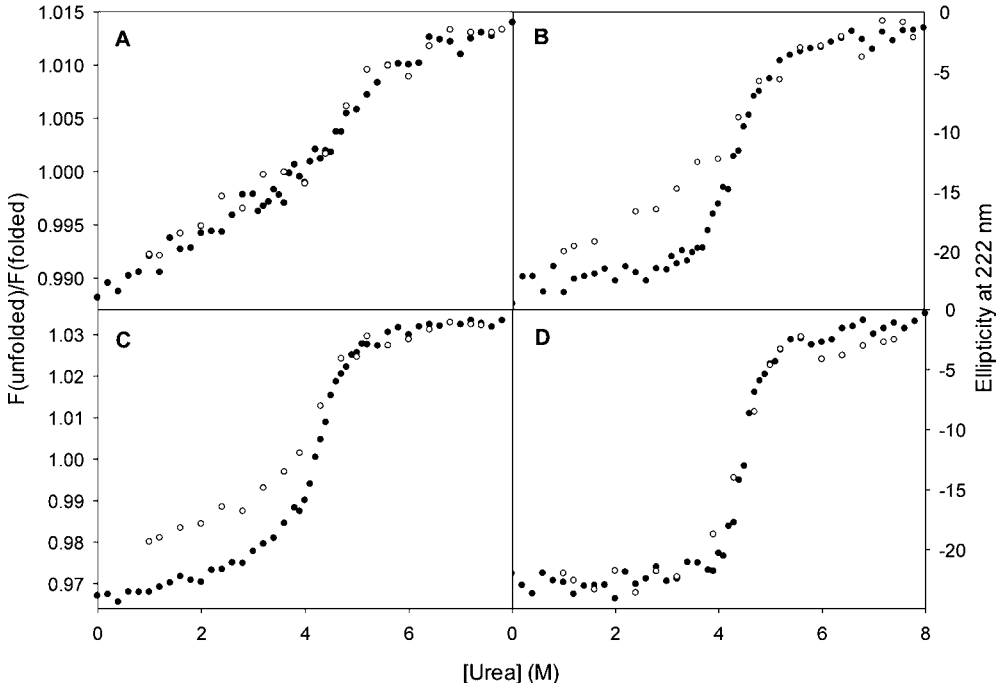

Figure 3. *S*-Nitrosation of GSTP1-1 introduces a refolding defect. Urea-induced unfolding (●) and refolding (○) of GSTP1-1 and *S*-nitrosated variants monitored by tryptophan fluorescence with a λ_{ex} of 280 nm (A and C) and circular dichroism at 222 nm (B and D). (A and B) Cys47/Cys101-NO and (C and D) Cys101-NO. Data points are the average of three replicates.

to reduced GSTP1-1 saturated with GSO_3^-, to control for the presence of the ligand.

***S*-Nitrosation Severely Impairs the Enzyme Activity but Does Not Substantially Alter the Structure of GSTP1-1.** GSTP1-1 catalyzes the conjugation of reduced glutathione to a variety of drugs and toxins, including several chemotherapeutic agents. Although neither Cys47 nor Cys101 is directly involved in catalysis, Cys47 is thought to contribute to maintaining the conformation of the active site by interacting with a hydrophobic pocket in domain 1 (Figure 1A) and, in the thiolate form, with Lys54.[31] Cys101 is highly solvent-exposed, and the Cys101 thiol does not appear to make any stabilizing interactions with the rest of the protein. The enzyme activity of reduced and *S*-nitrosated GSTP1-1 was evaluated using the standard CDNB/GSH conjugation assay.[24] *S*-Nitrosation at Cys47 and Cys101 caused a 94% decrease in the specific activity of the enzyme, from 96 μmol min^{-1} mg^{-1} (reduced) to 6 μmol min^{-1} mg^{-1} (Cys47/Cys101-NO).

We used several spectroscopic methods to probe the effect of *S*-nitrosation on the structure of GSTP1-1 in solution. Circular dichroism spectra are similar for reduced and *S*-nitrosated GSTP1-1, although a small decrease in the level of α-helical structure is apparent for the Cys47/Cys101-NO and Cys101-NO proteins (Figure 1B). Steady-state fluorescence (λ_{ex} = 280 nm) shows substantial quenching of tryptophan fluorescence for Cys47/Cys101-NO GSTP1-1 (Figure 1C). This quenching effect is most likely due to Förster resonance energy transfer between the two tryptophan residues in each subunit (Trp28 and Trp38) and Cys47-NO (Figure 1A)[32] and does not necessarily indicate a structural change in the vicinity of the tryptophans. In support of this interpretation, no significant shift in the maximal emission wavelength is apparent. Acrylamide quenching was used to compare the accessibility of tryptophan residues in reduced and *S*-nitrosated GSTP1-1. Within error, the effective quenching constants (K_Q) for reduced (1.7 ± 0.4 M^{-1}) and Cys101-NO (1.8 ± 0.5 M^{-1}) GSTP1-1 are identical, and very similar to that reported previously.[33,34] The K_Q for quenching of Cys47/Cys101-NO GSTP1-1 (2.8 ± 0.3 M^{-1}) is slightly elevated, however, suggesting that one or both tryptophans are more solvent-exposed in the *S*-nitrosated protein.

***S*-Nitrosation Reduces the Unfolding Cooperativity in Domain 1 of GSTP1-1.** To investigate the effect of *S*-nitrosation on the stability of GSTP1-1, we monitored the unfolding equilibrium of the protein using circular dichroism and fluorescence spectroscopy (Figure 2). The majority of the helical structure of GSTP1-1 is located in domain 2, while both tryptophan residues are in domain 1 (Figure 1A). CD ellipticity at 222 nm is therefore primarily a probe of domain 2 unfolding, while tryptophan fluorescence reports on the unfolding of domain 1.[35] Neither *S*-nitrosation at Cys47 and Cys101 nor *S*-nitrosation at Cys101 alone affects the unfolding of domain 2 of GSTP1-1 (ellipticity at 222 nm) (Figure 2B,D). *S*-Nitrosation does, however, significantly influence the unfolding equilibrium of domain 1. While the unfolding of the reduced protein shows a sigmoidal, cooperative transition, the profile for Cys47/Cys101 nitrosated GSTP1-1 is almost linear (Figure 2A). The dependence of unfolding on denaturant concentration (*m* value) is therefore significantly decreased. This implies that *S*-nitrosation at both cysteines severely impairs the cooperativity of unfolding of domain 1 and reduces the change in solvent accessible surface area upon unfolding.[36] In addition, the starting point of the unfolding curve is higher for the modified protein, but the denaturation end point is lower than that for reduced GSTP1-1. *S*-Nitrosation of GSTP1-1 may therefore result in a partially unfolded "native" state that fails to unfold to the same degree as the reduced protein, even at high denaturant concentrations. This observation is supported by acrylamide quenching experiments in 8 M urea. While the tryptophans of reduced GSTP1-1 in the denatured state are completely

dx.doi.org/10.1021/bi401414c | *Biochemistry* XXXX, XXX, XXX−XXX

accessible to quencher, the Lehrer plot for the *S*-nitrosated protein indicates that 34% of its tryptophan fluorescence is inaccessible to quenching by acrylamide. The denatured state of *S*-nitrosated GSTP1-1 is therefore unusually compact.

Similar to double nitrosation at Cys47 and Cys101, Cys101 nitrosation results in a less cooperative unfolding transition for domain 1 of GSTP1-1 (Figure 2C). In addition, the starting and ending points of the curve suggest that the modified protein is partially unfolded initially but retains more "folded" character than the unmodified protein when denaturation is complete. This effect is much less pronounced, however, than for Cys47/Cys101-NO GSTP1-1.

Because of refolding hysteresis (discussed below), the unfolding transitions in Figure 2 could not be fit to a model for equilibrium unfolding.

S-Nitrosation Causes a Refolding Defect in GSTP1-1. We examined the refolding equilibrium of reduced and *S*-nitrosated GSTP1-1 using circular dichroism and fluorescence spectroscopy (Figure 3). Unlike the reduced protein, which unfolds and refolds reversibly (not shown), *S*-nitrosated GSTP1-1 refolds defectively. Domain 1 of Cys47/Cys101-NO GSTP1-1 (monitored by fluorescence) refolds reversibly (Figure 3A). Circular dichroism measurements, however, reveal hysteresis in domain 2 refolding (Figure 3B). The shallow slope of the refolding transition suggests that domain 2 folds less cooperatively than it unfolds and implies a smaller change in solvent accessible surface area upon folding.[36] Despite the hysteresis, the native state is essentially completely recovered at low urea concentrations.

While circular dichroism measurements suggest that the α-helical structure of Cys101-NO GSTP1-1 is completely and reversibly recovered upon dilution of the denaturant (Figure 3D), folding hysteresis is detected by tryptophan fluorescence (Figure 3C). The hysteresis is apparent from approximately 4 M urea (the midpoint of the unfolding transition), with the folding transition displaying a slope that is shallower than that for unfolding. In addition, the fluorescence signal, and therefore the structure of domain 1, is not completely recovered at low urea concentrations. Light scattering data (not shown) suggest that the hysteresis and lack of recovery of the native state are not the result of protein aggregation.

S-Nitrosation Alters the Unfolding Pathway of GSTP1-1. Equilibrium unfolding experiments demonstrate that *S*-nitrosation severely destabilizes domain 1 of GSTP1-1. To further understand the effect of *S*-nitrosation on the unfolding of the protein, we measured unfolding kinetics using a stopped-flow instrument (Figure 4). Structural changes were followed by intrinsic fluorescence, thereby focusing on the local environment of Trp28 and Trp38 in domain 1 (Figure 1A).

The unfolding of the reduced protein shows two phases: a positive amplitude burst phase followed by a negative amplitude phase (Figure 4A). The positive amplitude phase has previously been attributed to the unfolding of helix 2.[35] This burst phase is largely unresolved, with approximately 1% of the signal captured, and was therefore excluded from the fit. In contrast, the negative amplitude phase is well-defined and was fit to a single-exponential decay function. The unfolding of reduced GSTP1-1 in complex with GSO_3^- follows kinetics very similar to those of the apoenzyme.

The *S*-nitrosated isoforms of GSTP1-1 show unfolding kinetics substantially different from those of the reduced proteins (Figure 4A). In contrast to the positive amplitude burst phase and negative amplitude slow phase of the reduced

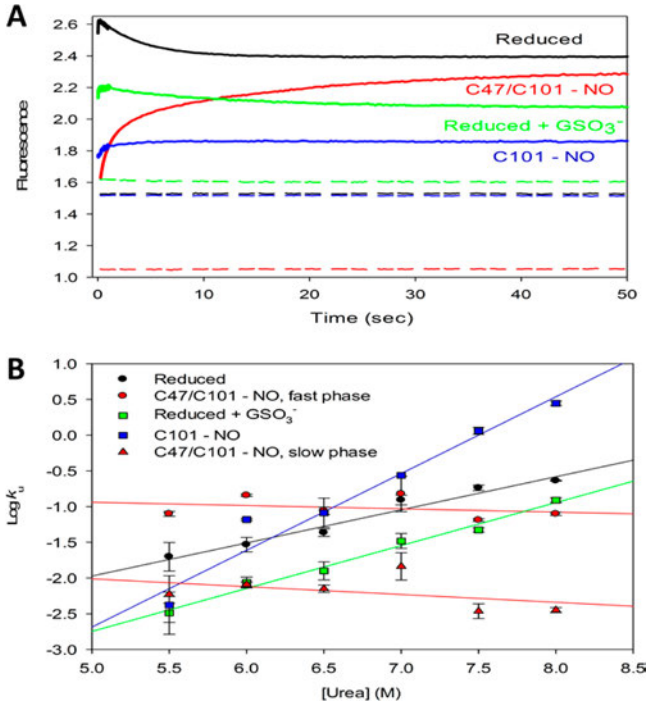

Figure 4. *S*-Nitrosation alters the unfolding pathway of GSTP1-1. (A) Fluorescence transients after mixing 1 μM reduced or *S*-nitrosated GSTP1-1 with 8 M urea: reduced (black), Cys47/Cys101-NO (red), reduced with GSO_3^- (green), and Cys101-NO (blue). Fluorescence transients for the protein mixed with buffer only are shown with dashed lines. λ_{ex} = 280 nm, and λ_{em} = 342 nm. For the reduced proteins (apo and liganded), the first phase (rapid increase in fluorescence) occurred too rapidly to be well resolved and only the second phase (slow decrease in fluorescence) was fit to a single-exponential decay function. The unfolding transient for Cys47/Cys101-NO was fit to a double-exponential function, while the transient for Cys101-NO fit well to a single-exponential function. (B) Urea dependence of the observed unfolding rate constants for the proteins in panel A. The data were fit to a linear function as described in Experimental Procedures, and the fit parameters are listed in Table 1. Data points are the average of three replicates, and error bars represent the standard deviation.

proteins, both Cys47/Cys101-NO and Cys101-NO GSTP1-1 show only positive amplitude phases. These events occur on a time scale much longer than that of the burst phase for the reduced proteins, and only a small proportion of the signal is not captured. While the unfolding of Cys101-NO GSTP1-1 fits well to a single-exponential function, the unfolding kinetics of Cys47/Cys101-NO GSTP1-1 are better described by a double-exponential function.

To characterize the unfolding kinetics further, the rate constants for the resolvable phases of unfolding were determined as a function of urea concentration (Figure 4B). Because the *S*-nitrosated and reduced proteins do not appear to follow the same unfolding pathway (Figure 4A), the constants reported in Table 1 are not necessarily for the same structural events and therefore cannot be directly compared. The data are nonetheless informative with regard to the character of the individual phases. For the reduced proteins, GSO_3^- binding does not significantly alter the kinetic cooperativity (m value). However, the ligand does appear to stabilize the native state of domain 1 of the reduced protein, which is evident in the 25-fold decrease in $k_u^{H_2O}$, consistent with previous work.[35] The unfolding of Cys101-NO GSTP1-1 is monophasic and different

dx.doi.org/10.1021/bi401414c | *Biochemistry* XXXX, XXX, XXX−XXX

Table 1. Kinetic Constants for the Unfolding of Reduced and *S*-Nitrosated GSTP1-1

	reduced	reduced with GSO_3^-	Cys101-NO (with GSO_3^-)	Cys47/Cys101-NO, fast phase	Cys47/Cys101-NO, slow phase
$k_u^{H_2O}$ (s^{-1})	$(5 \pm 2) \times 10^{-5}$	$1.8 \times 10^{-6} \pm 6 \times 10^{-7}$	$(3 \pm 2) \times 10^{-8}$	0.21 ± 0.11	0.04 ± 0.02
$m_u^{\ddagger}$ (kcal mol^{-1} M^{-1})	0.62 ± 0.04	0.81 ± 0.04	1.3 ± 0.1	-0.07 ± 0.06	-0.06 ± 0.08

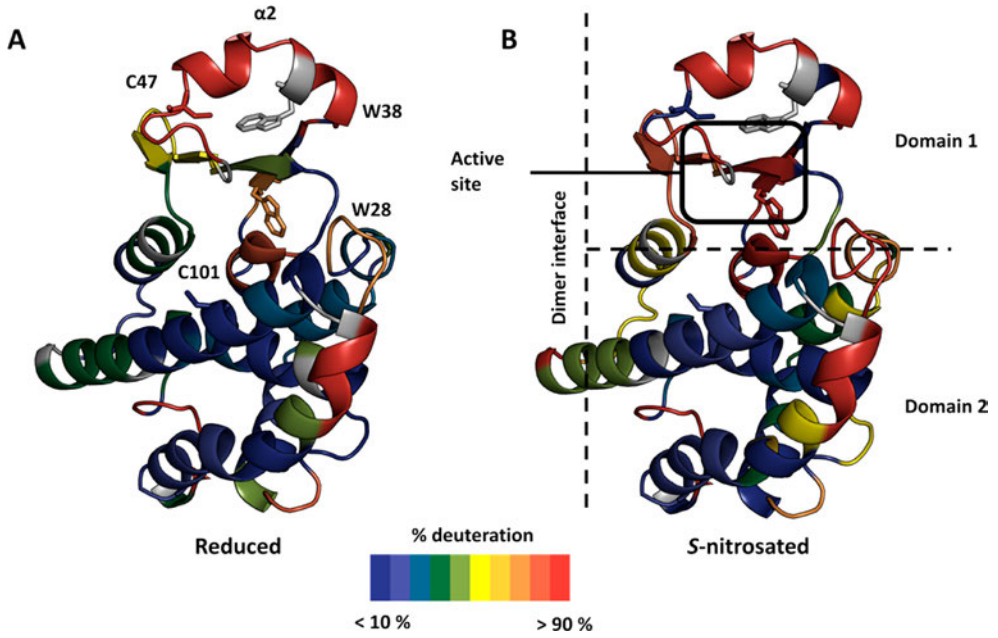

Figure 5. Conformational dynamics of reduced and *S*-nitrosated GSTP1-1 probed by DXMS. The percentages of deuteration of (A) reduced and (B) *S*-nitrosated GSTP1-1 after 100 s are mapped onto the structure of a single subunit of the protein (PDB entry 6GSS). The highly dynamic α2 helix is indicated, as are the *S*-nitrosation target cysteines (C47 and C101) and the dominant fluorophores (W28 and W38).

from that of the reduced proteins. The large $m_u^{\ddagger}$ and small $k_u^{H_2O}$ indicate that this phase represents the highly cooperative unfolding of a stable structural element in domain 1. The two phases (fast and slow) in the unfolding of Cys47/Cys101-NO GSTP1-1 are both characterized by a very low $m_u^{\ddagger}$ and a high $k_u^{H_2O}$. In contrast to Cys101-NO GSTP1-1, this suggests the unfolding of an unstable structural element that experiences a small change in solvent accessible surface area between the native and transition states.

***S*-Nitrosation Increases the Conformational Dynamics of GSTP1-1.** To rationalize the effect of *S*-nitrosation on the stability and activity of GSTP1-1, the dynamics of the reduced and modified proteins were probed using amide hydrogen−deuterium exchange mass spectrometry (DXMS) (Figure 5). In both reduced and *S*-nitrosated GSTP1-1, α2 rapidly exchanges nearly all of its amide protons. This is consistent with NMR data that showed that α2 is largely disordered above 17 °C[37] and therefore poorly protected from deuterium exchange. In contrast, the helical bundle comprising domain 2 is relatively stable in both proteins, in agreement with DXMS data for class mu GSTM1-1[38] and the GST homologue CLIC1.[39]

The deuteration difference map and peptide deuteration kinetics reveal substantial differences in amide hydrogen exchange behavior between reduced and *S*-nitrosated GSTP1-1 (Figure 6 and Figures S1 and S2 of the Supporting Information). Although α2 is equally susceptible to deuteration in both proteins, the rest of domain 1 is significantly more dynamic in *S*-nitrosated GSTP1-1. Specifically, strands β1−β3, helices α1 and α3, and the apex of helix α8 all show higher levels of deuteration in the modified protein over 10−3600 s. The exception to this trend is part of the peptide that includes *S*-nitrosated Cys47 (residues 37−47), which exchanges fewer deuterons than in the reduced protein, suggesting that this region is locally protected from deuterium exchange. The dynamics of domain 2 are also affected by *S*-nitrosation, particularly over longer time scales (>30 s), evident in the increased level of deuteration of α4, α5, and α7. Together, the DXMS data show that *S*-nitrosation at Cys47 and Cys101 destabilizes both domain 1 and domain 2 of GSTP1-1.

DISCUSSION

S-Nitrosation is a post-translational modification with a wide range of substrates and clear physiological relevance. Despite this, the molecular mechanisms by which this cysteine modification effects changes in protein function remain poorly understood. Here, we investigated the effect of *S*-nitrosation on the activity, stability, structure, and dynamics of GSTP1-1, with the aim of understanding how the activity of this ubiquitous enzyme is regulated. We found that *S*-nitrosation destabilizes GSTP1-1, causing domain 1 of the protein to unfold with low cooperativity and introducing a global refolding defect.

S-Nitrosation was previously observed to reduce the activity of GSTP1-1 *in vitro* by 30%.[22] We observed a substantially larger reduction in activity (94%), possibly due to the fact that we nitrosated the protein at 37 °C instead of 25 °C, resulting in a larger proportion of the population of the protein being modified.[30] Despite the significant decrease in enzyme activity, our spectroscopic analyses revealed little structural difference between the *S*-nitrosated and reduced isoforms, except for a small reduction in α-helical content and a change in acrylamide

dx.doi.org/10.1021/bi401414c | *Biochemistry* XXXX, XXX, XXX−XXX

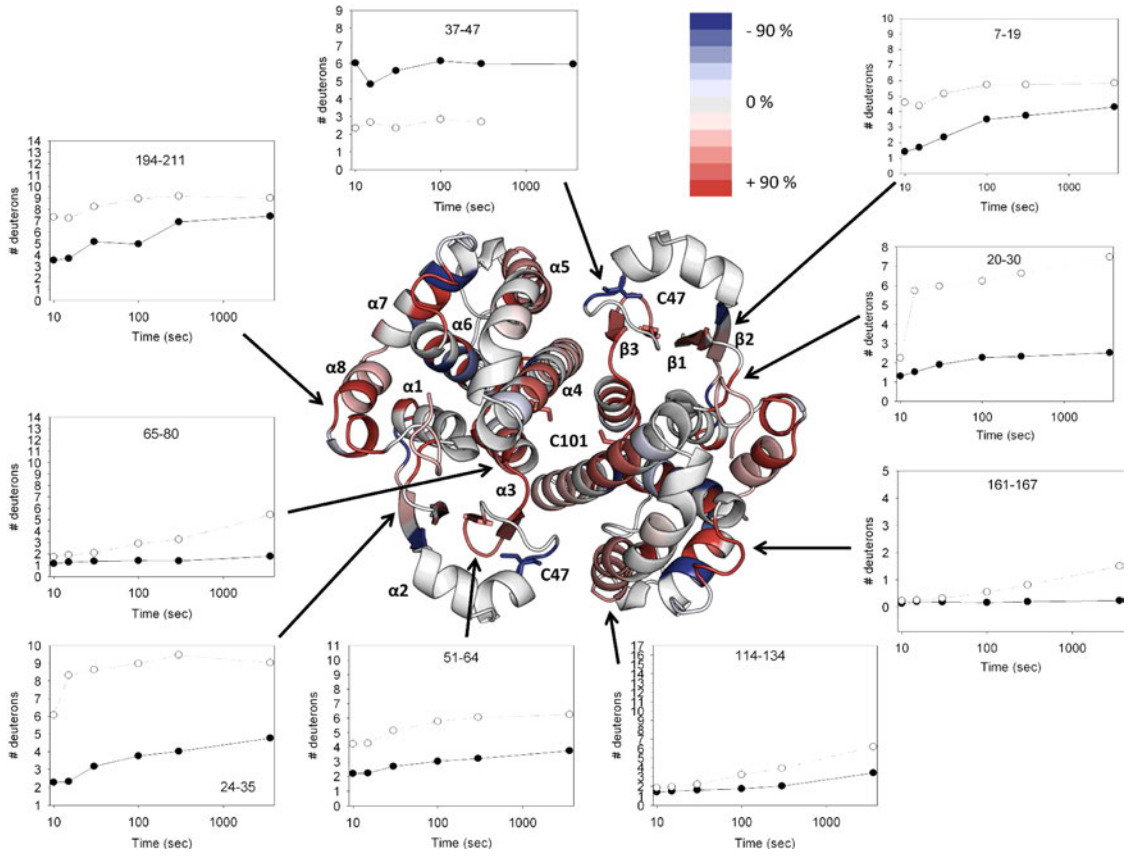

Figure 6. *S*-Nitrosation increases the conformational flexibility of GSTP1-1. The percentage differences in deuteration between reduced and *S*-nitrosated GSTP1-1 after 100 s are mapped onto the structure of dimeric GSTP1-1 (PDB entry 6GSS), calculated as the percentage of deuteration (*S*-nitrosated) minus the percentage of deuteration (reduced). Red coloring indicates that the level of deuterium exchange is higher for the nitrosated protein, while blue coloring indicates that the level of deuterium exchange is higher for the reduced protein. Helices $\alpha1-\alpha8$ are labeled, and the target cysteines (Cys47 and Cys101) are shown as sticks. The deuteron uptake plots compare deuteron incorporation of reduced (●) and *S*-nitrosated (○) GSTP1-1 over time for representative peptides. Lines through the points are guides for the eye only. The plots are scaled according to the maximal number of exchangeable amide hydrogens for that peptide, assumed to equal the number of non-proline residues in the peptide minus the first two residues, which are subject to rapid back exchange.

quenching behavior (Figure 1). Cys47 does not participate directly in catalysis,[40] but chemical modification of the thiol impairs the activity of the enzyme.[41−43] Our DXMS data suggest that *S*-nitrosation at this residue inactivates GSTP1-1 by substantially increasing the dynamics of the active site (Figures 5 and 6).

Equilibrium unfolding experiments showed, strikingly, that *S*-nitrosation significantly reduces the unfolding cooperativity of GSTP1-1 (Figure 2). This indicates that the modification decreases the difference in solvent accessible surface area between the native and denatured states.[36] Acrylamide quenching experiments in 8 M urea support this by suggesting that the denatured state of *S*-nitrosated GSTP1-1 retains significant residual structure. Furthermore, data for the unfolding kinetics show that *S*-nitrosated GSTP1-1 unfolds quickly (high $k_u^{H_2O}$) and via a low-energy transition state (low $m_u^{\ddagger}$) (Figure 4). Together, these data indicate that *S*-nitrosation at Cys47 and Cys101 smoothes the unfolding energy landscape of GSTP1-1.

Trp28 is the dominant fluorophore of GSTP1-1, contributing 70% of the fluorescence signal.[44] Unlike Trp38, which is solvent-exposed even in the native state because of its position on the highly dynamic $\alpha2$, Trp28 is relatively solvent inaccessible in reduced GSTP1-1 (Figure 6). This is consistent with the cooperative transition observed when the unfolding of the reduced protein is probed by tryptophan fluorescence; as the protein unfolds, the buried Trp28 becomes solvent-exposed in a concerted manner. The very low unfolding cooperativity of *S*-nitrosated GSTP1-1 is explained by our DXMS experiments, which reveal that the local environment of Trp28 becomes less ordered and more solvent accessible upon *S*-nitrosation (Figures 5 and 6). *S*-Nitrosation appears to substantially destabilize domain 1 of GSTP1-1 (proximal to Trp28 and -38), resulting in a partially disordered state that unfolds with low kinetic and thermodynamic cooperativity.

In addition to destabilizing domain 1, *S*-nitrosation increases the conformational flexibility of parts of domain 2, which is particularly stable in reduced GSTP1-1 (Figures 5 and 6). This is most apparent at longer deuteration times (>30 s), indicating that the conformational transitions that expose the amide hydrogens in domain 2 are much slower than those associated with domain 1. The increased dynamics of domain 2 may alter the folding energy landscape of *S*-nitrosated GSTP1-1, potentially explaining the low refolding cooperativity of this domain (Figure 3).

S-Nitrosation at Cys47 is disfavored whenever the G-site of GSTP1-1 is occupied,[30] for example, by GSH, glutathione disulfide, or the dinitrosyl−diglutathionyl−iron complex.[45] In addition, Cys47-NO is highly susceptible to denitrosation by GSH.[30] These factors are consistent with the low level of

dx.doi.org/10.1021/bi401414c | *Biochemistry* XXXX, XXX, XXX−XXX

Cys47-NO GSTP1-1 observed *in vivo* (3−55% depending on the concentration of the NO donor).[21] *S*-Nitrosation at Cys47 is therefore only likely to occur under conditions of oxidative stress, when GSH concentrations are low and NO donors (GSNO and CysNO) are more abundant.[20] Cys101-NO of GSTP1-1 is relatively kinetically resistant to denitrosation by GSH[30] and unusually persistent *in vivo*.[19] We therefore also analyzed the stability and unfolding of Cys101-NO GSTP1-1, prepared by saturating the protein with GSO_3^- prior to *S*-nitrosation with GSNO. GSO_3^- binds the G-site of GSTP1-1, biasing the closed state of $\alpha 2$[37] and preventing *S*-nitrosation of Cys47.[30] *S*-Nitrosation at Cys101 reduces the cooperativity of unfolding of domain 1 of GSTP1-1, although not to the same extent as the fully nitrosated protein (Figure 2). It also introduces a refolding defect in the same domain, preventing the full recovery of the native state (Figure 3). In contrast to *S*-nitrosation at both cysteines, Cys101 nitrosation stabilizes the protein kinetically (Figure 4). This kinetic stabilization may compensate *in vivo* for the apparent thermodynamic destabilization and refolding defect. Although *S*-nitrosation at Cys101 alone does not affect the enzymatic activity of GSTP1-1,[22] it may affect the ability of GSTP1-1 to inhibit c-jun N-terminal kinase[46] or bind peroxiredoxin.[47]

GSTP1-1 is tightly regulated by *S*-nitrosation. GSNO spontaneously and rapidly *S*-nitrosates Cys47 when $\alpha 2$ is in its open conformation,[30] thereby introducing local disorder, destabilizing domain 1, and smoothing the unfolding energy landscape. Cys101 is nitrosated more slowly but persists *in vivo*,[19,30] introducing a refolding defect but kinetically stabilizing GSTP1-1. This work elucidates the regulation of GSTP1-1 by *S*-nitrosation at a molecular level, contributing to a general understanding of how cysteine *S*-nitrosation controls protein stability and activity.

■ ASSOCIATED CONTENT

Ⓢ Supporting Information

DXMS deuteration difference heat map (Figure S1) and a complete set of DXMS peptide uptake plots (Figure S2). This material is available free of charge via the Internet at http://pubs.acs.org.

■ AUTHOR INFORMATION

Corresponding Author

*Protein Structure-Function Research Unit, School of Molecular and Cell Biology, University of the Witwatersrand, Johannesburg, South Africa. E-mail: heinrich.dirr@wits.ac.za. Telephone: (+27) 11 717 6352.

Funding

Supported by the University of the Witwatersrand, South African National Research Foundation Grant 68898, and the South African Research Chairs Initiative of the Department of Science and Technology and National Research Foundation Grant 64788.

Notes

The authors declare no competing financial interest.

■ ABBREVIATIONS

$\alpha 2$, helix 2 of glutathione transferase P1-1; DXMS, hydrogen−deuterium exchange mass spectrometry; GST, glutathione transferase; GSH, glutathione; GSNO, *S*-nitrosoglutathione; GSO_3^-, glutathione sulfonate; S-NO, *S*-nitrosothiol; PDB, Protein Data Bank.

■ REFERENCES

(1) Lee, T.-Y., Chen, Y.-J., Lu, C.-T., Ching, W.-C., Teng, Y.-C., Huang, H.-D., and Chen, Y.-J. (2012) dbSNO: A database of cysteine S-Nitrosylation. *Bioinformatics 2012*, 2293−2295.

(2) Hess, D. T., Matsumoto, A., Kim, S., Marshall, H. E., and Stamler, J. S. (2005) Protein S-nitrosylation: Purview and parameters. *Nat. Rev. Mol. Cell Biol. 6*, 150−166.

(3) Hess, D. T., and Stamler, J. S. (2011) Regulation by S-nitrosylation of Protein Posttranslational Modification. *J. Biol. Chem. 287*, 4411−4418.

(4) Foster, M. W., Hess, D. T., and Stamler, J. S. (2009) Protein S-nitrosylation in health and disease: A current perspective. *Trends Mol. Med. 15*, 391−404.

(5) Hausladen, A., Privalle, C. T., Keng, T., DeAngelo, J., and Stamler, J. S. (1996) Nitrosative stress: Activation of the transcription factor OxyR. *Cell 86*, 719−729.

(6) Rössig, L., Fichtlscherer, B., Breitschopf, K., Haendeler, J., Zeiher, A. M., Mülsch, A., and Dimmeler, S. (1999) Nitric oxide inhibits caspase-3 by S-nitrosation in vivo. *J. Biol. Chem. 274*, 6823−6826.

(7) Xu, L. (1998) Activation of the Cardiac Calcium Release Channel (Ryanodine Receptor) by Poly-S-Nitrosylation. *Science 279*, 234−237.

(8) Asada, K., Kurokawa, J., and Furukawa, T. (2009) Redox- and calmodulin-dependent S-nitrosylation of the KCNQ1 channel. *J. Biol. Chem. 284*, 6014−6020.

(9) Wolzt, M., MacAllister, R. J., Davis, D., Feelisch, M., Moncada, S., Vallance, P., and Hobbs, A. J. (1999) Biochemical characterization of S-nitrosohemoglobin. Mechanisms underlying synthesis, no release, and biological activity. *J. Biol. Chem. 274*, 28983−28990.

(10) Kim, S. O., Merchant, K., Nudelman, R., Beyer, W. F., Jr., Keng, T., DeAngelo, J., Hausladen, A., and Stamler, J. S. (2002) OxyR: A Molecular Code for Redox-Related Signaling. *Cell 109*, 383−396.

(11) Malik, M., Shukla, A., Amin, P., Niedelman, W., Lee, J., Jividen, K., Phang, J. M., Ding, J., Suh, K. S., Curmi, P. M. G., et al. (2010) S-Nitrosylation Regulates Nuclear Translocation of Chloride Intracellular Channel Protein CLIC4. *J. Biol. Chem. 285*, 23818−23828.

(12) Tada, Y., Spoel, S. H., Pajerowska-Mukhtar, K., Mou, Z., Song, J., Wang, C., Zuo, J., and Dong, X. (2008) Plant immunity requires conformational changes [corrected] of NPR1 via S-nitrosylation and thioredoxins. *Science 321*, 952−956.

(13) Schreiter, E. R., Rodr1, M., Weichsel, A., Montfort, W. R., and Bonaventura, J. (2007) S-Nitrosylation-induced Conformational Change in Blackfin Tuna Myoglobin. *J. Biol. Chem. 282*, 19773−19780.

(14) Weichsel, A., Brailey, J. L., and Montfort, W. R. (2007) Buried S-nitrosocysteine revealed in crystal structures of human thioredoxin. *Biochemistry 46*, 1219−1227.

(15) Chen, Y. Y., Chu, H. M., Pan, K. T., Teng, C., Wang, D. L., Wang, A. H. J., Khoo, K. H., and Meng, T. C. (2008) Cysteine S-nitrosylation protects protein-tyrosine phosphatase 1B against oxidation-induced permanent inactivation. *J. Biol. Chem. 283*, 35265−35272.

(16) Weichsel, A., Maes, E. M., Andersen, J. F., Valenzuela, J. G., Shokhireva, T. K., Walker, F. A., and Montfort, W. R. (2005) Heme-assisted S-nitrosation of a proximal thiolate in a nitric oxide transport protein. *Proc. Natl. Acad. Sci. U.S.A. 102*, 594−599.

(17) Williams, J., and Pappu, K. (2003) Structural and biochemical studies of p21Ras S-nitrosylation and nitric oxide-mediated guanine nucleotide exchange. *Proc. Natl. Acad. Sci. U.S.A. 100*, 6376−6381.

(18) Lenarcic Zivkovic, M., Zareba-Koziol, M., Zhukova, L., Poznanski, J., Zhukov, I., and Wyslouch-Cieszynska, A. (2012) Post-translational S-Nitrosylation Is an Endogenous Factor Fine Tuning the Properties of Human S100A1 Protein. *J. Biol. Chem. 287*, 40457−40470.

(19) Paige, J. S., Xu, G., Stancevic, B., and Jaffrey, S. R. (2008) Nitrosothiol reactivity profiling identifies S-nitrosylated proteins with unexpected stability. *Chem. Biol. 15*, 1307−1316.

(20) Beltrán, B., Orsi, A., Clementi, E., and Moncada, S. (2000) Oxidative stress and S-nitrosylation of proteins in cells. *Br. J. Pharmacol. 129*, 953−960.

(21) Sinha, V., Wijewickrama, G. T., Chandrasena, R. E. P., Xu, H., Edirisinghe, P. D., Schiefer, I. T., and Thatcher, G. R. J. (2010) Proteomic and mass spectroscopic quantitation of protein S-nitrosation differentiates NO-donors. *ACS Chem. Biol. 5*, 667−680.
(22) Lo Bello, M., Nuccetelli, M., Caccuri, A. M., Stella, L., Parker, M. W., Rossjohn, J., McKinstry, W. J., Mozzi, A. F., Federici, G., Polizio, F., Pedersen, J. Z., and Ricci, G. (2001) Human glutathione transferase P1-1 and nitric oxide carriers; a new role for an old enzyme. *J. Biol. Chem. 276*, 42138−42145.
(23) Chang, M., Bolton, J. L., and Blond, S. Y. (1999) Expression and purification of hexahistidine-tagged human glutathione S-transferase P1-1 in *Escherichia coli*. *Protein Expression Purif. 17*, 443−448.
(24) Habig, W., and Jakoby, W. (1981) Assays for differentiation of glutathione S-transferases. *Methods Enzymol. 77*, 398−405.
(25) Lehrer, S. S. (1971) Solute perturbation of protein fluorescence. The quenching of the tryptophyl fluorescence of model compounds and of lysozyme by iodide ion. *Biochemistry 10*, 3254−3263.
(26) Eftink, M. R., and Ghiron, C. A. (1976) Exposure of tryptophanyl residues in proteins. Quantitative determination by fluorescence quenching studies. *Biochemistry 15*, 672−680.
(27) Zhang, H., Mcloughlin, S. M., Frausto, S. D., Tang, H., Mark, R., and Marshall, A. G. (2010) Simultaneous Reduction and Digestion of Proteins with Disulfide Bonds for Hydrogen/Deuterium Exchange Monitored by Mass Spectrometry. *Anal. Chem. 82*, 1450−1454.
(28) Téllez-Sanz, R., Cesareo, E., Nuccetelli, M., Aguilera, A. M., Barón, C., Parker, L. J., Adams, J. J., Morton, C. J., Lo Bello, M., Parker, M. W., et al. (2006) Calorimetric and structural studies of the nitric oxide carrier S-nitrosoglutathione bound to human glutathione transferase P1-1. *Protein Sci. 15*, 1093−1105.
(29) Liu, L., Hausladen, A., Zeng, M., Que, L., Heitman, J., and Stamler, J. S. (2001) A metabolic enzyme for S-nitrosothiol conserved from bacteria to humans. *Nature 410*, 490−494.
(30) Balchin, D., Wallace, L., and Dirr, H. W. (2013) S-Nitrosation of Glutathione Transferase P1-1 Is Controlled by the Conformation of a Dynamic Active Site Helix. *J. Biol. Chem. 288*, 14973−14984.
(31) Lo Bello, M., Parker, M. W., Desideri, A., Polticelli, F., Falconi, M., Del Boccio, G., Pennelli, A., Federici, G., and Ricci, G. (1993) Peculiar Spectroscopic and Kinetic Properties of Cys-47 in human placental glutathione transferase. *J. Biol. Chem. 268*, 19033−19038.
(32) Chen, X., Wen, Z., Xian, M., Wang, K., Ramachandran, N., Tang, X., Schlegel, H. B., Mutus, B., and Wang, P. G. (2001) Fluorophore-labeled S-nitrosothiols. *J. Org. Chem. 66*, 6064−6073.
(33) Bico, P., Erhardt, J., Kaplan, W., and Dirr, H. (1995) Porcine class pi glutathione S-transferase: Anionic ligand binding and conformational analysis. *Biochim. Biophys. Acta 1247*, 225−230.
(34) Dirr, H., and Reinemer, P. (1991) Equilibrium unfolding of class glutathione S-transferase. *Biochem. Biophys. Res. Commun. 180*, 294−300.
(35) Gildenhuys, S., Wallace, L. A., Burke, J. P., Balchin, D., Sayed, Y., and Dirr, H. W. (2010) Class pi glutathione transferase unfolds via a dimeric and not monomeric intermediate: Functional implications for an unstable monomer. *Biochemistry 49*, 5074−5081.
(36) Myers, J. K. K., Pace, C. N. N., and Scholtz, J. M. M. (1995) Denaturant m values and heat capacity changes: Relation to changes in accessible surface areas of protein unfolding. *Protein Sci. 4*, 2138−2148.
(37) Hitchens, T. K., Mannervik, B., and Gordon, S. (2001) Disorder-to-order transition of the active site of human class pi glutathione transferase, GST P1-1. *Biochemistry 40*, 11660−11669.
(38) Thompson, L. C., Walters, J., Burke, J., Parsons, J. F., Armstrong, R. N., and Dirr, H. W. (2006) Double mutation at the subunit interface of glutathione transferase rGSTM1-1 results in a stable, folded monomer. *Biochemistry 45*, 2267−2273.
(39) Stoychev, S. H., Nathaniel, C., Fanucchi, S., Brock, M., Li, S., Asmus, K., Woods, V. L., and Dirr, H. W. (2009) Structural dynamics of soluble chloride intracellular channel protein CLIC1 examined by amide hydrogen-deuterium exchange mass spectrometry. *Biochemistry 48*, 8413−8421.
(40) Kong, K.-H., Inoue, H., and Takahashi, K. (1991) Non-essentiality of cysteine and histidine residues for the activity of human class pi glutathione S-transferase. *Biochem. Biophys. Res. Commun. 181*, 748−755.
(41) Townsend, D. M., Manevich, Y., He, L., Hutchens, S., Pazoles, C. J., and Tew, K. D. (2009) Novel role for glutathione S-transferase pi. Regulator of protein S-glutathionylation following oxidative and nitrosative stress. *J. Biol. Chem. 284*, 436−445.
(42) Caccuri, A. M., Petruzzelli, R., Polizio, F., Federici, G., and Desiderittl, A. (1992) Inhibition of Glutathione Transferase 7r from Human Placenta by 1-Chloro-2,4-dinitrobenzene Occurs Because of Covalent Reaction with Cysteine 47. *Arch. Biochem. Biophys. 297*, 119−122.
(43) Sluis-cremer, N., and Dirr, H. (1995) Conformational stability of Cys45-alkylated and hydrogen peroxide-oxidised glutathione S-transferase. *FEBS Lett. 371*, 94−98.
(44) Stella, L., Caccuri, A., Rosato, N., Nicotra, M., Lo Bello, M., De Matteis, F., Mazzetti, A. P., Federici, G., and Ricci, G. (1998) Flexibility of helix 2 in the human glutathione transferase P1-1. *J. Biol. Chem. 273*, 23267−23273.
(45) De Maria, F., Pedersen, J. Z., Caccuri, A. M., Antonini, G., Turella, P., Stella, L., Lo Bello, M., Federici, G., and Ricci, G. (2003) The specific interaction of dinitrosyl-diglutathionyl-iron complex, a natural NO carrier, with the glutathione transferase superfamily: Suggestion for an evolutionary pressure in the direction of the storage of nitric oxide. *J. Biol. Chem. 278*, 42283−42293.
(46) Adler, V., Yin, Z., Fuchs, S. Y., Benezra, M., Rosario, L., Tew, K. D., Pincus, M. R., Sardana, M., Henderson, C. J., Wolf, C. R., Davis, R. J., and Ronai, Z. (1999) Regulation of JNK signaling by GSTp. *EMBO J. 18*, 1321−1334.
(47) Ralat, L. A., Misquitta, S. A., Manevich, Y., Fisher, A. B., and Colman, R. F. (2008) Characterization of the complex of glutathione S-transferase pi and 1-cysteine peroxiredoxin. *Arch. Biochem. Biophys. 474*, 109−118.

dx.doi.org/10.1021/bi401414c | *Biochemistry* XXXX, XXX, XXX−XXX

Chapter 4

General discussion

4.1 A minimal mechanism for transnitrosation of GSTP1-1

Using transient kinetic techniques, a minimal mechanism was defined for the transnitrosation of GSTP1-1 by CysNO or GSNO [132] (Scheme 2).

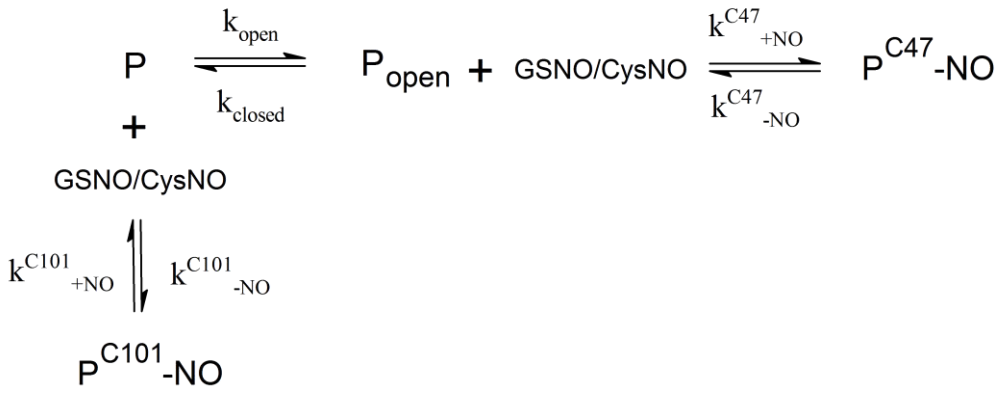

Scheme 2. Minimal mechanism for *S*-nitrosation of GSTP1-1. P and P_{open} represent GSTP1-1 with α2 in the closed and open conformations, respectively. k^{C47} and k^{C101} are the rate constants for *S*-nitrosation (+NO) and denitrosation (-NO) at Cys47 and Cys101.

S-Nitrosation caused a decrease in the fluorescence intensity of GSTP1-1 following excitation at 280 nm. This allowed the kinetics of nitrosation to be measured by stopped-flow fluorimetry. *S*-Nitrosation at Cys101 was found to occur in a single step, with relatively slow kinetics. A concurrent experiment using CysNO as the NO donor suggested that transnitrosation by GSNO is limited by steric hindrance at this cysteine, resulting in apparent negative cooperativity. This is consistent with the limited space between Cys101 residues on

adjacent subunits, preventing the dimer interface cleft from accommodating two GSNO molecules simultaneously.

Due to its low pK_a [116], Cys47 of GSTP1-1 would be expected to be transnitrosated more rapidly than Cys101. It was demonstrated, however, that the rate of Cys47 nitrosation is controlled by the conformation of α2 at the active site. When α2 is closed, the Cys47 thiol is not solvent accessible and cannot react with GSNO. *S*-Nitrosation therefore selects for the conformation of GSTP1-1 in which α2 is open. The kinetic mechanism reported here – conformational selection – is seldom invoked to explain two-step biochemical interactions. Instead, data similar to those reported in this work are commonly assumed to indicate an induced-fit mechanism of bimolecular recognition. Indeed, this interpretation has previously been applied to explain the behaviour of α2 of GSTP1-1 during ligand binding at the active site [133]. In light of the detailed kinetic data reported here [132], and the well-established conformational heterogeneity of α2 [112], it is more likely that ligand binding by GSTP1-1 follows a conformational selection mechanism. In fact, a recent study argues that conformational selection is able to account for almost all ligand binding behaviours [134].

GSNO is essentially identical in structure to GSH, the natural ligand of GSTP1-1. It was therefore initially proposed that *S*-nitrosation of GSTP1-1 at Cys47 is preceded by GSNO binding to the active site [129]. Although superficially plausible, this mechanism is inconsistent with the binding mode of GSNO, which positions the NO group far from the Cys47 thiol (PDB codes 2A2S; 2A2R [129]). Indeed, it was demonstrated in this work that GSNO does not bind GSTP1-1 with measurable affinity, and that CysNO (which has no binding site on GSTP1-1) can readily nitrosate Cys47. GSNO binding does not, therefore, precede *S*-nitrosation of GSTP1-1. Instead, GSNO binding to any extent is likely to *compete* with *S*-nitrosation by biasing the closed state of α2.

The mechanism of transnitrosation reported here is the first for any protein, and represents an important step towards understanding the mechanics of protein *S*-nitrosation at a molecular level. Furthermore, this work suggests a new view of ligand recognition by GSTP1-1, where ligand binding selects between slow-exchanging conformers of α2.

4.2 Targeted cysteine nitrosation by *S*-nitrosoglutathione

How *S*-nitrosation is targeted to specific cysteines is an important, unresolved question. To properly answer this question, the rates and mechanisms of *S*-nitrosation must be compared across different cysteines. This requires detailed kinetic data, such as that reported here for GSTP1-1.

Three factors have been proposed to target specific cysteines for transnitrosation: an acid-base motif near the cysteine thiol [81], low thiol pK_a [80], and a proximal GSNO binding site [14,28,81]. Neither Cys101 nor Cys47 of GSTP1-1 is near an appropriate acid-base motif. Furthermore, although the protein may bind GSNO, it was demonstrated in this work that GSNO binding is not linked to *S*-nitrosation of Cys47. Cys47 does have an unusually low pK_a due to stabilisation of the thiolate by Lys44 [116]. However, because the α2 equilibrium limits the rate of nitrosation at Cys47, the low pK_a of this group does not ultimately determine its reactivity. These considerations point to thiol solvent accessibility as the major determinant of *S*-nitrosation specificity in GSTP1-1. Cys101 is the most solvent accessible cysteine residue out of the four on each subunit, and Cys47 is readily nitrosated when α2 is open and the thiol is exposed.

Previous NMR work [112], as well as the energetics of α2 opening reported here, argue for α2 being largely unfolded or disordered in the open conformation. This suggests that significant tertiary or secondary structure is not required to target GSNO or CysNO to a specific cysteine. The apparent selection of unstructured regions of proteins by post-translational modifications has been extensively reported [135], and includes phosphorylation of disordered regions of p53 [136] and acetylation of histone tails [137]. This is the first time that this phenomenon has been reported for protein *S*-nitrosation, but it would be unsurprising if similar behaviour were found for other proteins.

4.3 *S*-Nitrosation introduces local disorder in domain 1 of GSTP1-1

The hydrogen-deuterium exchange mass spectrometry data reported here reveal that *S*-nitrosation at Cys47 and Cys101 substantially increases the susceptibility of GSTP1-1 to deuteration. This is particularly evident in domain 1, even at short time points (less than 10 seconds). This result indicates that *S*-nitrosation induces local disorder in domain 1 of GSTP1-1. In fact, given that Cys47 is nitrosated only when α2 is unfolded, *S*-nitrosation may select for transiently disordered conformations of domain 1, and prevent the domain from reforming its stable, native structure. The crystal structure of Cys-alkylated mouse GSTP1-1 lacked well-defined electron density for most of domain 1 [122]. This suggests that other modifications of Cys47 may alter the dynamics of domain 1, and that the integrity of the Cys47 thiol is vital for the proper folding and packing of the domain.

The introduction of local disorder is the likely cause of the low activity of the *S*-nitrosated enzyme. The highly dynamic active site of *S*-nitrosated GSTP1-1 is unlikely to be able to form a functional GSH binding site, much less position the thiol group optimally for conjugation to the electrophilic substrate. This is consistent with the increase in the K_M for GSH noted previously upon *S*-nitrosation of Cys47 of GSTP1-1 [128]. Whether the introduction of domain 1 disorder affects the interaction of GSTP1-1 with its numerous cellular binding partners [102,104,105] remains to be evaluated.

4.4 *S*-Nitrosation remodels the unfolding energy landscape of GSTP1-1

The unfolding kinetics of reduced GSTP1-1 have previously been explored in detail by Gildenhuys *et al*. [115]. These authors mapped the burst phase in the kinetics experiment to the rapid unfolding of helix α2. They also concluded, based on an initial conditions test, that the native state is heterogeneous in α2 conformation, and unfolding proceeds via parallel pathways. No evidence was found for a stable monomeric species, and the intermediate state was suggested to be dimeric, but with α2 unfolded. The burst phase for the unfolding of reduced GSTP1-1 is hyperfluorescent. This suggests that the unfolding of α2 either buries the tryptophan residues in a more hydrophobic environment, shifts the fluorophores away from quenching groups [138], or simply increases conformational dynamics [139]. The second phase of unfolding is characterised by a decrease in fluorescence intensity, which most likely

corresponds to an increase in solvent exposure of the tryptophan residues as domain 1 (and the bulk protein) unfolds completely [138].

In contrast to reduced GSTP1-1, the *S*-nitrosated proteins lack a hypofluorescent phase corresponding to solvent exposure as domain 1 unfolds [140]. This is consistent with biophysical data for Cys47/Cys101-NO GSTP1-1. DXMS experiments indicate that much of domain 1 of the *S*-nitrosated protein is highly dynamic and solvent exposed, even in the native state. Furthermore, this isoform unfolds rapidly, and with low kinetic cooperativity. This implies the unfolding of a highly dynamic structure that experiences a small change in ASA between the native and denatured states. Together, the data suggest that *S*-nitrosation at Cys47 and Cys101 induces partial unfolding of GSTP1-1, which then undergoes only limited further unfolding at high denaturant concentrations. Although the unfolding transients for Cys101-NO GSTP1-1 appear similar to those for the double-nitrosated protein, the unfolding events are quite different in character. Cys101 nitrosated GSTP1-1 unfolds two orders of magnitude more slowly than the reduced control, and with higher kinetic cooperativity. *S*-Nitrosation at Cys101 therefore appears to stabilise GSTP1-1 kinetically, while confining the unfolding pathway to a limited set of conformations, evidenced by the lack of a hypofluorescent phase in the unfolding transient.

Equilibrium and pre-equilibrium unfolding data demonstrate that *S*-nitrosation remodels the energy landscape of GSTP1-1 (Figure 9). For Cys47/Cys101-NO GSTP1-1, DXMS experiments indicate that the native state is destabilised, while acrylamide quenching data suggest stabilisation of the denatured state. This is consistent with equilibrium unfolding data, which show that *S*-nitrosation substantially decreases the cooperativity of unfolding of domain 1. Furthermore, unfolding kinetics experiments reveal a high k_u^{H2O} and very low $m_u^{\ddagger}$, evidence for a lower energy unfolding transition state and overall much smoother unfolding energy landscape. The effect of *S*-nitrosation at Cys101 alone is quite different. In this instance, the modified protein unfolds more slowly than reduced GSTP1-1, and with higher kinetic cooperativity. This implies that *S*-nitrosation at Cys101 destabilises the transition state for the unfolding reaction.

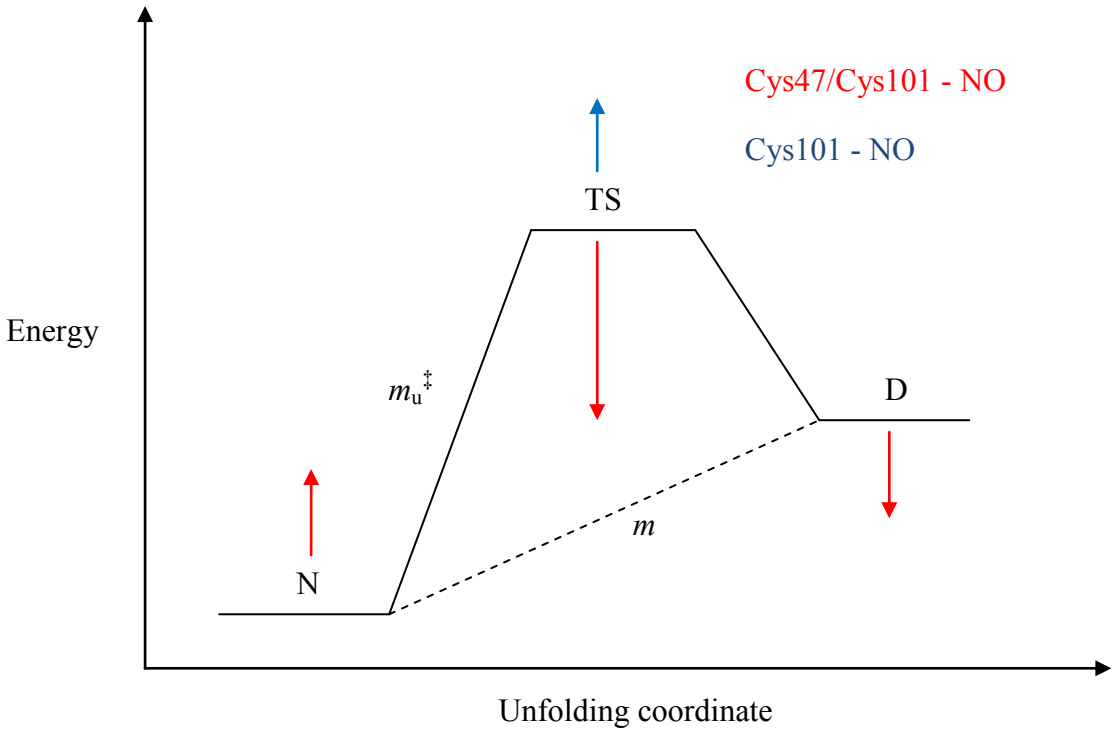

Figure 9. *S*-Nitrosation remodels the unfolding energy landscape of domain 1 of GSTP1-1. *S*-nitrosation at Cys47 and Cys101 destabilises the native state (N), while stabilising the transition state (TS) and denatured state (D). *S*-nitrosation at both cysteines reduces both the equilibrium (m) and kinetic ($m_u^{\ddagger}$) unfolding cooperativity. Nitrosation at Cys101 alone decreases the k_u^{H2O} and increases the $m_u^{\ddagger}$, suggesting that the transition state is destabilised.

The structure and stability of the denatured and transition states have important implications for the folding of GSTP1-1. Domain 1 Cys47/Cys101-NO GSTP1-1 folds without hysteresis, but the Cys101-NO isoform shows folding hysteresis in the same domain. Folding hysteresis following chemical denaturation is rare in the GST fold, but has been reported for Ure2, the yeast prion protein [141,142]. In the case of Ure2, the accumulation of an aggregation-prone monomeric species prevents equilibrium from being reached. In the case of Cys101-NO GSTP1-1, the hysteresis occurs without aggregation, and can be explained by the modification destabilising the transition state. A higher energy transition state implies a larger energy barrier for protein folding – the energy difference between the denatured and transition states is increased (Figure 9). It is possible that a fraction of the denatured protein is kinetically trapped in an unfolded (or partially folded) state, altering the unfolding-refolding equilibrium and causing hysteresis.

Despite its physiological importance, the effects of post-translational modifications on protein unfolding and stability have been explored in only a few instances. Both

phosphorylation [143] and ubiquitination [144] are known to promote local protein unfolding. *S*-Nitrosation causes a small reduction of the melting temperature of CLIC4 [93], although the implications for the stability and unfolding of the protein are unknown. Glycosylation has been shown to stabilise or destabilise proteins in a site-specific manner [145], with the stabilising effects attributed to a destabilisation of the denatured state [146]. This latter case is similar to the results presented here, which reveal site-specific stability effects upon *S*-nitrosation. More generally, these examples imply that the modulation of protein stability may be a generic strategy for post-translational control of protein function.

4.5 Cellular regulation of GSTP1-1 by *S*-nitrosation

GSTP1-1 functions *in vivo* to detoxify xenobiotics [147] and regulate c-jun N-terminal kinase 1 (JNK1) activity [102]. The GSH conjugation activity of GSTP1-1 is clearly impacted by *S*-nitrosation, as demonstrated in this study and previously [128]. Although various chemical modifications of the active site cysteine (Cys47) of GSTP1-1 have long been known to affect its enzymatic activity [119–121], the physiological relevance of these modifications is unclear. Thus far, the only post-translational modifications of GSTP1-1 demonstrated *in vivo* are *S*-nitrosation [41,131] and *S*-glutathionylation [126]. Both modifications have been shown to reduce GSTP1-1 enzymatic activity, demonstrating that the enzyme is under post-translational control.

Cellular oxidative or nitrosative stress would likely trigger *S*-nitrosation of GSTP1-1. Under these conditions, GSNO/CysNO concentrations are high and Cys47 is rapidly *S*-nitrosated. Cys47 nitrosation introduces local disorder, destabilising domain 1 and severely disrupting the detoxification activity of the enzyme. These consequences are mitigated in the presence of ligands which bind the G-site of GSTP1-1 and induce the closed conformation of α2, such as glutathione disulfide and dinitrosyl-di-glutathionyl-iron complex [148]. Furthermore, the reduced form of the protein is readily restored by GSH, which rapidly denitrosates Cys47, thereby limiting the duration of the stress response.

Cys101 nitrosation occurs slowly, especially at high GSNO, due to steric hindrance at the dimer interface of GSTP1-1. However, the Cys101-NO site is significantly stable against denitrosation by GSH [41,132]. Cys101-NO GSTP1-1 may, therefore, accumulate to high levels even in healthy cells. The physiological relevance of this is not obvious. *S*-Nitrosation at

Cys101 does not affect the detoxification activity of GSTP1-1 [128], and the refolding defect caused by this modification appears to be compensated for by enhanced kinetic stability. Speculatively, *S*-nitrosation at Cys101 may allow GSTP1-1 to transnitrosate other proteins, or affect the interaction between GSTP1-1 and JNK [102], peroxiredoxin [104] or AMP-activated protein kinase [105].

The effect of post-translational modifications on the ability of GSTP1-1 to inhibit JNK is unclear. *S*-Glutathionylation at Cys47 and Cys101 has been suggested to inhibit the interaction [126], although this has not been directly demonstrated. GSTP1-1 inhibits JNK activity by binding phosphorylated (active) JNK either directly or via a JNK substrate [102,103,149]. This interaction appears to be sensitive to the conformation of domain 1 of GSTP1-1. The binding of various active-site inhibitors prevents GSTP1-1 binding to JNK [102,150], as does the double mutation at the active site, W38H/C47S [151]. Given the severe consequences of *S*-nitrosation to the stability and dynamics of domain 1, it seems likely that the association of GSTP1-1 with JNK would be affected by this modification.

It is possible to speculate on the effects of disruption of the GSTP1-1 – JNK complex *in vivo.* Upon activation, JNK1 phosphorylates the c-jun component of the AP1 transcription factor at Ser63 and Ser73 [152], which activates the transcription of genes involved in cell proliferation, cell death, inflammation, and DNA repair [153]. JNK1 can also phosphorylate (and thereby stabilise) ATF2 and p53 [154] or (in its inactive form) target substrates for ubiquitination and subsequent degradation [155], depending on the stress conditions of the cell. As a consequence of these roles, JNK1 has been linked to autoimmune, neurodegenerative and metabolic diseases, as well as various cancers [156]. Under normal physiological conditions, GSTP1-1 likely sequesters JNK in an inactive complex, retarding AP1 activation. Oxidative stress would potentially disrupt this interaction by stimulating *S*-nitrosation of GSTP1-1, thereby releasing active JNK and causing the activation of pro-apoptotic genes. In normal cells, this may represent a mechanism by which apoptosis is induced in response to oxidative stress. Interestingly, tumor cells are typically hypoxic [157]. Hypoxia would mitigate protein *S*-nitrosation [30] and might in this way suppress JNK-mediated apoptosis in cancerous cells.

4.6 Conclusions

Despite its role in cellular physiology and pathophysiology, the phenomenon of protein *S*-nitrosation is poorly understood at a molecular level. In this research, the mechanism and biophysical consequences of *S*-nitrosation of GSTP1-1 were determined. The mechanism of transnitrosation reported here is the first for any protein, and represents an important step towards understanding how protein *S*-nitrosation is controlled and targeted *in vivo*. Furthermore, this is the first time that the effect of *S*-nitrosation on the stability and dynamics of a protein has been evaluated. These results constitute a detailed characterisation of the regulation of GSTP1-1 by *S*-nitrosation, and also offer novel insights into the control of protein function by *S*-nitrosation in general.

References

(1) Dunker, A. K., Brown, C. J., Lawson, J. D., Iakoucheva, L. M., and Obradovic, Z. (2002) Intrinsic disorder and protein function. *Biochemistry 41*, 6573–6582.

(2) Scott, N. (2005) Protein structure: unusual covalent bonds. *Encycl. Life Sci.* 1–10.

(3) Walsh, C. T., Garneau-tsodikova, S., and Gatto, G. J. (2005) Protein Posttranslational Modifications : The Chemistry of Proteome Diversifications. *Angew. Chem. Int. Ed. Engl. 44*, 7342–7372.

(4) Itzen, A., Blankenfeldt, W., and Goody, R. S. (2011) Adenylylation: renaissance of a forgotten post-translational modification. *Trends Biochem. Sci. 36*, 221–228.

(5) Hofmann, K., and Falquet, L. (2001) A ubiquitin-interacting motif conserved in components of the proteasomal and lysosomal protein degradation systems. *Trends Biochem. Sci. 26*, 347–350.

(6) Grunstein, M. (1997) Histone acetylation in chromatin structure and transcription. *Nature 389*, 349–352.

(7) Zhang, F., and Casey, P. (1996) Protein Prenylation: Molecular Mechanisms and Functional Consequences. *Annu. Rev. Biochem. 65*, 241–269.

(8) Smotrys, J., and Linder, M. (2004) PALMITOYLATION OF INTRACELLULAR SIGNALING PROTEINS: Regulation and Function. *Annu. Rev. Biochem. 73*, 559–597.

(9) Farazi, T., Waksman, G., and Gordon, J. (2001) The Biology and Enzymology of Protein N-Myristoylation. *J. Biol. Chem. 276*, 39501–39504.

(10) Manning, G., Whyte, D. B., Martinez, R., Hunter, T., and Sudarsanam, S. (2002) The Protein Kinase Complement of the Human Genome. *Science 298*, 1912–1934.

(11) Johnson, L. N., and Lewis, R. J. (2001) Structural Basis for Control by Phosphorylation. *Chem. Rev. 101*, 2209–2242.

(12) Giles, N. M., Giles, G., and Jacob, C. (2003) Multiple roles ofcysteine in biocatalysis. *Biochem. Biophys. Res. Commun.* 1–4.

(13) Marino, S. M., and Gladyshev, V. N. (2011) Analysis and functional prediction of reactive cysteine residues. *J. Biol. Chem. 287*, 4419–4425.

(14) Kim, S. O., Merchant, K., Nudelman, R., Beyer Jr, W. F., Keng, T., DeAngelo, J., Hausladen, A., and Stamler, J. S. (2002) OxyR:: A Molecular Code for Redox-Related Signaling. *Cell 109*, 383–396.

(15) Marino, S. ., and Gladyshev, V. N. (2010) Cysteine Function Governs Its Conservation and Degeneration and Restricts Its Utilization on Protein Surfaces. *J. Mol. Biol. 404*, 902–916.

(16) Hess, D. T., Matsumoto, A., Kim, S., Marshall, H. E., and Stamler, J. S. (2005) Protein S-nitrosylation: purview and parameters. *Nat. Rev. Mol. Cell Biol. 6*, 150–166.

(17) Reddie, K., and Carrol, K. . (2008) Expanding the functional diversity of proteins through cysteine oxidation. *Curr. Opin. Chem. Biol. 12*, 746–754.

(18) Bredt, D. . (1999) Endogenous nitric oxide synthesis: biological functions and pathophysiology. *Free Radic. Biol. Med. 31*, 577–596.

(19) Hill, B. G., Dranka, B. P., Bailey, S., Lancaster, J., and Darley-Usmar, V. (2010) What part of NO don't you understand? Some answers to the cardinal questions in nitric oxide biology. *J. Biol. Chem. 285*, 19699–19704.

(20) Butler, A. R., and Megson, I. . (2002) Non-Heme Iron Nitrosyls in Biology. *Chem. Rev. 102*, 1155–1166.

(21) Thomas, D. T., Miranda, K. M., Colton, C. A., Citrin, D., Espey, M. G., and Wink, D. A. (2003) Heme Proteins and Nitric Oxide (NO): The Neglected, Eloquent Chemistry in NO Redox Signaling and Regulation. *Antioxid. Redox Signal 5*, 307–317.

(22) Stamler, J. S., Simon, D. I., Osborne, J. a, Mullins, M. E., Jaraki, O., Michel, T., Singel, D. J., and Loscalzo, J. (1992) S-nitrosylation of proteins with nitric oxide: synthesis and characterization of biologically active compounds. *Proc. Natl. Acad. Sci. U. S. A. 89*, 444–448.

(23) Gow, A. J., Luchsinger, B. P., Pawloski, J. R., Singel, D. J., and Stamler, J. S. (1999) The oxyhemoglobin reaction of nitric oxide. *Proc. Natl. Acad. Sci. USA 96*, 9027–9032.

(24) Murad, F. (1986) Cyclic guanosine monophosphate as a mediator of vasodilation. *J. Clin. Invest. 78*, 1–5.

(25) Xue, Y., Liu, Z., Gao, X., Jin, C., Wen, L., Yao, X., and Ren, J. (2010) GPS-SNO: computational prediction of protein S-nitrosylation sites with a modified GPS algorithm. *PLoS One 5*, e11290.

(26) Liu, L., Yan, Y., Zeng, M., Zhang, J., Hanes, M. a, Ahearn, G., McMahon, T. J., Dickfeld, T., Marshall, H. E., Que, L. G., and Stamler, J. S. (2004) Essential roles of S-nitrosothiols in vascular homeostasis and endotoxic shock. *Cell 116*, 617–28.

(27) Sarkar, S., Korolchuk, V. I., Renna, M., Imarisio, S., Fleming, A., Williams, A., Garcia-Arencibia, M., Rose, C., Luo, S., Underwood, B. R., Kroemer, G., O'Kane, C. J., and Rubinsztein, D. C. (2011) Complex inhibitory effects of nitric oxide on autophagy. *Mol. Cell 43*, 19–32.

(28) Savidge, T. C., Urvil, P., Oezguen, N., Ali, K., Choudhury, A., Acharya, V., Pinchuk, I., Torres, A. G., English, R. D., Wiktorowicz, J. E., Loeffelholz, M., Kumar, R., Shi, L., Nie,

W., Braun, W., Herman, B., Hausladen, A., Feng, H., Stamler, J. S., and Pothoulakis, C. (2011) Host S-nitrosylation inhibits clostridial small molecule-activated glucosylating toxins. *Nat. Med. 17*, 1136–1141.

(29) Hess, D. T., and Stamler, J. S. (2011) Regulation by S-nitrosylation of Protein Posttranslational Modification. *J. Biol. Chem. 287*, 4411–4418.

(30) Foster, M. W., Hess, D. T., and Stamler, J. S. (2009) Protein S-nitrosylation in health and disease: a current perspective. *Trends Mol. Med. 15*, 391–404.

(31) Bartberger, M. D., Houk, K. N., Powell, S. C., Mannion, J. D., Lo, K. Y., Stamler, J. S., and Toone, E. J. (2000) Theory, Spectroscopy, and Crystallographic Analysis of S - Nitrosothiols: Conformational Distribution Dictates Spectroscopic Behavior. *J. Am. Chem. Soc. 122*, 5889–5890.

(32) Chan, N. L., Rogers, P. H., and Arnone, A. (1998) Crystal structure of the S-nitroso form of liganded human hemoglobin. *Biochemistry 37*, 16459–64.

(33) Schreiter, E. R., Rodrı, M., Weichsel, A., Montfort, W. R., and Bonaventura, J. (2007) S-Nitrosylation-induced Conformational Change in Blackfin Tuna Myoglobin. *J. Biol. Chem. 282*, 19773–19780.

(34) Weichsel, A., Brailey, J. L., and Montfort, W. R. (2007) Buried S-nitrosocysteine revealed in crystal structures of human thioredoxin. *Biochemistry 46*, 1219–1227.

(35) Chen, Y. Y., Chu, H. M., Pan, K. T., Teng, C., Wang, D. L., Wang, A. H. J., Khoo, K. H., and Meng, T. C. (2008) Cysteine S-nitrosylation protects protein-tyrosine phosphatase 1B against oxidation-induced permanent inactivation. *J. Biol. Chem. 283*, 35265–35272.

(36) Zhao, Y. L., and Houk, K. N. (2006) Thionitroxides, RSNHO•: The Structure of the SNO Moiety in "S-Nitrosohemoglobin", A Possible NO Reservoir and Transporter. *J. Am. Chem. Soc. 128*, 1422–1423.

(37) Bartberger, M. D., Mannion, J. D., Powell, S. C., Stamler, J. S., Houk, K. N., and Toone, E. J. (2001) S-N dissociation energies of S-nitrosothiols: on the origins of nitrosothiol decomposition rates. *J. Am. Chem. Soc. 123*, 8868–8869.

(38) Dicks, A. P., Swift, H. R., Williams, D. L. H., Butler, A. R., Al-Sadoni, H. H., and Cox, B. G. (1996) Identification of Cu+ as the effective reagent in nitric oxide formation from S-nitrosothiols (RSNO). *J. Chem. Soc. Perkin Trans. 2*, 481–487.

(39) Sexton, D. J., Muruganandam, A., McKenney, D. J., and Mutus, B. (1994) Visible Light Photochemical Release of Nitric Oxide from S-Nitrosoglutathione. *Photochem. Photobiol. 59*, 463–467.

(40) Williams, D. L. H. (1999) The Chemistry of S-Nitrosothiols. *Acc. Chem. Res. 32*, 869–876.

(41) Paige, J. S., Xu, G., Stancevic, B., and Jaffrey, S. R. (2008) Nitrosothiol reactivity profiling identifies S-nitrosylated proteins with unexpected stability. *Chem. Biol. 15*, 1307–1316.

(42) Knowles, R. G., and Moncada, S. (1994) Nitric oxide synthases in mammals. *Biochem. J. 298*, 249–58.

(43) Smith, B. C., and Marletta, M. a. (2012) Mechanisms of S-nitrosothiol formation and selectivity in nitric oxide signaling. *Curr. Opin. Chem. Biol. 16*, 498–506.

(44) Goldstein, S., and Czapski, G. (1996) Mechanism of the nitrosation of thiols and amines by oxygenated NO solutions: the nature of the nitrosating intermediates. *J. Am. Chem. Soc. 118*, 3419–3425.

(45) Hofstetter, D., Nauser, T., and Koppenol, W. H. (2007) The glutathione thiyl radical does not react with nitrogen monoxide. *Biochem. Biophys. Res. Commun. 360*, 146–148.

(46) Madej, E., Folkes, L. K., Wardman, P., Czapski, G., and Goldstein, S. (2008) Thiyl radicals react with nitric oxide to form S-nitrosothiols with rate constants near the diffusion-controlled limit. *Free Radic. Biol. Med. 44*, 2013–2018.

(47) Grierson, L., Hildenbrand, K., and Bothe, E. (1992) Intramolecular Transformation Reaction of the Glutathione Thiyl Radical into a Non-sulphur-centred Radical: A Pulse-radiolysis and EPR Study. *Int. J. Radiat. Biol. 62*, 265–277.

(48) Hofstetter, D., Nauser, T., and Koppenol, W. H. (2010) Hydrogen exchange equilibria in glutathione radicals: rate constants. *Chem. Res. Toxicol. 23*, 1596–600.

(49) Lancaster, J. R. (2006) Nitroxidative, nitrosative, and nitrative stress: kinetic predictions of reactive nitrogen species chemistry under biological conditions. *Chem. Res. Toxicol. 19*, 1160–1174.

(50) Koppenol, W. (2012) Nitrosation, Thiols, and Hemoglobin: Energetics and Kinetics. *Inorg. Chem.51,* 5637-5641.

(51) Basu, S., Keszler, A., Azarova, N. A., Nwanze, N., Perlegas, A., Shiva, S., Broniowska, K. A., Hogg, N., and Kim-Shapiro, D. B. (2010) A novel role for cytochrome c: Efficient catalysis of S-nitrosothiol formation. *Free Radic. Biol. Med. 48*, 255–263.

(52) Fernhoff, N. B., Derbyshire, E. R., Underbakke, E. S., and Marletta, M. a. (2012) Heme-assisted S-Nitrosation Desensitizes Ferric Soluble Guanylate Cyclase (sGC) to Nitric Oxide. *J. Biol. Chem. 287*, 43053–43062.

(53) Herold, S., and Rock, G. (2003) Reactions of deoxy-, oxy-, and methemoglobin with nitrogen monoxide. Mechanistic studies of the S-nitrosothiol formation under different mixing conditions. *J. Biol. Chem. 278*, 6623–6034.

(54) Tejero, J., Basu, S., Helms, C., Hogg, N., King, S. B., Kim-Shapiro, D. B., and Gladwin, M. T. (2012) Low NO concentration dependence of reductive nitrosylation reaction of hemoglobin. *J. Biol. Chem. 287*, 18262–18274.

(55) Jourd'heuil, D., Jourd'heuil, F. L., and Feelisch, M. (2003) Oxidation and nitrosation of thiols at low micromolar exposure to nitric oxide. Evidence for a free radical mechanism. *J. Biol. Chem. 278*, 15720–15726.

(56) Bosworth, C., Toledo, J., Zmijewsjki, J., Li, Q., and Lancaster, J. (2009) Dinitrosyliron complexes and the mechanism (s) of cellular protein nitrosothiol formation from nitric oxide. *Proc. Natl. Acad. Sci. USA 106*, 4671–4676.

(57) Foster, M. W., Liu, L., Zeng, M., Hess, D. T., and Stamler, J. S. (2009) A genetic analysis of nitrosative stress. *Biochemistry 48*, 792–799.

(58) Kharitonov, V. G., Sundquist, a R., and Sharma, V. S. (1995) Kinetics of nitrosation of thiols by nitric oxide in the presence of oxygen. *J. Biol. Chem. 270*, 28158–28164.

(59) Ford, E., Hughes, M. N., and Wardman, P. (2002) Kinetics of the reactions of nitrogen dioxide with glutathione, cysteine, and uric acid at physiological pH. *Free Radic. Biol. Med. 32*, 1314–1323.

(60) Yap, L.-P., Sancheti, H., Ybanez, M. D., Garcia, J., Cadenas, E., and Han, D. (2010) Determination of GSH, GSSG, and GSNO using HPLC with electrochemical detection. *Methods Enzymol. 473*, 137–147.

(61) Gaston, B. (1993) Endogenous nitrogen oxides and bronchodilator S-nitrosothiols in human airways. *Proc. Natl. Acad. Sci. U. S. A. 90*, 10957–10961.

(62) Foster, M. W., Forrester, M. T., and Stamler, J. S. (2009) A protein microarray-based analysis of S-nitrosylation. *Proc. Natl. Acad. Sci. U. S. A. 106*, 18948–18953.

(63) Liu, L., Hausladen, A., Zeng, M., Que, L., Heitman, J., and Stamler, J. S. (2001) A metabolic enzyme for S-nitrosothiol conserved from bacteria to humans. *Nature 410*, 490–494.

(64) Hogg, N. (1999) The kinetics of S-transnitrosation--a reversible second-order reaction. *Anal. Biochem. 272*, 257–262.

(65) Giustarini, D., Milzani, A., Colombo, R., Dalle-Donne, I., and Rossi, R. (2003) Nitric oxide and S-nitrosothiols in human blood. *Clin. Chim. Acta 330*, 85–98.

(66) Houk, K. N., Hietbrink, B. N., Bartberger, M. D., McCarren, P. R., Choi, B. Y., Voyksner, R. D., Stamler, J. S., and Toone, E. J. (2003) Nitroxyl disulfides, novel intermediates in transnitrosation reactions. *J. Am. Chem. Soc. 125*, 6972–696.

(67) Perissinotti, L. L., Turjanski, A. G., Estrin, D. a, and Doctorovich, F. (2005) Transnitrosation of nitrosothiols: characterization of an elusive intermediate. *J. Am. Chem. Soc. 127*, 486–487.

(68) Rossi, R., Lusini, L., Giannerini, F., Giustarini, D., Lungarella, G., and Di Simplicio, P. (1997) A method to study kinetics of transnitrosation with nitrosoglutathione: reactions with hemoglobin and other thiols. *Anal. Biochem. 254*, 215–220.

(69) Zhang, Y., and Hogg, N. (2004) Formation and stability of S-nitrosothiols in RAW 264.7 cells. *Am. J. Physiol. Lung Cell. Mol. Physiol. 287*, L467–L474.

(70) Anand, P., and Stamler, J. S. (2012) Enzymatic mechanisms regulating protein S-nitrosylation: implications in health and disease. *J. Mol. Med. 90*, 233–244.

(71) Mitchell, D. A., Morton, S. U., Fernhoff, N. B., and Marletta, M. A. (2007) Thioredoxin is required for S-nitrosation of procaspase-3 and the inhibition of apoptosis in Jurkat cells. *Proc. Natl. Acad. Sci. USA 104*, 11609–11614.

(72) Benhar, M., Forrester, M. T., Hess, D. T., and Stamler, J. S. (2008) Regulated protein denitrosylation by cytosolic and mitochondrial thioredoxins. *Science 320*, 1050–1054.

(73) Barglow, K. T., Knutson, C. G., Wishnok, J. S., Tannenbaum, S. R., and Marletta, M. A. (2011) Site-specific and redox-controlled S-nitrosation of thioredoxin. *Proc. Natl. Acad. Sci. U. S. A. 108*, E600–E606.

(74) Romeo, A. A., Capobianco, J. A., and English, A. M. (2003) Superoxide dismutase targets NO from GSNO to Cysβ93 of oxyhemoglobin in concentrated but not dilute solutions of the protein. *J. Am. Chem. Soc. 125*, 14370–14378.

(75) Broniowska, K. a, Keszler, A., Basu, S., Kim-Shapiro, D. B., and Hogg, N. (2012) Cytochrome c-mediated formation of S-nitrosothiol in cells. *Biochem. J. 442*, 191–197.

(76) Bateman, R., Rauh, D., Tavshanjian, B., and Shokat, K. (2008) Human carbonyl reductase 1 is an S-nitrosoglutathione reductase. *J. Biol. Chem. 283*, 35756–35762.

(77) Benhar, M., Forrester, M. T., and Stamler, J. S. (2009) Protein denitrosylation: enzymatic mechanisms and cellular functions. *Nat. Rev. Mol. Cell Biol. 10*, 721–732.

(78) Foster, M. W. (2011) Methodologies for the characterization, identification and quantification of S-nitrosylated proteins. *Biochim. Biophys. Acta.1820,*675-683.

(79) Hao, G., Derakhshan, B., Shi, L., Campagne, F., and Gross, S. . (2006) SNOSID, a proteomic method for identification of cysteine S-nitrosylation sites in complex protein mixtures. *Proc. Natl. Acad. Sci. U. S. A. 103*, 1012–1017.

(80) Doulias, P., Greene, J. L., Greco, T. M., Tenopoulou, M., Seeholzer, S. H., Dunbrack, R. L., and Ischiropoulos, H. (2010) Structural profiling of endogenous S-nitrosocysteine residues reveals unique features that accommodate diverse mechanisms for protein S-nitrosylation. *Proc. Natl. Acad. Sci. U. S. A. 107*, 16958–16963.

(81) Marino, S. M., and Gladyshev, V. N. (2010) Structural analysis of cysteine S-nitrosylation: a modified acid-based motif and the emerging role of trans-nitrosylation. *J. Mol. Biol. 395*, 844–859.

(82) Zhang, H., Andrekopoulos, C., Xu, Y., Joseph, J., Hogg, N., Feix, J., and Kalyanaraman, B. (2009) DECREASED S-NITROSATION OF PEPTIDE THIOLS IN THE MEMBRANE INTERIOR. *Free Radic. Biol. Med. 47*, 962–968.

(83) Kornberg, M., Sen, N., Hara, M., Juluri, K., Nguyen, J., Snowman, A., Law, L., LD, H., and Snyder, S. (2010) GAPDH mediates nitrosylation of nuclear proteins. *Nat. Cell Biol. 12*, 1094–1100.

(84) Wu, C., Liu, T., Chen, W., Oka, S.-I., Fu, C., Jain, M., Parrott, A., Baykal, A., Sadoshima, J., and Li, H. (2010) Redox regulatory mechanism of transnitrosylation by thioredoxin. *Mol. Cell. proteomics 9*, 2262–2275.

(85) Dunn, J., Gutbrod, S., Webb, A., Pak, A., Jandu, S. K., Bhunia, A., Berkowitz, D. E., and Santhanam, L. (2011) S-nitrosation of arginase 1 requires direct interaction with inducible nitric oxide synthase. *Mol. Cell. Biochem. 355*, 83–89.

(86) Iwakiri, Y., Satoh, A., Chatterjee, S., Toomre, D. K., Chalouni, C. M., Fulton, D., Groszmann, R. J., Shah, V. H., and Sessa, W. C. (2006) Nitric oxide synthase generates nitric oxide locally to regulate compartmentalized protein S-nitrosylation and protein trafficking. *Proc. Natl. Acad. Sci. 103*, 19777-19782.

(87) Rössig, L., Fichtlscherer, B., Breitschopf, K., Haendeler, J., Zeiher, A. M., Mülsch, A., and Dimmeler, S. (1999) Nitric oxide inhibits caspase-3 by S-nitrosation in vivo. *J. Biol. Chem. 274*, 6823–6826.

(88) Hashemy, S. I., and Holmgren, A. (2008) Regulation of the catalytic activity and structure of human thioredoxin 1 via oxidation and S-nitrosylation of cysteine residues. *J. Biol. Chem. 283*, 21890–21898.

(89) Hausladen, A., Privalle, C. T., Keng, T., DeAngelo, J., and Stamler, J. S. (1996) Nitrosative stress: activation of the transcription factor OxyR. *Cell 86*, 719–729.

(90) Xu, L. (1998) Activation of the Cardiac Calcium Release Channel (Ryanodine Receptor) by Poly-S-Nitrosylation. *Science 279*, 234–237.

(91) Asada, K., Kurokawa, J., and Furukawa, T. (2009) Redox- and calmodulin-dependent S-nitrosylation of the KCNQ1 channel. *J. Biol. Chem. 284*, 6014–6020.

(92) Wolzt, M., MacAllister, R. J., Davis, D., Feelisch, M., Moncada, S., Vallance, P., and Hobbs, a J. (1999) Biochemical characterization of S-nitrosohemoglobin. Mechanisms underlying synthesis, no release, and biological activity. *J. Biol. Chem. 274*, 28983–28990.

(93) Malik, M., Shukla, A., Amin, P., Niedelman, W., Lee, J., Jividen, K., Phang, J. M., Ding, J., Suh, K. S., Curmi, P. M. G., and others. (2010) S-Nitrosylation Regulates Nuclear Translocation of Chloride Intracellular Channel Protein CLIC4. *J. Biol. Chem. 285*, 23818–23828.

(94) Tada, Y., Spoel, S. H., Pajerowska-Mukhtar, K., Mou, Z., Song, J., Wang, C., Zuo, J., and Dong, X. (2008) Plant immunity requires conformational changes [corrected] of NPR1 via S-nitrosylation and thioredoxins. *Science 321*, 952–956.

(95) Weichsel, A., Maes, E. M., Andersen, J. F., Valenzuela, J. G., Shokhireva, T. K., Walker, F. A., and Montfort, W. R. (2005) Heme-assisted S-nitrosation of a proximal thiolate in a nitric oxide transport protein. *Proc. Natl. Acad. Sci. U. S. A. 102*, 594–599.

(96) Kumar, V., Martin, F. E., Hahn, M. G., Schaefer, M., Stamler, J. S., Stasch, J.-P., and van den Akker, F. (2013) Insights into BAY 60-2770 activation and S-nitrosylation-dependent desensitization of soluble guanylyl cyclase via crystal structures of homologous Nostoc H-NOX domain complexes. *Biochemistry 52,* 3601-3608.

(97) Williams, J., and Pappu, K. (2003) Structural and biochemical studies of p21Ras S-nitrosylation and nitric oxide-mediated guanine nucleotide exchange. *Proc. Natl. Acad. Sci. U. S. A. 100*, 6376–6381.

(98) Lenarcic Zivkovic, M., Zareba-Koziol, M., Zhukova, L., Poznanski, J., Zhukov, I., and Wyslouch-Cieszynska, A. (2012) Post-translational S-Nitrosylation Is an Endogenous Factor Fine Tuning the Properties of Human S100A1 Protein. *J. Biol. Chem. 287*, 40457–40470.

(99) Sheehan, D., Meade, G., Foley, V. M., and Dowd, C. A. (2001) Structure, function and evolution of glutathione transferases: implications for classification of an ancient enzyme superfamily. *Biochem. J. 360*, 1–16.

(100) Tew, K. D. (1994) Glutathione-associated Enzymes in Anticancer Drug Resistance. *Cancer Res. 54*, 4313–4320.

(101) Henderson, C. J., McLaren, A. W., Moffat, G. J., Bacon, E. J., and Wolf, C. R. (1998) Pi-class glutathione S-transferase: regulation and function. *Chem. Biol. Interact. 111*, 69–82.

(102) Adler, V., Yin, Z., Fuchs, S. Y., Benezra, M., Rosario, L., Tew, K. D., Pincus, M. R., Sardana, M., Henderson, C. J., Wolf, C. R., and others. (1999) Regulation of JNK signaling by GSTp. *EMBO J. 18*, 1321–1334.

(103) Thévenin, A. F., Zony, C. L., Bahnson, B. J., and Colman, R. F. (2011) GSTpi modulates JNK activity through a direct interaction with JNK substrate, ATF2. *Protein Sci.* 1–45.

(104) Ralat, L., Manevich, Y., Fisher, A., and Colman, R. (2006) Direct Evidence for the Formation of a Complex between 1-Cysteine Peroxiredoxin and Glutathione S-Transferase π with Activity Changes in Both Enzymes. *Biochemistry 45*, 360–372.

(105) Klaus, A., Zorman, S., Berthier, A., Polge, C., Ramirez, S., Michelland, S., Sève, M., Vertommen, D., Rider, M., Lentze, N., Auerbach, D., and Schlattner, U. (2013) Glutathione S-transferases interact with AMP-activated protein kinase: evidence for S-glutathionylation and activation in vitro. *PLoS One 8*, e62497.

(106) Fabrini, R., De Luca, A., Stella, L., Mei, G., Orioni, B., Ciccone, S., Federici, G., Lo Bello, M., and Ricci, G. (2009) Monomer-dimer equilibrium in glutathione transferases: a critical re-examination. *Biochemistry 48*, 10473–82.

(107) Reinemer, P., Dirr, H. W., Ladenstein, R., Schaffer, J., Gallay, O., and Huber, R. (1991) The three-dimensional structure of class pi glutathione S-transferase in complex with glutathione sulfonate at 2 . 3 A resolution. *EMBO J. 10*, 1997–2005.

(108) Armstrong, R. N. (1991) Glutathione S-transferases: reaction mechanism, structure, and function. *Chem. Res. Toxicol. 4*, 131–140.

(109) Dirr, H., Reinemer, P., and Huber, R. (1994) X-ray crystal structures of cytosolic glutathione S-transferases Implications for protein architecture , substrate recognition and catalytic function. *Eur. J. Biochem. 220*, 645–661.

(110) Honaker, M. T., Acchione, M., Sumida, J. P., and Atkins, W. M. (2011) An ensemble perspective for catalytic promiscuity: calorimetric analysis of the active site conformational landscape of a detoxification enzyme. *J. Biol. Chem. 286*, 42770 –42776.

(111) Oakley, a J., Lo Bello, M., Ricci, G., Federici, G., and Parker, M. W. (1998) Evidence for an induced-fit mechanism operating in pi class glutathione transferases. *Biochemistry 37*, 9912–9917.

(112) Hitchens, T. K., Mannervik, B., and Gordon, S. (2001) Disorder-to-order transition of the active site of human class Pi glutathione transferase, GST P1-1. *Biochemistry 40*, 11660–11669.

(113) Ricci, G., Caccuri, A. M., Bello, M. L., Rosato, N., Mei, G., Nicotra, M., Chiessi, E., Mazzetti, A. P., and Federici, G. (1996) Structural Flexibility Modulates the Activity of Human Glutathione Transferase P1-1. *J. Biol. Chem. 271*, 16187-16192.

(114) Dalke, H. W., and Schulten, K. (1996) VMD - Visual Molecular Dynamics. *J. Molec. Graph. 14*, 33–38.

(115) Gildenhuys, S., Wallace, L. A., Burke, J. P., Balchin, D., Sayed, Y., and Dirr, H. W. (2010) Class Pi glutathione transferase unfolds via a dimeric and not monomeric intermediate: functional implications for an unstable monomer. *Biochemistry 49*, 5074–81.

(116) Lo Bello, M., Parker, M. W., Desideri, A., Polticelli, F., Falconi, M., Del Boccio, G., Pennelli, A., Federici, G., and Ricci, G. (1993) Peculiar Spectroscopic and Kinetic Properties of Cys-47 in human placental glutathione transferase. *J. Biol. Chem. 268*, 19033–19038.

(117) Orton, C. R., and Liebler, D. C. (2007) Analysis of protein adduction kinetics by quantitative mass spectrometry: competing adduction reactions of glutathione-S-transferase P1-1 with electrophiles. *Chem. Biol. Interact. 168*, 117–27.

(118) Kong, K.-H., Inoue, H., and Takahashi, K. (1991) Non-essentiality of cysteine and histidine residues for the activity of human class pi glutathione S-transferase. *Biochem. Biophys. Res. Commun. 181*, 748–755.

(119) Lo Bello, M., Petruzzelli, R., De Stefano, E., Tenedini, C., Barra, D., and Federici, G. (1990) Identification of a highly reactive sulphydryl group in human placental glutathione transferase by a site-directed fluorescent reagent. *FEBS Lett. 263*, 389–391.

(120) Shen, H., Tamai, K., and Tsuchida, S. (1991) Modulation of Class Pi Glutathione transferase activity by Sulfhydryl Group Modification. *Arch. Biochem. Biophys. 286*, 178–182.

(121) Sluis-Cremer, N., and Dirr, H. (1995) Conformational stability of Cys45-alkylated and hydrogen peroxide-oxidised glutathione S-transferase. *FEBS Lett. 371*, 94–98.

(122) Vega, M. C., Walsh, S. B., Mantles, T. J., and Coll, M. (1998) The three-dimensional structure of Cys-47-modified mouse liver glutathione S-transferase P1-1. *J. Biol. Chem. 273*, 2844–2850.

(123) Bico, P., Erhardt, J., Kaplan, W., and Dirr, H. (1995) Porcine class Pi glutathione S-transferase: Anionic ligand binding and conformational analysis. *Biochim. Biophys. Acta 1247*, 225–230.

(124) Ricci, G., Boccio, G. Del, Pennelli, A., Bello, L., Petruzzelli, R., Caccuri, A. M., Barra, D., and Federici, G. (1991) Redox Forms of Human Placenta Glutathione Transferase. *J. Biol. Chem. 266*, 21409–21415.

(125) Stella, L., Di Iorio, E. E., Nicotra, M., and Ricci, G. (1999) Molecular dynamics simulations of human glutathione transferase P1-1: conformational fluctuations of the apo-structure. *Proteins 37*, 10–19.

(126) Townsend, D. M., Manevich, Y., He, L., Hutchens, S., Pazoles, C. J., and Tew, K. D. (2009) Novel role for glutathione S-transferase pi. Regulator of protein S-Glutathionylation following oxidative and nitrosative stress. *J. Biol. Chem. 284*, 436–445.

(127) Oakley, a J., Lo Bello, M., Battistoni, A., Ricci, G., Rossjohn, J., Villar, H. O., and Parker, M. W. (1997) The structures of human glutathione transferase P1-1 in complex with glutathione and various inhibitors at high resolution. *J. Mol. Biol. 274*, 84–100.

(128) Lo Bello, M., Nuccetelli, M., Caccuri, A. M., Stella, L., Parker, M. W., Rossjohn, J., McKinstry, W. J., Mozzi, A. F., Federici, G., Polizio, F., Pedersen, J. Z., and Ricci, G. (2001) Human glutathione transferase P1-1 and nitric oxide carriers; a new role for an old enzyme. *J. Biol. Chem. 276*, 42138–42145.

(129) Téllez-Sanz, R., Cesareo, E., Nuccetelli, M., Aguilera, A. M., Barón, C., Parker, L. J., Adams, J. J., Morton, C. J., Lo Bello, M., Parker, M. W., and others. (2006) Calorimetric and structural studies of the nitric oxide carrier S-nitrosoglutathione bound to human glutathione transferase P1-1. *Protein Sci. 15*, 1093–1105.

(130) Beltrán, B., Orsi, A., Clementi, E., and Moncada, S. (2000) Oxidative stress and S-nitrosylation of proteins in cells. *Br. J. Pharmacol. 129*, 953–960.

(131) Sinha, V., Wijewickrama, G. T., Chandrasena, R. E. P., Xu, H., Edirisinghe, P. D., Schiefer, I. T., and Thatcher, G. R. J. (2010) Proteomic and mass spectroscopic quantitation of protein S-nitrosation differentiates NO-donors. *ACS Chem. Biol. 5*, 667–680.

(132) Balchin, D., Wallace, L., and Dirr, H. W. (2013) S-nitrosation of glutathione transferase P1-1 is controlled by the conformation of a dynamic active-site helix. *J. Biol. Chem.* 14973–14984.

(133) Nieslanik, B. S., Ibarra, C., and Atkins, W. M. (2001) The C-terminus of glutathione S-transferase A1-1 is required for entropically-driven ligand binding. *Biochemistry 40*, 3536–3543.

(134) Vogt, A. D., and Di Cera, E. (2013) Conformational Selection Is a Dominant Mechanism of Ligand Binding. *Biochemistry 52*, 5723-5729.

(135) Xie, H., Vucetic, S., Iakoucheva, L. M., Oldfield, C. J., Dunker, A. K., Obradovic, Z., and Uversky, V. N. (2007) Functional Anthology of Intrinsic Disorder . 3 . Ligands , Post-Translational Modifications , and Diseases Associated with Intrinsically Disordered Proteins research articles 1917–1932.

(136) Bell, S., Klein, C., Müller, L., Hansen, S., and Buchner, J. (2002) p53 Contains Large Unstructured Regions in its Native State. *J. Mol. Biol. 322*, 917–927.

(137) Jenuwein, T., and Allis, C. D. (2001) Translating the histone code. *Science 293*, 1074–1080.

(138) Lakowicz, J. R., and Masters, B. R. (2008) Principles of Fluorescence Spectroscopy, Third Edition. *J. Biomed. Opt. 13*, 029901.

(139) Ervin, J., Larios, E., Osváth, S., Schulten, K., and Gruebele, M. (2002) What causes hyperfluorescence: folding intermediates or conformationally flexible native states? *Biophys. J. 83*, 473–483.

(140) Balchin, D., Stoychev, S. H., and Dirr, H. W. (2013) S-Nitrosation destabilizes glutathione transferase P1-1. *Biochemistry*. **DOI:** 10.1021/bi401414c

(141) Perrett, S., Freeman, S. J., Butler, P. J. G., and Fersht, A. R. (1999) Equilibrium folding properties of the yeast prion protein determinant Ure2. *J. Mol. Biol. 290*, 331–345.

(142) Galani, D., Fersht, A. R., and Perrett, S. (2002) Folding of the yeast prion protein Ure2: kinetic evidence for folding and unfolding intermediates. *J. Mol. Biol. 315*, 213–227.

(143) Huffine, M. E., and Scholtz, J. M. (1996) Energetic implications for protein phosphorylation. Conformational stability of HPr variants that mimic phosphorylated forms. *J. Biol. Chem. 271*, 28898–28902.

(144) Hagai, T., and Levy, Y. (2010) Ubiquitin not only serves as a tag but also assists degradation by inducing protein unfolding. *Proc. Natl. Acad. Sci. U. S. A. 107*, 2001–2006.

(145) Chen, M. M., Bartlett, A. I., Nerenberg, P. S., Friel, C. T., Hackenberger, C. P. R., Stultz, C. M., Radford, S. E., and Imperiali, B. (2010) Perturbing the folding energy landscape of the bacterial immunity protein Im7 by site-specific N-linked glycosylation. *Proc. Natl. Acad. Sci. U. S. A. 107*, 22528–22533.

(146) Shental-Bechor, D., and Levy, Y. (2008) Effect of glycosylation on protein folding: a close look at thermodynamic stabilization. *Proc. Natl. Acad. Sci. U. S. A. 105*, 8256–8261.

(147) Armstrong, R. N. (1997) Structure, catalytic mechanism, and evolution of the glutathione transferases. *Chem. Res. Toxicol. 10*, 2–18.

(148) De Maria, F., Pedersen, J. Z., Caccuri, A. M., Antonini, G., Turella, P., Stella, L., Lo Bello, M., Federici, G., and Ricci, G. (2003) The specific interaction of dinitrosyl-

diglutathionyl-iron complex, a natural NO carrier, with the glutathione transferase superfamily: suggestion for an evolutionary pressure in the direction of the storage of nitric oxide. *J. Biol. Chem. 278*, 42283–42293.

(149) Wang, T., Arifoglu, P., Ronai, Z., and Tew, K. D. (2001) Glutathione S-transferase (GSTP1-1) inhibits c-Jun N-terminal Kinase (JNK1) Signaling through Interaction with the C Terminus. *J. Biol. Chem. 276*, 20999 –21003.

(150) Monaco, R., Friedman, F., Hyde, M., and Chen, J. (1999) Identification of a glutathione-S-transferase effector domain for inhibition of jun kinase, by molecular dynamics. *J. Protein Chem. 18*, 859–866.

(151) Asakura, T., Sasagawa, A., Takeuchi, H., Shibata, S.-I., Marushima, H., Mamori, S., and Ohkawa, K. (2007) Conformational change in the active center region of GST P1-1, due to binding of a synthetic conjugate of DXR with GSH, enhanced JNK-mediated apoptosis. *Apoptosis 12*, 1269–1280.

(152) Hibi, M., Lin, A., Smeal, T., Minden, A., and Karin, M. (1993) Identification of an oncoprotein- and UV-responsive protein kinase that binds and potentiates the c-Jun activation domain. *Genes Dev. 7*, 2135–2148.

(153) Karin, M., and Gallagher, E. (2005) From JNK to pay dirt: jun kinases, their biochemistry, physiology and clinical importance. *IUBMB Life 57*, 283–295.

(154) Fuchs, S. Y., Adler, V., Pincus, M. R., and Ronai, Z. (1998) MEKK1/JNK signaling stabilizes and activates p53. *Proc. Natl. Acad. Sci. U. S. A. 95*, 10541-10546.

(155) Fuchs, S. ., Xie, B., Adler, V., Fried, V. A., Davis, R. J., and Ronai, Z. (1997) c-Jun NH2-terminal kinases target the ubiquitination of their associated transcription factors. *J. Biol. Chem. 272*, 32163–32168.

(156) Manning, A. M., and Davis, R. J. (2003) Targeting JNK for therapeutic benefit: from junk to gold? *Nat. Rev. Drug Discov. 2*, 554–565.

(157) Vaupel, P., Kallinowski, F., and Okunieff, P. (1989) Blood Flow , Oxygen and Nutrient Supply , and Metabolic Microenvironment of Human Tumors : A Review. *Cancer Res. 49*, 6449–6465.